Characterisation of proton exchange membranes in an H_2SO_4 environment

R Peach

21640904

Dissertation submitted in partial fulfilment of the requirements for the degree *Magister Scientiae* in *Chemistry* at the Potchefstroom Campus of the North-West University

Supervisor: Prof H Krieg

Co-supervisor: Mr AJ Krüger

Assistant supervisor: Mr D van der Westhuizen

September 2014

Academic Contributions Resulting from this Research

Article published in peer reviewed journal:

Peach R, Krieg HM, Krüger AJ, van der Westhuizen D, Bessarabov D, Kerres J. 2014. Comparison of ionically and ionical-covalently cross-linked polyaromatic membranes for SO_2 electrolysis. *International Journal of Hydrogen Energy.* 2014. 39(1): p.28-40.

Acknowledgements

I herein express my sincerest gratitude towards:

- My Heavenly Farther for providing me with the strength, ability, determination and support of loved ones to complete the research for my dissertation.
- My parents for all their support, unconditional love and words of encouragement throughout my studies and research work.
- Professor Henning M. Krieg, Membrane Technology, for all his effort, support and guidance during my research work. I learned a great deal and am truly grateful for the opportunities he has given me.
- Derik van der Westhuizen, Membrane Technology, and Andries J. Krüger, DST HySA, for their guidance, advice and contribution to my dissertation and research as co-supervisors.
- Dr. Jochen A. Kerres and Dr. Andreas Chromik, Institute of Chemical Process Engineering, University of Stuttgart, for hosting us in Germany at ICVT for two weeks while sharing their knowledge and providing us with the membrane materials on which my dissertation is based.
- Dr. Vladimir Atanasov, Institute of Chemical Process Engineering, University of Stuttgart, for the insight on our results and discussion of my dissertation.
- Dr. L. Tiedt and Dr. A. Jordaan at the Laboratory of Electron Microscopy, North-West University, for their support and assistance with the SEM analysis.
- Dr S. Ellis from the statistical consultation services at the North-West University for guidance in the processing of my data.
- Chemical Research Beneficiation, North-West University, Potchefstroom Campus for the use of their laboratories and analytical apparatus (Coal Chemistry, Membrane Technology and Catalysis and Synthesis halls) during the course of my research.
- Mrs Hestelle Stoppel, secretary at Chemical Research Beneficiation, North-West University, for her time and effort in the handling of orders and deliveries.
- The DFG for their financial support within our collaboration with Dr. Kerres (DFG project number KE 673/11-1).
- Lastly, but not least, my brother and friends for providing me with the needed distractions and motivation during the course of my studies.

Abstract

In light of the world's growing demand for energy that is environmentally friendly and sustainable, energy sources such as hydrogen have been considered potential contenders. Hydrogen, which can be used for energy storage, can be produced efficiently by the membrane based Hybrid Sulfur (HyS) thermo-chemical process consisting of a decomposition and an electrolysis step. During the HyS electrolysis step, SO_2 and H_2O are converted to H_2 and H_2SO_4, which implies that the proton exchange membranes (PEMs) to be used for this process should have a high proton conductivity, limited SO_2 cross-over and good H_2SO_4 stability.

In order to find alternatives to the costly and high-temperature unstable Nafion®, the aim of this study was to evaluate the H_2SO_4 stability of various novel membranes. To structure the study, the novel PEM materials were grouped according to the PBI-type base component within the blend membranes, resulting in three groups comprising non-PBI based membranes, PBIOO based membranes and F_6-PBI based membranes. Nafion®212 was included as reference PEM. By repeating the H_2SO_4 treatment with three different Nafion®212 samples, the obtained Nafion® data was also used to determine the experimental and analytical error margins for the study. The stability of all membranes was determined by submerging the membrane samples in 80 wt% H_2SO_4 at 80 °C for 120 hours. To determine the influence of the acid on the membranes, all samples were characterised before and after the H_2SO_4 treatment and compared in terms of their acid stability. Physical characterisation of the PEMs included the evaluation of weight and thickness changes, while IEC, SEM-EDX, FTIR and TGA were used to elucidate possible chemical changes due to the H_2SO_4 treatment.

According to the Nafion®212 data, which had been obtained in triplicate for each of the analytical techniques, the experimental error of both the analytical and H_2SO_4 treatment remained below 10 %, except for the SEM-EDX sulfur-content where significantly larger errors were observed. In spite of the high error margins of the SEM-EDX data (S-content), its results, combined with the results from the other analytical techniques, resulted in a better understanding (both physical and chemical) of the effect the H_2SO_4 had on the membrane. This further facilitated the evaluation and comparison of the various blended PEM materials in terms of their H_2SO_4 stability, and the subsequent relation obtained between the observed stability and the chemical constitution and cross-linking of the membranes.

After the 80 wt% H_2SO_4 treatment, significant weight losses were reported for the non-PBI based and PBIOO based membrane groups in comparison with the minimal changes noted for the F_6-PBI based group and Nafion®212. Furthermore, significant thickness changes were

reported for most of the PBIOO based membranes. The small weight and thickness changes observed for the F_6-PBI confirmed the improved stability of this group of membranes in an H_2SO_4 environment, most likely due to the protective role of the partially fluorinated basic polymer and the known strength of the C-F bonds present.

The results showed a clear correlation between the H_2SO_4 stability and the specific polymers present in the PEM blends investigated. Specific effects found included sulfonation, salt formation, hydrolysis and the accompanied dissolution of membrane fragments. Significant physical changes, for example ascribed to sulfonation of the concerned polymers, were supported by increased IEC measurements and peak intensities of the FTIR spectra, corresponding to the additional $–SO_3H$ groups present, while a variation in TGA signals served to further support the altered membrane composition and structure due to the H_2SO_4 treatment. In the case of dissolution, the corresponding chemical changes (analytical techniques) were supported by the decreased peak intensities of FTIR spectra, IEC measurements and TGA signals associated with degradation of the polymer backbone.

It was shown that the stability of the blended membranes depended on the composition (blend components) of the membrane and the effective cross-linking (interaction) between the blend components. For all three groups examined, it became apparent that blend components sFS and sPSU were, for example, more stable than sPEEK and that ionical cross-linking seemed more effective than covalent cross-linking of blend components.

When considering all membranes tested, the non-PBI based blend membranes consisting of (s)PSU and PFS copolymers in the presence of fluorinated cross-linkers and the PBIOO-sPSU blended membranes including most of the F_6-PBI based membranes showed sufficient stability to be recommended for SO_2 electrolysis.

Keywords

Proton exchange membranes, H_2SO_4 stability, physical and chemical characterisation, Nafion®212 reference, polymer evaluation (cross-linking)

Table of Contents

Academic Contributions Resulting from this Research ..... **i**

Acknowledgements ..... **ii**

Abstract ..... **iii**

Keywords ..... **v**

Chapter 1: Introduction **1**

Chapter 2: Literature study **9**

Chapter 3: Experimental **37**

Chapter 4: Results and Discussion **44**

Chapter 5: Evaluation and recommendations **84**

Appendix A: **100**

Appendix B: **102**

Appendix C: **105**

Appendix D: **108**

Chapter 1: Introduction

Contents

1.1 Background 2

1.1.1 Hydrogen supply..... 2

1.1.2 Producing hydrogen 2

1.2 Problem statement 4

1.3 Aim and objectives 5

1.4 Outline of the dissertation 5

1.5 References 7

1.1 Background

The rapidly increasing demand for energy and the reality of depleting fossil fuels have raised concerns for future energy security and environmental sustainability. Renewable energy sources, such as wind, hydroelectricity and solar energy, are limited to seasonal fluctuations and application [1]. Fuel cells, on the other hand, represent an energy conversion technology with a high-energy conversion efficiency and a variety of applications, both stationary and instationary [2,3]. While proton exchange membrane (PEM) based fuel cells are promising for applications in automobiles and portable devices, PEMs are also currently the most popular fuel cells used for the generation of electrical energy [4].

As hydrogen is a clean alternative energy carrier, the production thereof using clean and non-polluting methods has become of interest [5,6]. Water electrolysis is one such method and is well-known to produce pure hydrogen and oxygen from water. Although significant advances have been made in recent years on water electrolysers, other more efficient electrolysis processes based on thermo-chemical cycles have been recently suggested [7].

1.1.1 Hydrogen supply

In nature, hydrogen is not available in a form that can be readily utilised in energy applications, but is found within a variety of compounds, including water and hydrocarbon fuels. In order to obtain hydrogen, energy is required to break the chemical bonds within these hydrogen-containing compounds. In an attempt to limit the air pollution emitted from fossil fuels in the production of hydrogen, more environmentally friendly hydrogen sources are being researched. For example, hydrogen can be produced from water with the addition of the valuable by-product oxygen. This considered, hydrogen can be seen as an energy-carrier and a means of transport and storage of energy rather than an energy source as would be the case for fossil fuels [5].

1.1.2 Producing hydrogen

As mentioned, hydrogen can be produced from an array of different methods, of which electrolysis and thermal-chemical processes will be discussed further.

1.1.2.1 Electrolysis

During electrolysis, an electric potential is applied to split water into gaseous hydrogen and oxygen [8]. The hydrogen produced by H_2O electrolysis is regarded pollutant-free, although the electrical energy needed for the splitting of the water exceeds the energy contained within the hydrogen product. Furthermore, since the cost of the needed electrical energy is high, the water-splitting process is only considered economical in areas where vast natural power sources (e.g. hydropower) are available [9].

1.1.2.2 Thermo-chemical cycles

Of the hydrogen production technologies investigated to date, the thermo-chemical processes, where the hydrogen source is chemically converted to pure hydrogen using an external heat source, seem most promising [10]. Similar to water electrolysis, hydrogen and oxygen is produced from water, with the difference that the additional chemicals that are used to reduce the electrical potential required are recycled. Furthermore, the temperature range required for the splitting of water in a thermo-chemical cycle (800-1000 °C) is much lower than that required for the direct thermal dissociation of water (>2500 °C) [6]. One of the most promising thermo-chemical cycles, using a proton exchange membrane (PEM) based electrolyser, is the Hybrid Sulfur (HyS) thermo-chemical cycle [11] which has received increased attention over the last years [12].

1.1.2.3 The HyS process

Investigating the decomposition of sulfuric acid, the HyS process was first presented by the Westinghouse Electric Corporation in the 1970's [6]. In the HyS cycle, the reactants are produced during the sulfuric acid decomposition step at approximately 800 ^{0}C [13] as shown in Equation 1.1. The formed SO_2 is fed, together with water, to the anodic side of the membrane electrode assembly (MEA) in the PEM electrolyser, where the SO_2 is then electrochemically oxidised at the anode and subsequently protons and electrons (Equation 1.2) are produced. The protons migrate through the PEM to produce H_2 and H_2SO_4 (Equation 1.3) at the cathode [14]. The formed H_2SO_4 is then recycled to the decomposition step (Equation 1.1).

$$H_2SO_4 \rightarrow SO_2 + ½\ O_2 + H_2O \quad (1.1)$$

$$SO_2 + 2H_2O \rightarrow H_2SO_4 + 2H^+ + 2e^- \quad (1.2)$$

$$2H^+ + 2e^- \rightarrow H_2 \quad (1.3)$$

The overall reaction is summarised in Equation 1.4 [15,16]:

$$2H_2O + SO_2 \rightarrow H_2 + H_2SO_4 \quad (1.4)$$

The electrolysis of water in the presence of SO_2 gas is of interest due to the significant reduction of potential required for the reaction (E^{theo}=0.158 V) compared to normal water electrolysis (E^{theo}=1.29 V), giving this process a higher overall efficiency [17]. However, the operating conditions determined for the SO_2 electrolyser in the HyS cycle includes elevated acid concentrations, temperatures and pressures which create a different environment for the PEM from the one found in a H_2O electrolyser. This gives rise to the challenge of developing PEM materials that will be able to withstand the harsh environment within such an SO_2 electrolyser.

1.1.2.4 PEM requirements

The PEM features as a core component in the PEM fuel cell and electrolyser operations. It is known that both the performance and lifetime of the fuel cell and electrolyser are affected by the mechanical and chemical properties of the membrane [18]. To ensure efficient operation, the membrane material has several functions to fulfill. In general, the desired properties of the membrane for fuel cell and electrolyser application include high proton conductivity, adequate thermal and mechanical strength, high chemical stability in the environment of operation, acting as a barrier to prohibit the mixing of reactant gasses and lastly, low cost [18,19]. Ultimately, the harsh environment prevailing during fuel cell and electrolyser operation determines the specific requirements of the membrane to ensure high efficiency and an acceptable life time. Thus, for improved performance, the proton conductivity and the durability of the membrane in terms of chemical, mechanical and thermal stability along with low costs are considered determining factors in the process of selecting appropriate PEM materials.

1.2 Problem statement

For the successful implementation of the HyS process, issues relating to the functionality and the development of stable polymers have to be addressed. Within the SO_2 electrolyser, the membrane forms an integral part of the system and should have a high chemical and thermal stability to withstand the harsh environment within the electrolyser, while having a high conductivity and selectivity towards proton transport. One of the challenges arising is the possible degradation of the PEM due to the presence of the concentrated H_2SO_4 within the electrolyser. Alternatively to the widely used perfluorosulfonic DuPont's Nafion® membranes, further research in the development of more cost-efficient membrane materials, as well as

membranes that can be used at temperatures >100 ºC, with improved functionality for SO_2 electrolysis and H_2SO_4 stability is required.

1.3 Aim and objectives

The aim of the study was to investigate the stability of a variety of PEM materials provided by the Kerres Group from the University of Stuttgart, Germany, in an H_2SO_4 environment. The stability of the membrane material was also compared with Nafion®212, which was included as a benchmark. Twenty five different blend membranes were investigated. For ease of the discussion, the membranes were divided into three groups according to the PBI component of the polymer, i.e. those materials that did not contain any PBI, those containing pure PBI and those containing partially fluorinated PBI.

For this study the characterisation of the membranes included determining the physical changes using weight and thickness change, and chemical changes using scanning electron microscopy (SEM) coupled EDX (elemental analysis), ion exchange capacity (IEC), Fourier Transform Infrared Spectroscopy (FTIR) in attenuated total reflection (ATR) mode and Thermo Gravimetric Analysis (TGA).

By determining which components contribute to the proton conductivity and chemical stability of the membrane within a SO_2 electrolyser environment, an improved membrane design with optimised chemical and mechanical properties can further be developed.

1.4 Outline of the dissertation

Chapter 1: Introduction
An overview of the energy demand is given showing hydrogen as an alternative, cleaner, more efficient and environmentally friendly energy source. Subsequently, the importance of the HyS process as a promising thermo-chemical cycle for the production of clean hydrogen from water is discussed. Finally, the challenges regarding the membrane material's stability within the identified H_2SO_4 environment are presented leading to the aim and objectives of the study and the outline of the dissertation.

Chapter 2: Literature study

A brief discussion of the PEMFC and SO_2 electrolyser, serving as introduction to the importance of the PEM material and desired properties for PEM fuel cell and electrolyser application, is presented, followed by the recent developments in membrane materials and known H_2SO_4 stability before discussing the analytical techniques employed for the characterisation of membranes in this study.

Chapter 3: Experimental methods

Before discussing the acid treatment, a composition table is provided in Chapter 3, summarising the membrane materials that were investigated in terms of their H_2SO_4 stability. The method and sample preparation requirements that were described for each analysis technique (used to investigate the acid stability) follow.

Chapter 4: Results and Discussion

In Chapter 4, the membrane's acid stability is evaluated based on the results obtained by the analytical techniques in terms of the three membrane groups mentioned in Section 1.3. The data from the analytical techniques presented in Chapter 3 will be used to investigate the mechanical, chemical and thermal degradations or changes the membranes underwent due to the H_2SO_4 treatment.

Chapter 5: Evaluation and recommendation

In the final chapter, the three separate membrane groups will be compared in terms of the presence and structure of the basic PBI-component, and the effect of the H_2SO_4 treatment on specific polymer structures present in the PEM blends. The research presented throughout the study will be reviewed and summarised in this chapter by identifying the main methods used and including a summarised evaluation thereof. Finally, recommendations for future studies on the membrane's acid stability are presented.

1.5 References

[1] X. Li, Principles of Fuel Cells., Taylor & Francis Group, New York, 2006, p. 1-2.

[2] K.D. Kreuer, On the development of proton conducting polymer membranes for hydrogen and methanol fuel cells., Journal of Membrane Science, 185 (2001) 29-39.

[3] L. Gubler, G.G. Scherer, A Proton-Conducting Polymer Membrane as Solid Electrolyte - Function and Required Properties., Springer, 2008, p. 1-14.

[4] J. Zhang, PEM fuel cell electrocatalysts and catalyst layers. Fundamentals and Applications., Gen Ed. Springer, 2008, p. 1137.

[5] R.L. Busby, Hydrogen and Fuel Cells: A Comprehensive Guide, 1st American ed., PennWell, Oklahoma, 2005.

[6] P. Sivasubramanian, R.P. Ramasamy, F.J. Freire, C.E. Holland, J.W. Weidner, Electrochemical hydrogen production from thermochemical cycles using a proton exchange membrane electrolyser., International Journal of Hydrogen Energy, 32 (2007) 463-468.

[7] M.B. Gorensek, J.A. Staser, T.G. Stanford, J.W. Weidner, A thermodynamic analysis of the SO2/H2SO4 system in SO2-depolarized electrolysis., International Journal of Hydrogen Energy, 34 (2009) 6089-6095.

[8] K. Zeng, D. Zhang, Recent progress in alkaline water electrolysis for hydrogen production and applications., Progress in Energy and Combustion Science, 36 (2010) 307-326.

[9] P. Hoffman, Tomorrow's Energy: Hydrogen, Fuel Cells, and the Prospects for a Cleaner Planet., The MIT Press: Cambridge, MA, 2001.

[10] H.R. Colon-Mercado, M.C. Elvington, D.T. Hobbs, FY08 Membrane Characterization Report for the hybrid Sulfur Electrolyzer., Contract Number DE-AC09-08SR22470, (2008).

[11] M.B. Gorensek, W.A. Summers, Hybrid sulfar flowsheets using PEM electrolysis and a bayonet decomposition reactor., International Journal of Hydrogen Energy, 34 (2009) 4097-4114.

[12] P. Millet, R. Ngameni, S.A. Grigoriev, N. Mbemba, F. Brisset, A. Ranjbari, C. Etiévant, PEM water electrolyzers: From electrocatalysis to stack development., International Journal of Hydrogen Energy, 35 (2010) 5043-5052.

[13] M.C. Elvington, H. Colon-Mercado, S. McCatty, S.G. Stone, D.T. Hobbs, Evaluation of proton-conducting membranes for use in a sulphur dioxide depolarized electrolyser., Journal of Power Sources, 195 (2010) 2823-2829.

[14] M.B. Gorensek, W.A. Summers, Hybrid sulfur flowsheets using PEM electrolysis and a bayonet decomposition reactor., International Journal of Hydrogen Energy, 34 (2008) 4097-4114.

[15] L.E. Brecher, S. Spewock, C.J. Warde, The Westinghouse Sulfur Cycle for the thermochemical decomposition of water., International Journal of Hydrogen Energy, 2 (1977) 7-15.
[16] J.V. Jayakumar, A. Gulledge, J.A. Staser, C. Kim, B.C. Benicewicz, J.W. Weidner, Polybenzimadazole Membranes for Hydrogen and Sulfuric Acid Production in the Hybrid Sulfur Electrolyzer., ECS Electrochemistry Letters, 1 (2012) F44-F48.
[17] H.R. Colòn-Mercado, D.T. Hobbs, Catalyst evaluation for a sulphur dioxidedepolarized electrolyzer., Electrochemistry Communications, 9 (2007) 2649-2653.
[18] T.J. Peckham, Y. Yang, S. Holdcroft, Proton Exchange Membranes., CRC Press, Boca Raton, London, New York, 2010.
[19] B. Smitha, S. Sridhar, A.A. Khan, Solid polymer electrolyte membranes for fuel cell applications- a review., Journal of Membrane Science, 259 (2005) 10-26.

Chapter 2: Literature study

Contents

2.1 Introduction 10

2.1.1 Membrane-based processes in the production of hydrogen 10

2.1.2 Properties of PEMs 14

2.2 PEM material development 18

2.2.1 Perfluorinated and partially fluorinated membranes 19

2.2.2 Non-fluorinated membrane materials 21

2.2.3 Blended membranes 23

2.3 PEM characterisation 28

2.3.1 Weight change 28

2.3.2 Change in thickness 28

2.3.3 SEM-EDX 28

2.3.4 IEC 29

2.3.5 FTIR 29

2.3.6 TGA 29

2.4 Conclusion 30

2.5 References 31

2.1 Introduction

The demand for cleaner, more environmentally friendly energy sources, alternatively to the traditional, known, depleting carbon based fuels, is growing. Lately, the development of more efficient methods for producing hydrogen, without contributing to global warming, has become a priority in the research world [1]. While hydrogen can be produced through various routes, the focus in Section 2.1.1 will be on membrane-based processes, with the attention on proton exchange membrane (PEM) based fuel cells and SO_2 electrolysis. A discussion on the importance of the polymer electrolyte and corresponding membrane requirements will follow in Section 2.1.2. Subsequently, the development of PEM materials for fuel cell application will be discussed in Section 2.2, focusing on the performance of existing PEM materials and a recent study completed on the stability in an H_2SO_4 environment. Lastly, the characterisation techniques that were used to investigate the stability of the membrane materials are discussed in Section 2.3.

2.1.1 Membrane-based processes in the production of hydrogen

Among the membrane-based processes, fuel cells are described as electrochemical devices that are able to convert the chemical energy of a supplied fuel and oxidant directly into electricity at high efficiencies. One reason for the high efficiency of fuels cells in comparison with internal combustion engines is related to the fact that the electrochemical process is not limited by the Carnot's cycle [2], making fuel cells attractive for application in transportation, portable and stationary electronic devices. A fuel cell needs no recharging, producing electrical power as long as the fuel in question is supplied.

A basic fuel cell consists of two electronically conducting gas diffusion electrodes, the fuel anode and oxidant cathode respectively, separated by an ionically conducting electrolyte. The membrane serves as a key component in the fuel cell not only as separator, but is responsible for the transport of protons from the anode to the cathode. The different fuel cells are distinguished from one another based on the type of the electrolyte and the temperature of operation [3]. Currently the most popular fuel cell used to generate electrical energy is the proton exchange membrane fuel cell (PEMFC) [4] with a polymer electrolyte in the form of a thin, permeable sheet.

2.1.1.1 PEM based fuel cell

The PEMFC is preferred to other fuel cells based on the perceived simple design, high power density operation at lower temperatures (~80 ^{0}C) and weight advantages [5,6], allowing, in combination with its high compatibility, a wide range of applications in portable as well as stationary systems [7]. The PEMFC is characterised by the use of a solid polymer electrolyte membrane, which forms an integral part of the fuel cell in allowing the transport of protons through the membrane. Both the transport of protons and water management of the fuel cell are crucial for efficient operation [2].

It is known that the type of fuel and the nature of the oxidant determine and restrict the operating conditions of a fuel cell [8]. Hydrogen or methanol can be used as fuel in the PEMFC system. For the purpose of this study we only elaborate on the use of hydrogen as fuel. In a PEMFC where hydrogen and oxygen are combined through an efficient electrochemical process, water vapour forms as the only by-product providing a clean and flameless process.

As illustrated in Figure 2.1, the hydrogen is supplied to the anodic side while the oxidant, oxygen, is supplied to the cathodic side of the membrane electrode assembly (MEA) within the fuel cell. A solid polymer electrolyte membrane is used to regulate the flow of ions, specifically protons, between the anode and cathode. The reactants are spatially separated and the electrons that flow between the fuel and oxidant are diverted for use in an external circuit, while the protons migrate across the membrane. When the electrons and protons reunite on the cathodic side of the MEA, water is formed as by-product in the presence of the supplied oxygen.

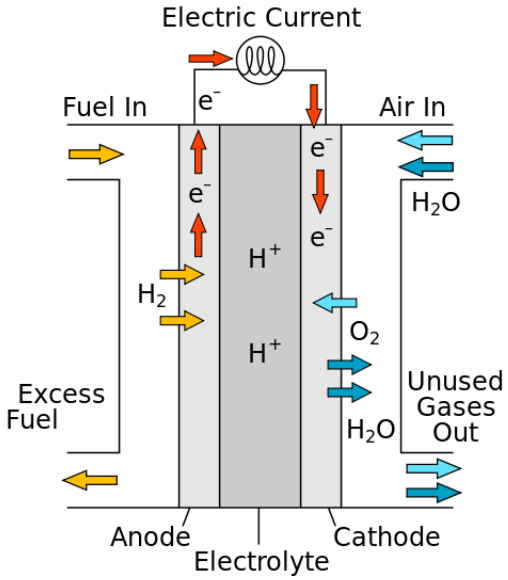

Figure 2.1: A schematic diagram of a PEM fuel cell [9].

2.1.1.2 SO_2 electrolyser

The reaction in a PEMFC is opposite from the process occurring in an H_2O electrolyser where energy and H_2O are used to produce H_2 and O_2 [10,11]. Water electrolysis is the most well-known membrane-based electrolyser process and has been extensively studied over recent years [12]. Pure hydrogen is obtained from the splitting of water by applying an electrical potential. However, a disadvantage of normal H_2O electrolysis is the low efficiency resulting from the high electrical voltage (E^{theo}=1.29 V) required for the conversion of H_2O into H_2 and O_2 [13]. To overcome this energetic disadvantage, various other thermo-chemical cycles have been proposed where additives are used to reduce the required voltage. For instance, the electrolysis of water in the presence of SO_2 results in a significant reduction in the potential required for the reaction (E^{theo}=0.158 V), giving this process a higher overall efficiency than normal H_2O electrolysis [13,14].

This sulfur based process where SO_2 is added to the H_2O electrolysis to reduce the potential required is currently the most promising thermo-chemical cycle [15]. Besides the better overall efficiency [13] in comparison with other thermodynamic cycles such as the sulfur iodine based cycle, the Hybrid Sulfur (HyS) process requires fewer reagents [16] while remaining a source of clean hydrogen [17]. The process first developed by the Westinghouse Electric Corporation in the 1970's [1] entails two steps. Firstly, SO_2, O_2 and H_2O are produced from the thermodynamic splitting (decomposition step) of H_2SO_4 at approximately 800 ^{0}C [18] as shown in Figure 2.2(a). The formed SO_2 is fed, together with water, to the anodic side of the membrane electrode assembly (MEA) in the PEM electrolyser in the second step (Figure 2.2(b)). The SO_2 is then electrochemically oxidised [17] at the anode side and subsequently protons and electrons (Equation 2.1) are produced. The protons migrate through the PEM, while the electrons are forced through the outer circuit. Protons and electrons are then united on the cathodic side of the MEA, reacting to produce H_2 and H_2SO_4 (Equation 2.2) [19,20]. The formed H_2SO_4 is then re-fed to the decomposition step, completing the cycle. The overall reaction (Equation 2.3) can be summarised as the cycling of water and SO_2 to the sulfur depolarized electrolyser (SDE) with the subsequent conversion to H_2 and H_2SO_4.

Anode reaction: $SO_2 + 2H_2O \rightarrow H_2SO_4 + 2H + 2e^-$ (2.1)

Cathode reaction: $2H^+ + 2e^- \rightarrow H_2$ (2.2)

Overall reaction: $2H_2O + SO_2 \rightarrow H_2 + H_2SO_4$ (2.3)

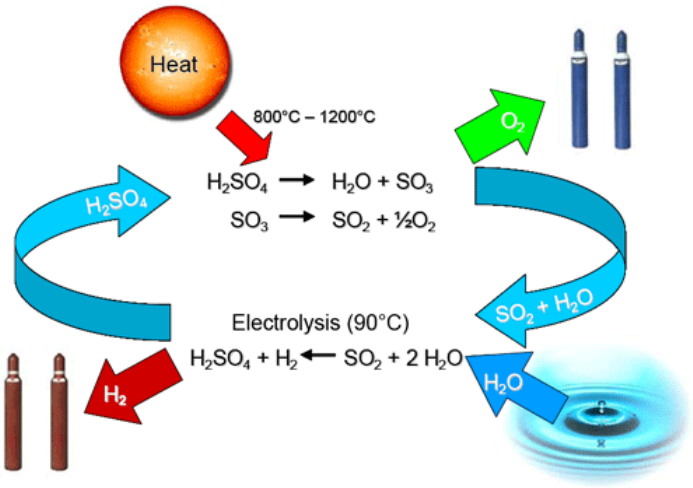

(a)

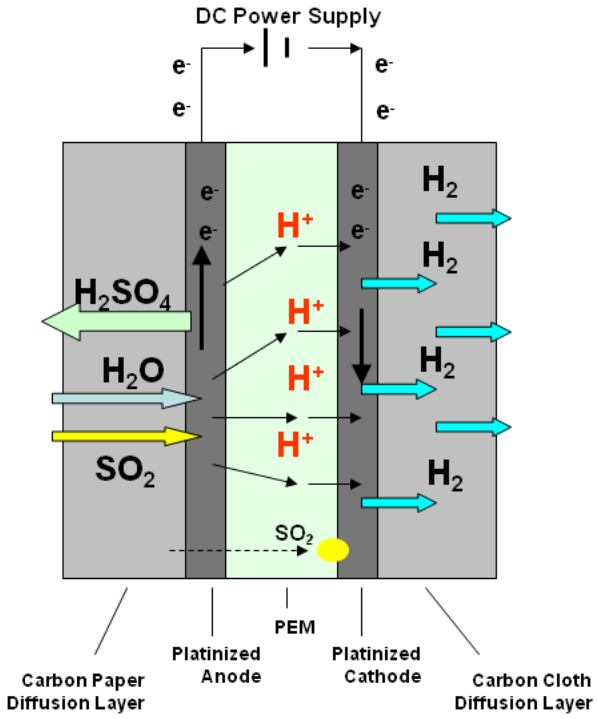

(b)

Figure 2.2: Schematic diagram of (a) the complete HyS cycle [21] and (b) the SO_2 electrolysis step [22].

As illustrated in Figure 2.2(b), it is possible that SO_2, along with the protons, can be carried across the PEM resulting in sulfur-based side reactions on the cathodic side of the MEA, ultimately resulting in SO_2 poisoning of the cathodic catalyst [20]. This results in an increase of the internal resistance of the MEA, resulting in more energy being required to maintain the

same hydrogen production process. Consequently, the efficiency of the SO_2 electrolyser is reduced. Another membrane related property results from the fact that the H_2SO_4 environment induced by the SO_2 electrolyser process may cause degradation of the PEM material. To date little has been published on the effect of the H_2SO_4 environment on membrane stability, while work has been done on the effect of H_2SO_4 on PBI-blended membrane materials [23].

2.1.2 Properties of PEMs

The membrane is an important constituent both for a PEM fuel cell and an electrolyser and crucial for efficient operation. The PEM material has several functions to fulfil to qualify as a possible candidate. Requirements of the membrane include the transport of protons over a wide range of temperatures and the ability to act as a barrier to prohibit and limit any crossover and subsequent mixing of reactant gases. The thermal and chemical stability along with mechanical robustness contributes to the membranes efficiency and life time. Lastly, the cost of the membrane is important to ensure commercial competitiveness. Ultimately, the lifetime of the fuel cell or electrolyser is limited by the membrane's stability in the harsh environment prevailing. Thus, for improved performance, further discussion on the required membrane properties will focus on proton conductivity and the durability of the membrane in terms of chemical and mechanical stability.

2.1.2.1 High Proton conductivity

Proton conductivity is considered a key parameter when evaluating membrane materials for fuel cell or electrolyser applications. This parameter is affected by the chemical structure and morphology of the membrane, acid strength, water content and temperature. In the development of better PEM materials, it is crucial to understand how these properties affect the proton conductivity.

The polymer microstructure and morphology are important factors that control the conductivity of PEMs. The protons dissociate and form hydronium ions (H_3O^+) in the presence of water, which acts as a proton solvent. For PEM materials such as Nafion®, a nano-phase-separated structure [24,25] is observed as hydrophilic and hydrophobic domains as shown in Figure 2.3. Proton conduction is thus limited to the water containing channels (hydrophilic domains) lined with the sulfonated counter-ions [26]. As a consequence, the water content strongly affects the proton mobility, while the hydrophilic domains are relied on to provide mechanical integrity to the membrane.

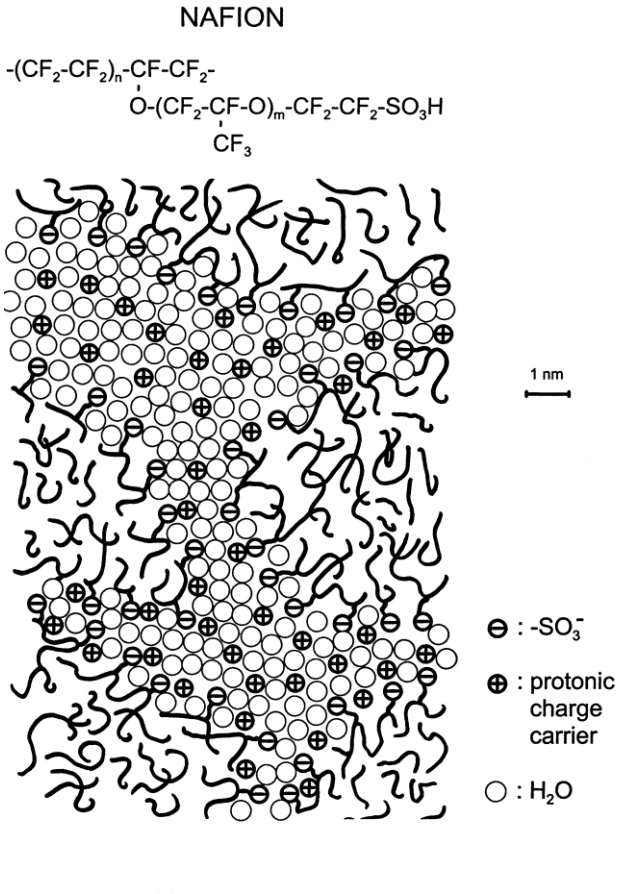

Figure 2.3: Nano-phase separated structure of Nafion® [27].

According to Peckham and Holdcroft [28], the transport of protons within these phase-separated systems (PEMs) occurs via a combination of mechanisms summarised in Figure 2.4. Firstly, movement by the vehicular mechanism is described as the diffusion of a solvated cation through the solution bound to a moving ‘‘vehicle’’ such as H_2O [29]. The protons produced in the fuel cell or electrolyser react with the water present, forming water-solvated species such as H_3O^+. Water then acts as facilitator in the diffusion of these hydronium ions across the membrane from a high to a low proton concentration [30].

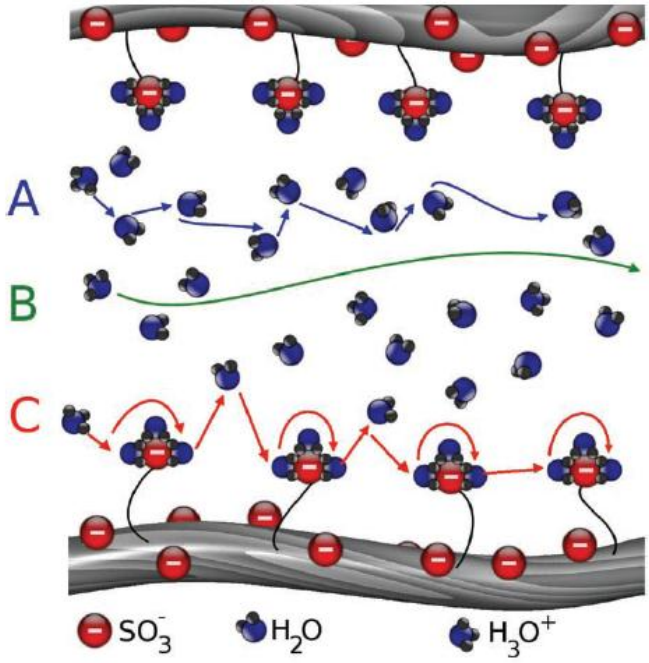

Figure 2.4: Possible modes of proton conduction in a phase-separated system summarised as A= Grotthus, B= vehicular, and C= surface mechanisms [28].

Protons transported through structural diffusion, also known as the Grotthus mechanism, are described by the migration of protons through the solution in Zundel and Eigen-complexes [31] as shown in Figure 2.5. In contrast to the vehicular mechanism, temporary hydronium ions are formed as the protons are passed from one water molecule to the neighbouring water molecule, relying on the breaking and forming of hydrogen bonds to act as the proton carriers.

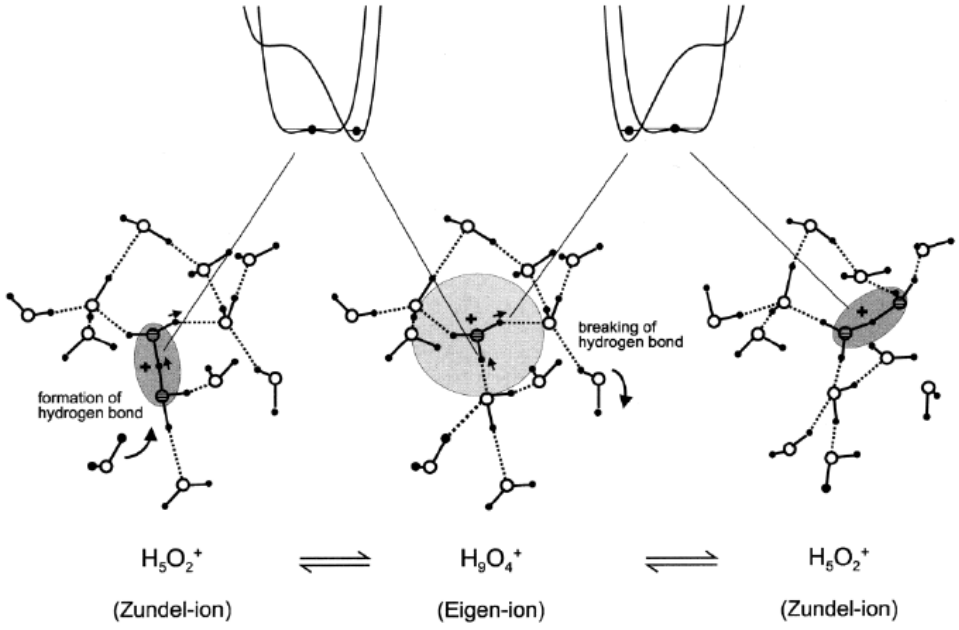

Figure 2.5: Proton conduction in water as described by the Grotthus mechanism [31].

Lastly, surface transport functions on the bound nature of the counter anion typically present as the $–SO_3^-$ species in sulfonic acid-based polymers. It is believed that the protons are transported between the $–SO_3^-$ groups found on the walls of the hydrophilic channels. Due to the high activation energy required for this model of transport, the mechanism only becomes evident as the water content decreases [28].

Proton transfer and conductivity in water tends to increase with the sulfonation of polymers and the subsequent increase of the polymer's hydrophilicity. The acid content (number of $–SO_3H$ groups present per gram of membrane) of a membrane can be determined by ion exchange capacity (IEC) measurements and is often used to characterise the proton conductivity of PEM materials.

2.1.2.2 Mechanical and thermo-mechanical properties

Fuel cell and electrolyser performance is affected by the mechanical and chemical properties of the membrane, while the lifetime of the fuel cell and electrolyser is dependent on the thermo-mechanical stability of the membrane, failure of which could result in the mixing of reactant gasses and a loss in conductivity [32]. The temperature and humidity necessary for fuel cell and electrolyser operation also affect the mechanical integrity of the membrane, along with the various degradation mechanisms prone to PEMs and are further discussed under chemical stability.

The thickness of the membrane is an important factor in managing the water crossover, conductivity and hydration of the membrane. Thinner membranes ensure rapid hydration, enhanced membrane conductivity and lower costs, but are limited by the compromise in mechanical strength. It has been suggested that specific conductivity can be sacrificed to the degree of sufficient mechanical strength and acceptable lifetime of thinner membranes (20-30 µm) [33]. For SO_2 electrolysis specifically, it has been shown that a higher water transport, due to the use of thinner membranes, results in a decrease in the acid concentration produced at the anode. However, apart from lowering the operation voltages, improved cell stability was also reported due to the decreased acid concentration [34].

2.1.2.3 Chemical stability

Chemical stability is important for enduring the harsh acidic environment and repeated thermal cycles, for example during the operation of a fuel cell. The stability of known PEM materials in an H_2SO_4 environment has to date not received much attention, limiting the available literature concerning the acid stability. It is believed that non-fluorinated membranes are more susceptible to chemical degradation than perfluoropolymers, due to the difference in bond strength reported

for the hydrogen-containing end groups in comparison with the bond strength of C-F bonds (410 and 460 kJ/ mol, respectively) [32].

The aromatic-based polymers, which are focussed on in this study, include poly(arylene ether), poly(ether ketone), and poly(ether sulfones). These polymers are considered most promising for the production of high-performance PEMs due to the associated low cost and commercial availability. In addition, improved proton conductivities along with high mechanical and thermal properties are achievable by the introduction of polar sites as pendant groups and sulfonation of the polymer structures [35,36]. However, pure sulfonated arylene membranes have the tendency to swell too much [37] and the possible hydrolysis of the aromatic ring's sulfonic acid group is troublesome, as it is well known that sulfonation is a reversible process in acidic environments at elevated temperatures [32]. Further investigation into the desulfonation process has indicated that, in the presence of an electron-withdrawing substituent, the sulfonic-acid bearing ring is prone to hydrolysis due to destabilisation of the aromatic sulfonic acid intermediate and the subsequent increase in hydrolytic ''stability'' [38]. Hydrolytic cleavage of the polymer backbone is also a concern as suggested by Iojoiu *et al*. [39] in the hydrolytic cleavage of the ether bond of aromatic-based PEMs.

2.2 PEM material development

The use of ion exchange membranes as solid electrolytes was reported as early as 1955 by General Electric (GE) and firstly described by William Thomas Grubb and Lee Niedrach in 1959 in the use of an organic cation exchange membrane [2]. In the interest of applying fuel cells as power sources in space, further development led to the production and testing of phenolic membranes [40]. Due to low power density ranging between 0.05 and 0.1 kW m^{-2}, low mechanical stability and a short lifetime, these membranes were, however, not suitable for fuel cell application, which led to the development of partially sulfonated poly(styrene sulfonic acid) membranes. Based on these membranes, the first PEMFC was built by GE during the mid-1960's to serve in the operational system of the GEMINI as a primary power source [41] with reported power densities of 0.4-0.6 kW m^{-2} [36]. In an attempt to further improve and address the brittleness exhibited by the poly(styrene sulfonic acid) membranes, they were replaced with the cross-linked polystyrene-divinyl benzene sulfonic acid membranes, but still insufficient proton conductivities were obtained [2]. Finally, in 1966, the perfluorinated Nafion® membrane was developed by Du Pont. This was regarded a breakthrough in the membrane development for PEM fuel cells as lifetimes up to 3 000 h and improved proton conductivity at lower current densities and temperatures of 50 ^{0}C were reported [36,42]. Since then the membrane

technology of Nafion® has developed greatly and is still regarded as the benchmark membrane [36] for use in PEM fuel cells as well as SO_2 electrolysers [18]. Simultaneously, other than the perfluorinated membranes, materials such as the sulfonated arylene main-chain ionomer membranes [43,44] and acid-base blends have received considerable attention and will further be discussed in terms of suitability for application within an SO_2 electrolyser.

2.2.1 Perfluorinated and partially fluorinated membranes

The perfluorocarbon based polymers are regarded as the most successful systems thus far to be implemented in the PEM technology of portable, stationary and commercial automotive applications [32]. In addition to reliable and good performance, perfluorosulfonic acid (PFSA) based polymers have proven highly durable and resistant to radically induced chemical degradation due to the strong C-F bonds present.

First in the class of perfluorinated ionomers, Nafion® was discovered by Dr. Walter Gustav Grot of DuPont and generated by the copolymerisation of tetrafluoroethylene (TFE) with a perfluorinated vinyl ether as comonomer [24]. Characteristically the polymer backbone is fluorinated and either consists of polytetrafluoroethylene (PTFE) or Teflon® with polyvinyl ether side chains and $–SO_3H$ ion exchange groups located at the endpoints as shown in Figure 2.6. The fluorinated nature gives Nafion® the ability to withstand harsh chemical environments while maintaining high mechanical strength and proton conductivity [45].

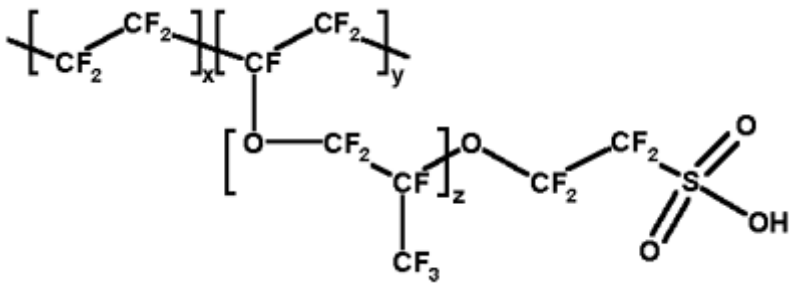

Figure 2.6: Nafion® structure [46].

Although Nafion® is still considered to be the benchmark membrane for fuel cell applications due to reported chemical stability and high proton conductivity at fairly high operating temperatures [18,47], a major disadvantage of PFSA based membranes is the high cost associated with the production of these materials. Other disadvantages, as reported by Smitha *et al*. [36], include safety concerns during the manufacturing process and the requirements of supporting equipment for the use of PFSA membranes. Lastly, the reported water loss and decreased mechanical strength of PFSA membranes at temperatures above 80 ^{0}C [48] limits application at elevated temperatures as would for example be appropriate for SO_2 electrolysis. It is known that the performance of PEM fuel cells are greatly influenced by temperature, pressure and relative humidity [36]. The effects of different operating parameters on the PEMFC were experimentally studied by Wang *et al*. [49], who confirmed that an increase in operating temperature and pressure improves the PEM fuel cell's performance, making the replacement of Nafion® with alternative membranes in the future for more efficient fuel cell operation likely [50]. Research into alternative materials is underway [37,51,52].

Considering the cost, difficulty of synthesising perfluorocarbon-based monomers and the polymer's temperature sensitivity, partially fluorinated polymers have received interest in recent years [32]. For example, the partially fluorinated polymer, sFS (Figure 2.7), was investigated as a potential sulfonated blend component which showed excellent hydrolysis stability when compared to Nafion® [53]. The high molecular weight (M_W) obtained by the polycondensation of decafluorobiphenyl and bisphenol A for the sFS polymer, ensured sufficient mechanical strength and an enhanced operational durability. The high thermal stability reported was likely due to the high M_W of the polymer.

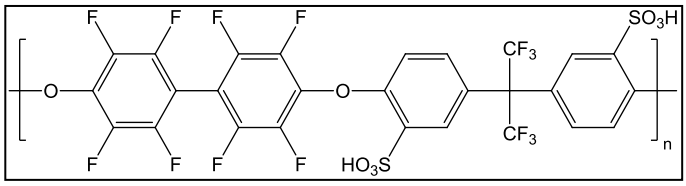

Figure 2.7: Partially fluorinated sulfonated polymer, sFS [53].

A study completed on the H_2SO_4 stability of the pure sFS polymer reported the dissolution of membrane fragments and a subsequent brittle, wrinkled appearance after a 30 and 60 wt% H_2SO_4 treatment [22]. The same study indicated a sulfonation of the polymer in a 90 wt% H_2SO_4 treatment illustrating the unstable character of the sFS membranes developed thus far in an H_2SO_4 environment.

2.2.2 Non-fluorinated membrane materials

This category of PEM materials broadly includes all membranes containing non-fluorinated backbones thus being hydrocarbon based. In most cases the membrane's backbones are functionalised by the introduction of sulfonic acid groups in an attempt to enhance proton-conducting properties, as the addition of the $-SO_3H$ groups to the polymer structure will result in an increased water uptake and improved proton conductivity.

Hydrocarbon-based polymers represent a large group of membrane materials of which the polyaromatics are favoured above other systems like polyesters for fuel cell application, due to their high thermal stability in comparison to the instability of the ester group in aqueous acids [36]. These speciality polymers also exhibited a high chemical stability in acidic, oxidising and reducing environments [54]. Within the polyaromatics, the polyarylene membrane group has received considerable attention in the development of various systems [32]. In the scope of this study the membrane material of interest, containing non-fluorinated backbones, will further be discussed under this group.

Polyarylene systems are characterised by the aryl or heteroaryl ring that is present in the main chain polymer. Polyarylenes are considered high temperature rigid polymers and report a T_g > 200 ^{0}C due to the presence of inflexible and bulky aromatic groups on the polymer backbone [55]. They were developed, with the expectation of improving the thermal, mechanical and oxidative stability found within the polystyrene-based membrane materials [35], by incorporating aromatic hydrocarbons directly into the polymer backbone thereby increasing their stability. Both electrophilic and aromatic substitution of the aromatic ring are possible and therefore sulfonated poly(ether ether ketone) (sPEEK), poly(ether sulfones) (PSU), poly(arylene ethers), polyesters and polyamides (PI) can be synthesised and are considered examples of main chain polyarylenes [36]. Both PEEK and PSU materials have been considered as substitutes for Nafion® in PEMFC applications due to their chemical stability [56]. The structures of sPEEK [57] and sPSU [58] are presented in Figure 2.8.

(a)

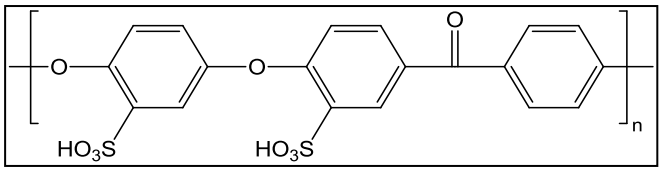

(b)

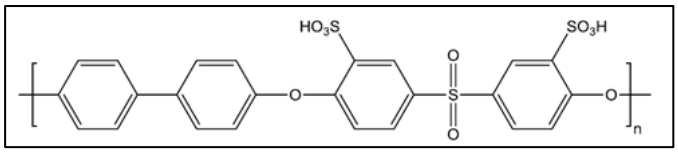

Figure 2.8: Structure of (a) the sPEEK and (b) the sPSU polymer.

The sPEEK polymer is an archetypical example of the sulfonated poly(arylene ether) group whereof the base polymer is readily available and cheap. The sulfonation procedure is easily performed with concentrated sulfuric acid, and when sufficient, ensures comparable or even higher proton conductivity values than Nafion® [59]. However, the statistical distribution of the sulfonic acid groups along the main chain creates a greater dependence upon water content in comparison to Nafion® for effective proton conduction [60]. Due to the good thermal stability and mechanical properties along with adequate conductivity [2,41], sPEEK is considered promising for fuel cell application. However, the proton conductivity and chemical durability of sPEEK reported at low relative humidity (RH) operation calls for improvement [2]. Also the stability of sPEEK in an SO_2 electrolyser environment has yet to be investigated.

The commercial processability and availability of the polysulfone (PSU) polymer and the accompanying low cost are favourable properties, but the proton conductivity in comparison with Nafion® is lower [2]. This can be attributed to the large phase-separation and hydrophobicity characteristic of the C-F chains present in Nafion®. The sulfonated PSU membrane was investigated in different concentrations of H_2SO_4 [23] and it was determined that the membrane only dissolved at a 90 wt% H_2SO_4 which was ascribed to sulfonation. It implies that this membrane could be suitable for SO_2 electrolysis as the H_2SO_4 concentrations rarely exceed 30-40 wt% in the electrolyser during operation [23].

The aromatic polybenzimidazole (PBI), as shown in Figure 2.9 [61], polymers are considered highly favourable for fuel cell application due to excellent thermal and mechanical properties. These heterocyclic polymers are inexpensive with proven chemical resistance in different environments [62]. The proton conducting properties of PBI are based on the (-NH-) and (-N=) basic functional groups of the imidazole ring, allowing proton migration and specific interactions

in blend membranes. In an H_2SO_4 stability study, the PBI membrane indicated the likeliness to form imidazolium hydrogen sulfate salts at lower H_2SO_4 concentrations, dissolving at a 90 wt% concentration due to direct sulfonation of the membrane backbone [22]. Blended sPSU-PBI and sFS-PBI were investigated in the same study and an improved stability in the H_2SO_4 environment was reported.

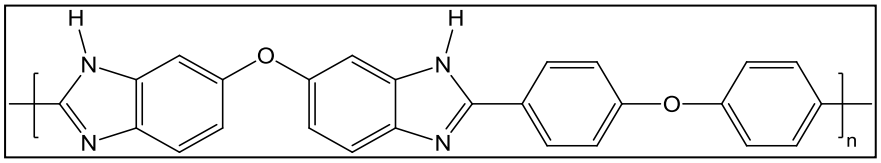

Figure 2.9: Basic structure of PBI [61].

2.2.3 Blended membranes

In an attempt to develop a membrane system combining stability and efficient proton transfer, the blending of two or more polymers has been suggested [37]. For example, an acid-base blend can provide an alternative for the polymer membranes where high conductivity is accompanied by dehydration effects. However, in order to develop novel PEM materials with the required membrane properties for optimal operation, the interaction between blend components have to be considered to ensure compatibility and subsequent miscibility. Chemical bonds can be introduced between the macromolecules to improve the mechanical and thermal stability as well as the homogeneity of the membranes [63]. This is evaluated by determining the impact of the various physical interactions that might occur between macromolecules and their influence on the polymer's structure and subsequently the membrane's stability. The different types of interactions present in polymers include van-der-Waals, dipole-dipole and electrostatic interactions (ionical cross-linking), hydrogen bridges and covalent cross-linking. Various ionomer systems containing these interaction forces between blend components have since been developed and the less successful blend types identified. In an attempt to develop novel ionomer membranes, Kerres *et al*. [37] concluded that van-der-Waals and dipole-dipole forces were too weak to ensure blend compatibility on their own. Poor mechanical stability due to high swelling was reported for the blend of unmodified and sulfonated PSU investigated. It was also found that blends solely relying on hydrogen-bridge interaction forces showed signs of incompatibility and reported an increase in swelling at elevated temperatures, followed by the dissolution of the membrane at temperatures exceeding 90 ^{0}C [37]. Acid-base polymer blends

containing interactions such as covalent cross-linking, ionical cross-linking and/ or hydrogen bonding bridges separately and in combination have proven to considerably reduce membrane swelling and improve mechanical and thermal stabilities [37,64]. Different acid-base complexes and blends that have been considered as promising alternatives to perfluorinated membranes (commercially available PEMs) will be included in the discussion under ionically, covalent and covalent-ionically cross-linked blends.

2.2.3.1 Ionically cross-linked acid-base blends

For the purpose of developing improved PEM materials, acid-base complexes that entail the integration of an acid component into an alkaline polymer base or simply by mixing a polymeric acid and base, have shown to be worthwhile alternatives [36,63] to Nafion®. The phosphoric acid-doped PBI (PBI/H_3PO_4) has been extensively researched and characterised in recent years due to its proven success in high temperature fuel cell applications [65]. Hasiotis *et al*. [66] for example, reported improved conductivities and mechanical properties for their sPSU-PBI blended membrane doped with H_3PO_4 in comparison with an unblended PBI/H_3PO_4 membrane under the same conditions.

Kerres *et al*. [37] have shown that blends containing a polysulfonate and polybase had improved thermal and mechanical stabilities compared to the sulfonated polymer alone. The mentioned improved properties can be ascribed to the ionic cross-links forming between the acidic and basic sites of the polymer components, as shown in Figure 2.10 [37]. The donation of protons from the acidic to basic sites results in the formation of hydrogen bonds and electrostatic forces (ionical cross-linking) between blend components, which lead to blend membranes reporting high proton conductivity, reduced crossover, low water uptake, good thermal stability and high mechanical strength [64].

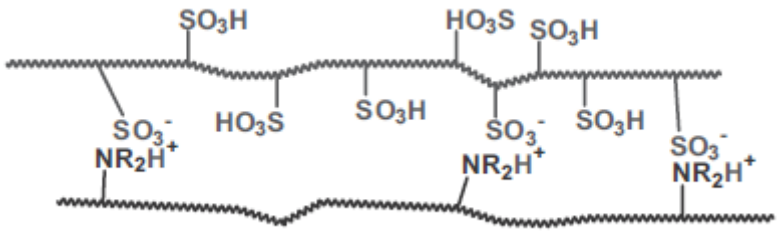

Figure 2.10: Schematic of the electrostatic interactions possible in ionically cross-linked acid-base blended membranes [37].

Wu *et al*. [63] attempted to improve the dimensional instability of the sulfonated poly (2,6-dimethyl-1,4-phenylene oxide) (sPPO) membrane by adding (3-aminopropyl) triethoxysilane (A1100) as inorganic component to establish acid-base interactions (ionical cross-linking and hydrogen bonding bridges) between the $–SO_3H$ groups of sPPO and the NH_2 groups of A1100. A homogeneous blend membrane was subsequently obtained with improved thermal and dimensional stabilities.

While various other acid-base polymer blends have since been studied [67-69], particularly blends where PBI was present as the basic polymer component are promising [70]. Due to the acid-base interactions forming between the benzimidazole groups of PBI and the acids, reduced swelling [71] and high proton conductivities at elevated temperatures [72] have been reported for PBI-blended membranes. The ionical cross-linking of PBI has also proven to effectively enhance the stability of linear PBI as determined by Li. *et al*. [65] in the monitoring of the membrane's degradation (weight loss) in an H_2O_2 environment over 120 h yielding stabilities that are comparable to Nafion®117.

A known disadvantage associated with acid-base blends is the reported swelling at temperatures between 70 and 90 ^0C due to the breaking of hydrogen bridges and electrostatic interactions (ionic bonds) in an aqueous environment [37,58]. The mechanical stability is greatly affected by the swelling which can contribute to the possible destruction of the blend membrane. In an attempt to address the problem, covalent cross-linking was suggested [37,73,74] and since developed by various research groups.

2.2.3.2 Covalently cross-linked blend membranes

In an effort to reduce the swelling associated with ionically cross-linked blend membranes, covalently cross-linked procedures yielding high chemical stability in an acidic environment were developed by Kerres *et al*. [37], leading to the development of two different covalently cross-linked membrane types.

Firstly, a blend type was prepared by dissolving both a sulfonated and a sulfinated polymer in the same solvent and adding a cross-linker. A broad range of properties were obtained by variation of the blend components, mass relation and cross-linker used. According to their results, the covalent network consists of the sulfinated polymer and cross-linker, while the polysulfonate macromolecules were found physically entangled within the network as illustrated in Figure 2.11(a). However, due to the low cross-linking density of this type of network, the polysulfonate macromolecules can easily diffuse from the network, leading to a loss in membrane constituents and the subsequent degradation of the membrane.

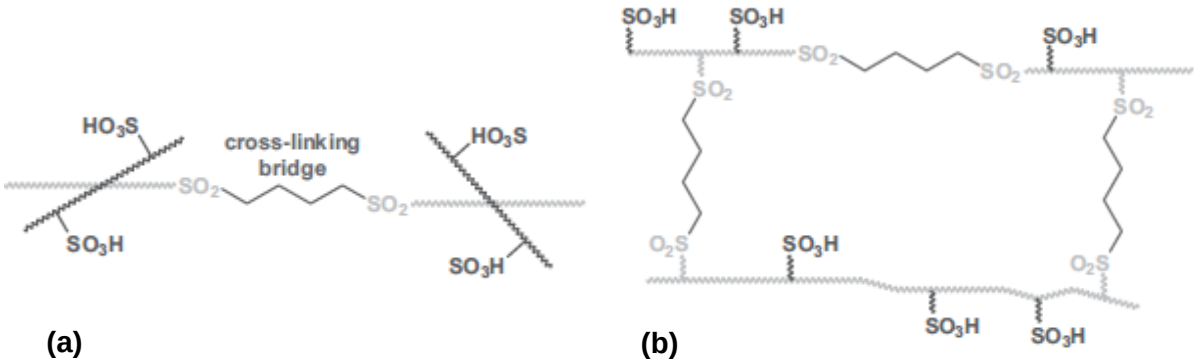

Figure 2.11: Covalently cross-linked membrane types 1 (a) and 2 (b) [37].

The second type consists of a polymer containing both the sulfonate and sulfinate groups on the same backbone as shown in Figure 2.11(b). Although the synthesis is more complicated, all macromolecules are involved in the network and diffusion of the sulfonated component is limited.

More recently Zhang *et al*. [75] developed covalently cross-linked sulfonated copolyimide (sPI) membranes containing benzimidazole groups. The covalent cross-linking used part of the $–SO_3H$ group as cross-linkable group, resulting in the formation of a highly stable sulfonyl group as illustrated in Figure 2.12. It was found that the cooperative effect of the covalent cross-linking and benzimidazole groups significantly enhanced the oxidative stability of the membranes.

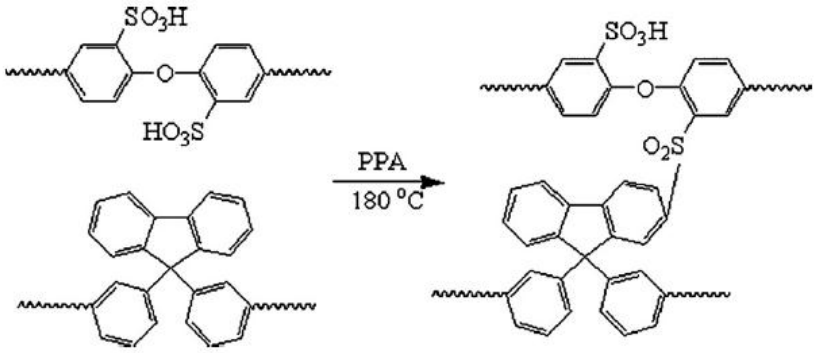

Figure 2.12: Covalent cross-linking of sPI resulting in highly stable sulfonyl groups [75].

However, during these type of covalent cross-linking processes, $–SO_3H$ groups are consumed, which leads to a decrease in the IECs and proton conductivities of the blended membranes [73,74]. Zhao and co-workers [76] addressed this problem by blending a sulfonated poly(arylene ether ketone) bearing carboxylic acid groups (SPAEK-C) with an o-diamino functional polybenzimidazole oligomer (PBI) where –COOH groups were involved in the cross-linking reaction instead of the $–SO_3H$ groups. Subsequently, the conductivity was only minimally affected resulting in a H_3PO_4 doped SPAEK-C/PBI blend membrane with reported proton conductivities comparable to Nafion®117.

2.2.3.3 Covalent-ionically cross-linked blend membranes

In an attempt to address the identified disadvantages of both the ionically and covalently cross-linked membranes, while maintaining the discussed advantages, combinations of these cross-linking types have been considered. The covalent-ionically cross-linked network as suggested by Kerres *et al*. [37] is illustrated in Figure 2.13. Various different membrane blend types have been investigated by Kerres *et al*. [37] and it was found that the incompatibility of suggested polysulfinate and polyamine blends could be limited by statistically distributing the different types of functional groups on the same polymer backbone. In another instance it was shown that, for a covalent-ionically cross-linked blended membrane of sulfonated-sulfinated PEEK and PSU base, containing tertiary basic N groups, the thermal stability and proton conductivity improved when compared with the purely covalent and ionically cross-linked membranes [77].

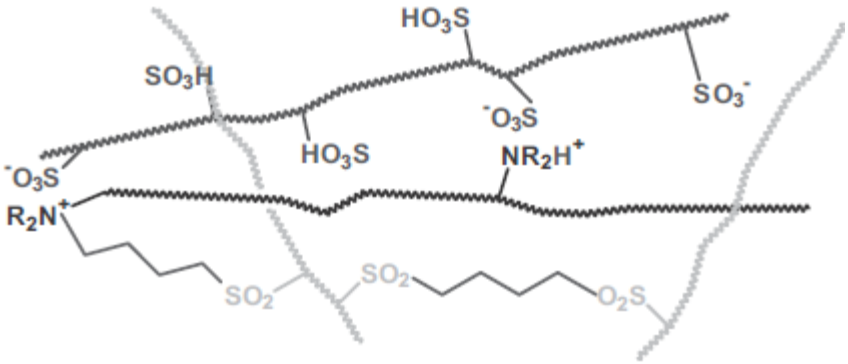

Figure 2.13: Structure of the suggested covalent-ionically cross-linked network [37].

In another study, Wang *et al*. [78] proposed a covalent-ionic network by cross-linking a carboxylic acid group bearing sPEEK (C-sPEEK) polymer with an amino-group-containing a PEEK (Am-PEEK) polymer. Improved oxidative stability and reduced swelling in addition to

enhanced thermal and mechanical stabilities were reported in comparison with the purely cross-linked membranes. Similarly, it was shown that the covalent-ionically cross-linked water soluble sulfonated–sulfinated poly(oxa-*p*-phenylene-3,3-phthalido-*p*-phenylene-oxa-*p*-phenylene-oxy phenylene) (SsPEEK-WC) membrane displayed significantly less water uptake and methanol permeability when compared to the solely covalent cross-linked PEEK-WC membrane [79].

In view of the studies that have been conducted in the field of blended and cross-linked membranes, it can be concluded that a wide variety of properties are attainable for covalent-ionically cross-linked (blend) membranes by variation of the acidic, basic and cross-linking components.

2.3 PEM characterisation

2.3.1 Weight change

The weight change is a physical measurement used to roughly evaluate the stability of the membrane materials in the subjected acidic environment. A large change in wt% can, before further characterisation, be used to determine whether the membranes underwent degradation due to the H_2SO_4 exposure. Further analytical studies can be used in support to investigate and describe the chemical changes the membrane material might have undergone.

2.3.2 Change in thickness

Another physical measurement used to obtain a rough estimate of the effect of the H_2SO_4 treatment on the membrane's stability is to monitor the change in thickness after treatment. Large changes reported in the thickness due to swelling during treatment may indicate a loss in mechanical stability and prove the membrane unsuitable for further applications [80].

2.3.3 SEM-EDX

Scanning electron microscopy (SEM) is used to examine the surface area or cross-section of the membrane under investigation by providing a three dimensional image of the inspected area. Visual images provided by the SEM can be used to indicate possible changes to the membrane due to the H_2SO_4 treatment. The energy dispersive X-ray spectroscopy analysis

(EDX) coupled to the SEM instrument provides a spectra of peaks which corresponds to the elemental composition of the sample area analysed [81]. With reference to characterisation work completed by Schoeman [22], it was suggested that the sulfur levels, relative to other elements found within the membrane material, could offer some insight into the effect of the H_2SO_4 treatment on the membrane.

2.3.4 IEC

The ion exchange capacity (IEC) gives the amount of ion-exchange groups, in this case the number of $-SO_3H$ groups, present per weight unit of dry membrane [meq/g] [82]. The amount of $-SO_3H$ groups, as determined by acid-base titrations [83], can be directly related to the proton conductivity of the membrane. The determined IEC_{total} provides information on all the $-SO_3H$ groups involved in the ionical cross-linking of the blend, while the IEC_{direct} represents only the $-SO_3H$ groups in the ionically cross-linked membranes where the protons contribute to the proton conductivity [82].

2.3.5 FTIR

The FTIR in attenuated total reflection (ATR) mode is used to determine whether the membrane underwent significant change in its chemical structure after the H_2SO_4 treatment by monitoring the amount and type of functional groups observable in the spectra. It is known that the intensity of an absorption band is directly related to the number of specific bonds present [84,85] and a change in the intensity observed is likely indicative of degradation (loss of membrane fragments) or sulfonation of the membrane.

2.3.6 TGA

Thermogravimetry (TGA) is a thermal analysis used to study the degradation of a sample by recording the change of mass as a function of time and temperature. Within the scope of this study the effect of the H_2SO_4 treatment on the thermal stability of the membrane material will be monitored by comparison of the obtained TGA signals.

2.4 Conclusion

The need for alternative energy sources in view of the depleting, environmentally hazardous fossil fuels have received significant attention over the years. Now, more than ever, scientists in various fields are searching for more efficient and more environmentally friendly sources. Hydrogen has been identified as such a source, or rather energy carrier, that can be produced via clean and non-polluting methods. Electrolysers offer the possibility of producing clean hydrogen through various processes, of which the Hybrid Sulfur thermo-chemical process currently seems most promising. The higher overall efficiency of the HyS process has drawn attention to the production of hydrogen in an SO_2 electrolyser.

The proton exchange membrane is considered an important fuel cell or electrolyser component which is crucial for efficient operation. High proton conductivity, durability, excellent barrier properties and low cost are considered desirable in the membrane material. Over the years, various membrane materials have been developed with the ideal of replacing the benchmark commercially available Nafion® membrane. Recently, different blended membranes have been synthesised with the hope of addressing the identified limitations of Nafion®. Due to the presence of H_2SO_4 in the SO_2 electrolyser, the chemical stability of the membrane becomes pertinent as well as the ability to prohibit SO_2 crossover. In order to determine whether membranes are suitable for SO_2 electrolysis, their stability in an H_2SO_4 environment could be investigated, where various characterisation techniques, including weight and thickness change, SEM-EDX, IEC, FTIR and TGA, could be used to monitor the influence of the H_2SO_4.

2.5 References

[1] P. Sivasubramanian, R.P. Ramasamy, F.J. Freire, C.E. Holland, J.W. Weidner, Electrochemical hydrogen production from thermochemical cycles using a proton exchange membrane electrolyser., International Journal of Hydrogen Energy, 32 (2007) 463-468.

[2] P. Trogadas, V. Ramani, Membrane and MEA Development in Polymer Electrolyte Fuel Cells., Springer, New York, 2009, p. 253-280.

[3] L. Gubler, G.G. Scherer, A Proton-Conducting Polymer Membrane as Solid Electrolyte - Function and Required Properties., Springer, 2008, p. 1-14.

[4] J. Zhang, PEM fuel cell electrocatalysts and catalyst layers. Fundamentals and Applications., Gen Ed. Springer, 2008, p. 1137.

[5] C. Wieser, Novel Polymer Electrolyte Membranes for Automotive Applications – Requirements and Benefits., Fuel Cells, 4 (2004) 245-250.

[6] V. Guarau, F. Barbir, H. Liu, An Analytical Solution of a Half-Cell Model for PEM Fuel Cells., Journal of Electrochemical Society, 147 (2000) 2468-2477.

[7] A.J. Appleby, F.R. Foulkes, EG & G Technical Services Inc. Science Application International Corporation, Fuel Cell Handbook., US Department of Energy, 2002, p. 82.

[8] W. Vielstich, H.A. Gasteiger, A. Lamm, Handbook of Fuel Cells- Fundamentals, Technology and Application., John Wiley & Sons, Chichester, 2003.

[9] R. Dervisoglu, In: Wikimedia Commons, Fuel Cell Schematic, Diagram of a proton conducting solid oxide fuel cell. http://en.wikipedia.org/wiki/File: Solid_oxide_fuel_cell_protonic.svg

[10] L. Ma, S. Sui, Y. Zhai, Investigations on high performance proton exchange membrane water electrolyzer., International Journal of Hydrogen Energy, 34 (2009) 678-684.

[11] G. Wei, Y. Wang, C. Huang, Q. Gao, Z. Wang, L. Xu, The stability of MEA in SPE water electrolysis for hydrogen production., International Journal of Hydrogen Energy, 35 (2010) 3951-3957.

[12] C. Stone, A.E. Morrison, From curiosity to “power to change the world®”., Solid State Ionics, 152–153 (2002) 1-13.

[13] H.R. Colòn-Mercado, D.T. Hobbs, Catalyst evaluation for a sulphur dioxidedepolarized electrolyzer., Electrochemistry Communications, 9 (2007) 2649-2653.

[14] T.L. Gibson, N.A. Kelly, Predicting efficiency of solar powered hydrogen generation using photovoltaic-electrolysis devices., International Journal of Hydrogen Energy, 35 (2010) 900-911.

[15] M.B. Gorensek, W.A. Summers, Hybrid sulfar flowsheets using PEM electrolysis and a bayonet decomposition reactor., International Journal of Hydrogen Energy, 34 (2009) 4097-4114.

[16] S. Charton, J. Janvier, P. Rivalier, E. Chainet, J. Caire, Hybrid sulfur cycle for H2 production: A sensitivity study of the electrolysis step in a filter-press cell., International Journal of Hydrogen Energy, 35 (2010) 1537-1547.
[17] M.B. Gorensek, J.A. Staser, T.G. Stanford, J.W. Weidner, A thermodynamic analysis of the SO2/H2SO4 system in SO2-depolarized electrolysis., International Journal of Hydrogen Energy, 34 (2009) 6089-6095.
[18] M.C. Elvington, H. Colon-Mercado, S. McCatty, S.G. Stone, D.T. Hobbs, Evaluation of proton-conducting membranes for use in a sulphur dioxide depolarized electrolyser., Journal of Power Sources, 195 (2010) 2823-2829.
[19] M.B. Gorensek, W.A. Summers, Hybrid sulfur flowsheets using PEM electrolysis and a bayonet decomposition reactor., International Journal of Hydrogen Energy, 34 (2008) 4097-4114.
[20] J.A. O'Brien, J.T. Hinkley, S.W. Donne, S. Lindquist, The electrochemical oxidation of aqueous sulfur dioxide: A critical review of work with respect to the hybrid sulphur cycle., Electrochemica acta, 55 (2010) 573-591.
[21] E. Zürich, Sulphur-based water-splitting thermochemical cycles, In: Departement of Mechanical and Process Engineering, Reaction scheme of the HyS thermochemical cycle. http://www.pre.ethz.ch/research/projects/?id=hycycles
[22] H. Schoeman, H2SO4 stability of PBI-blend membranes for SO2 electrolysis., MSc dissertation, Faculty of Natural Science, Focus Area: Chemical Resource Beneficiation, North-West University, Potchefstroom 2520, South Africa, 2011.
[23] H. Schoeman, H.M. Krieg, A.J. Kruger, A. Chromik, K. Krajinovic, J. Kerres, H2SO4 stability of PBI-blend membranes for SO2 electrolysis., International Journal of Hydrogen Energy, 37 (2012) 603-614.
[24] K.A. Mauritz, R.B. Moore, State of Understanding of Nafion., Chemical reviews, 104 (2004) 4535-4585.
[25] K. Schmidt-Rohr, Q. Chen, Parallel cylindrical water nanochannels in Nafion fuel-cell membranes., Nature Materials, 7 (2008) 75-83.
[26] L. Gubler, G.G. Scherer, Trends for fuel cell membrane development., Desalination, 250 (2010) 1034-1037.
[27] K.D. Kreuer, On the development of proton conducting polymer membranes for hydrogen and methanol fuel cells., Journal of Membrane Science, 185 (2001) 29-39.
[28] T.J. Peckham, S. Holdcroft, Structure-Morphology-Property Relationships of Non-Perfluorinated Proton-Conducting Membranes., Advanced Materials, 22 (2010) 4667-4690.
[29] K.D. Kreuer, A. Rabenau, W. Weppner, Vehicle Mechanism, A New Model for the Interpretation of the Conductivity of Fast Proton Conductors., Angewandte Chemistry International Edition English, 21 (1982) 208-209.

[30] X. Li, K. Jioa, Water transport in polymer electrolyte membrane fuel cells., Progress in energy and combustion science, 37 (2011) 221-291.
[31] K.D. Kreuer, S.J. Paddison, E. Spohr, M. Schuster, Transport in proton conductors for fuel-cell applications: Simulations, elementary reactions, and phenomenology., Chemical reviews, 104 (2004) 4637-4678.
[32] T.J. Peckham, Y. Yang, S. Holdcroft, Proton Exchange Membranes., CRC Press, Boca Raton, London, New York, 2010, p. 107-189.
[33] C. Wieser, Novel polymer electrolyte membranes for automotive applications - Requirements and benefits., Fuel Cells, 4 (2004) 245-250.
[34] J.A. Staser, J.W. Weidner, Effect of Water Transport on the Production of Hydrogen and Sulfuric Acid in a PEM Electrolyzer., Journal of Electrochemical Society, 156 (2009) B16-B21.
[35] J. Kerres, Development of ionomer membranes for fuel cells., Journal of Membrane Science, 185 (2001) 3-27.
[36] B. Smitha, S. Sridhar, A.A. Khan, Solid polymer electrolyte membranes for fuel cell applications- a review., Journal of Membrane Science, 259 (2005) 10-26.
[37] J. Kerres, Blended and Cross-Linked Ionimer Membrane for Appliction in Membrane Fuel Cells., Fuel Cells, 2 (2005) 230-247.
[38] M. Schuster, K.D. Kreuer, H.T. Andersen, J. Maier, Sulfonated Poly(phenylene sulfone) Polymers as Hydrolitically and Thermooxidatively Stable Proton Conducting Ionomers., Macromolecules, 40 (2006) 598-607.
[39] C. Iojoiu, M. Marechal, F. Chabert, J.Y. Sanchez, Mastering Sulfonation of Aromatic Polysulfones: Crucial for Membranes for Fuel Cell Application., Fuel Cells, 5 (2005) 344-354.
[40] K. Kordesch, G. Simader, Fuel Cells and Their Application., VCH Publishers, New York, 1996.
[41] M. Rikukawa, K. Sanui, Proton-conducting polymer electrolyte membranes based on hydrocarbon polymers., Progress Polymer Science, 25 (2000) 1463-1502.
[42] A.E. Steck, Membrane materials in fuel cells, In: First International Symposium on New Materials for Electrochemical systems., Montreal, 1995, p. 74-94.
[43] C. Hartnig, L. Jörissen, J. Kerres, W. Lehnert, J. Scholta, Materials for fuel cells 1st ed., CRC Press & Cambridge: Woodhead Publishing Ltd., Boca Raton, New York, Boston, Washington DC, 2008, p. 101-184.
[44] J. Kerres, F. Schönberger, Chapter III: Proton exchange membranes and fuel cells., In: Tongwen Xu, editor. Advances in membrane science and technology, Nova Science Publishers, Inc. p. 75-118.
[45] P.W. Majsztrik, Mechanical and transport properties of Nafion® for PEM fuel cells; temperature and hydration effects., Thesis PhD (Chemistry), Princeton Univesity, 2008.

[46] Kebes, Nafion structure, In: Wikimedia Commons, Nafion, a polymeric sulfonic acid useful in fuel cells., 2005. http://commons.wikimedia.org/wiki/File:Nafion_structure.png
[47] H. Tang, Z. Wan, M. Pan, S.P. Jiang, Self-assembled Nafion–silica nanoparticles for elevated-high temperature polymer electrolyte membrane fuel cells., Electrochemical communications, 9 (2007) 2003-2008.
[48] T. Higashihara, K. Matsumoto, M. Ueda, Sulfonated aromatic hydrocarbon polymers as proton exchange membranes for fuel cells., Polymer, 50 (2009) 5341-5357.
[49] L. Wang, A. Husar, T. Zhou, H. Liu, A parametric study of PEM fuel cell performances., International Journal of Hydrogen Energy, 28 (2003) 1263-1272.
[50] L.J.M.J. Blomen, M.N. Mugerwa, Fuel Cell Systems., Plenum Press, New York, 1993, p. 493.
[51] B. Smitha, S. Sridhar, A.A. Khan, Synthesis and characterization of proton conducting polymer membranes for fuel cells., Journal of Membrane Science, 225 (2003) 63-76.
[52] B. Smitha, S. Sridhar, A.A. Khan, Polyelectrolyte complexes of chitosan and poly(acrylic acid) for fuel cell applications., Macromolecules, 37 (2004) 2233-2239.
[53] J. Kerres, F. Schönberger, A. Chromik, T. Häring, Q. Li, J.O. Jensen, C. Pan, P. Noyé, N.J. Bjerrum, Partially Fluorinated Arylene Polyethers and Their Ternary Blend Membranes with PBI and H3PO4. Part I. Synthesis and Characterisation of Polymers and Binary Blend Membranes., Fuel Cells, 8 (2008) 175-187.
[54] G. Hoogers, Fuel Cell Technology Handbook., CRC Press, Washington DC, 2003.
[55] Soczka-Guth, T. et al., International Patent WO99/29763, 1999.
[56] S. Koter, P. Piotrowski, J. Kerres, Comparative investigations of ion-exchange membranes., Journal of Membrane Science, 153 (1999) 83-90.
[57] M. Gil, X. Ji, X. Li, H. Na, J. Eric Hampsey, Y. Lu, Direct synthesis of sulfonated aromatic poly(ether ether ketone) proton exchange membranes for fuel cell applications., Journal of Membrane Science, 234 (2004) 75-81.
[58] D. Xing, J. Kerres, Improved performance of sulphonated polyarylene ethers for proton exchange membrane fuel cells., Polymers For Advanced Technologies, 17 (2006) 591-597.
[59] B. Yang, A. Manthiram, Sulfonated Poly(ether ether ketone) Membranes for Direct Methanol Fuel Cells., Electrochemical and Solid-State Letters, 6 (2003) A229-A231.
[60] K.D. Kreuer, On the development of proton conducting membranes for hydrogen and methanol fuel cells., Journal of Membrane Science, 185 (2001) 29-39.
[61] S. Mitov, B. Vogel, E. Roduner, H. Zhang, X. Zhu, V. Gogel, L. Jörissen, M. Hein, D. Xing, F. Schönberger, J. Kerres, Preparation and Characterization of Stable Ionomers and Ionomer Membranes for Fuel Cells., Fuel Cells, 6 (2006) 413-424.
[62] N.N. Krishnan, H.J. Lee, H.J. Kim, J.Y. Kim, I. Hwang, J.H. Jang, E.A. Cho, S.K. Kim, D. Henkensmeier, S.A. Hong, T.H. Lim, Sulfonated poly(ether sulfone)/sulfonated

polybenzimidazole blend membrane for fuel cell applications., European Polymer Journal, 46 (2010) 1633-1641.
[63] D. Wu, T. Xu, L. Wu, Y. Wu, Hybrid acid–base polymer membranes prepared for application in fuel cells., Journal of Power Sources, 186 (2009) 286-292.
[64] S.J. Peighambardoust, S. Rowshanzamir, M. Amjadi, Review of the proton exchange membranes for fuel cell applications., International Journal of Hydrogen Energy, 35 (2010) 9349-9384.
[65] Q. Li, J.O. Jensen, R.F. Savinell, N.J. Bjerrum, High temperature proton exchange membranes based on polybenzimidazoles for fuel cells., Progress in Polymer Science, 34 (2009) 449-477.
[66] C. Hasiotis, V. Qingfeng, J.K. Deimede, C.G. Kallitsis, N.J. Kontoyannis, Development and characterization acid-doped polybenzimidazolesulfonated polysulfone blend polymer electrolytes for fuel cells., Journal of Electrohemical Society, 148 (2001) A513-A519.
[67] Y.F. Lin, Y.H. Hsiao, C.Y. Yen, C.L. Chiang, C.H. Lee, C.C. Huang, C.C.M. Ma, Sulfonated poly(propylene oxide) oligomers/Nafion® acid-base blend membranes for DMFC., Journal of Power Sources, 172 (2007) 570-577.
[68] H.L. Wu, C.C.M. Ma, H.C. Kuan, C.H. Wang, C.Y. Chen, C.L. Chiang, Sulfonated poly(ether ether ketone)/poly(vinylpyrrolidone) acid–base polymer blends for direct methanol fuel cell application., Journal of Polymer Science Part B: Polymer Physics, 44 (2006) 565-572.
[69] Y. Fu, A. Manthiram, M.D. Guiver, Acid–base blend membranes based on 2-amino-benzimidazole and sulfonated poly(ether ether ketone) for direct methanol fuel cells., Electrochemistry Communications, 9 (2007) 905-910.
[70] J. Kerres, A. Ulrich, T. Häring, M. Baldauf, U. Gebhardt, W. Preidel, Preparation, characterization and fuel cell application of new acid-base blend membranes., Journal of New Materials for Electrochemical Systems, 3 (2000) 229-239.
[71] D. Liu, H. Liao, N. Tan, G. Xiao, D. Yan, Sulfonated poly(arylene thioether phosphine oxide)/sulfonated benzimidazole blends for proton exchange membranes., Journal of Membrane Science, 372 (2011) 125-133.
[72] Z. Zuo, Y. Fu, A. Manthiram, Novel Blend Membranes Based on Acid-Base Interactions for Fuel Cells., Polymers, (2012) 1627-1644.
[73] S.D. Mikhailenko, G.P. Robertson, M.D. Guiver, S. Kaliaguine, Properties of PEMs based on cross-linked sulfonated poly(ether ether ketone)., Journal of Membrane Science, 285 (2006) 306-316.
[74] C. Zhang, X. Guo, J. Fang, H. Xu, M. Yuan, B. Chen, A new and facile approach for the preparation of cross-linked sulfonated poly(sulfide sulfone) membranes for fuel cell application., Journal of Power Sources, 170 (2007) 42.

[75] G. Zhang, X. Guo, J. Fang, K. Chen, K.I. Okamoto, Preparation and properties of covalently cross-linked sulfonated copolyimide membranes containing benzimidazole groups., Journal of Membrane Science, 326 (2009) 708-713.
[76] C. Zhao, H. Lin, M. Han, H. Na, Covalently cross-linked proton exchange membranes based on sulfonated poly(arylene ether ketone) and polybenzimidazole oligomer., Journal of Membrane Science, 353 (2010) 10-16.
[77] J. Kerres, Covalent-ionically cross-linked poly(etheretherketone)-basic polysulfone blend ionomer membranes., Fuel Cells, 6 (2006) 251-260.
[78] J. Wang, C. Zhao, G. Zhang, Y. Zhang, J. Ni, W. Ma, H. Na, Novel covalent-ionically cross-linked membranes with extremely low water swelling and methanol crossover for direct methanol fuel cell applications., Journal of Membrane Science, 363 (2010) 112-119.
[79] H. Luo, G. Vaivars, M. Mathe, Covalent-ionically cross-linked polyetheretherketone proton exchange membrane for direct methanol fuel cell., Journal of Power Sources, 195 (2010) 5197-5200.
[80] J. Kerres, W. Cui, R. Disson, W. Neubrand, Development and characterization of crosslinked ionomer membranes based upon sulfinated and sulfonated PSU crosslinked PSU blend membranes by disproportionation of sulfinic acid groups., Journal of Membrane Science, 139 (1998) 211-225.
[81] Ammrf, EDS Precision, In: Australian Microscopy and Microanalysis Research Facility. My scope training for advanced research., 2012. http://www.ammrf.org.au/ myscope/analysis/eds/accuracy/
[82] J. Kerres, D. Xing, F. Schönberger, Comparative Investigation of Novel PBI Blend Ionomer Membranes from Nonfluorinated and Partially Fluorinated Poly Arylene Ethers., Journal of Polymer Science: Part B: Polymer Physics, 44 (2006) 2311-2326.
[83] J. Kerres, W. Zhang, L. Jörissen, V. Gogel, Application of Different Types of Polyaryl-Blend-Membranes in DMFC., Journal of New Materials for Electrochemical Systems, 5 (2002) 97-107.
[84] P.R. Griffiths, H.J. Sloane, Fourier Transform Infrared Spectroscopy., John Wiley & Sons, 1986, p. 83.
[85] J. Coats, Interpretation of Infrared Spectra, A Practical Approach., John Wiley & Sons Ltd, Chichester, 2000, p. 10815-10837.

Chapter 3: Experimental

Contents

3.1 Introduction 38

3.2 Materials 38

3.2.1 Membranes 38

3.2.2 Chemicals 38

3.3 Membrane H_2SO_4 treatment 40

3.3.1 Pre-treatment 40

3.3.2 H_2SO_4 treatment 40

3.3.3 Post-treatment 40

3.4 Characterisation 40

3.4.1 Weight change 41

3.4.2 Thickness change 41

3.4.3 IEC 41

3.4.4 SEM and EDX 42

3.4.5 FTIR 42

3.4.6 TGA 42

3.5 References 43

3.1 Introduction

Within this chapter the analytical techniques and experimental procedures that were used to determine the H_2SO_4 stability of various proton exchange membrane (PEM) materials in an 80 wt% H_2SO_4 environment at 80 ºC are described. Membranes were characterised before and after acid treatment using weight and thickness changes, IEC, SEM (EDX), FTIR and TGA data.

3.2 Materials

3.2.1 Membranes

The 30 PEM materials that were studied comprised 25 different blends with repeats completed on 4 membrane types. The membranes listed in Table 3.1, with the exception of Nafion®212, were provided by Dr. Kerres and his co-workers from the University of Stuttgart, Germany. Nafion®212 was obtained from Ion Power and was used as is. In Table 3.1 both the composition and the amount of the components used for the manufacture of the membranes are presented. For clarity, the membranes were divided according to the PBI-type base component within the blend membranes consisting of i) the non-PBI based (NB), ii) the PBIOO based (PB) and iii) the F_6-PBI based membranes (FPB). For reference purposes three identical Nafion®212 samples (N212 A, B and C) were included in the H_2SO_4 stability study and used for the error determination (see Section 3.4). The structures of all the components presented in Table 3.1 are given in Appendix A.

3.2.2 Chemicals

The 80 wt% H_2SO_4 used for the membrane treatment was prepared from the dilution of a 96 wt% H_2SO_4 (Merck, SA) with DI water (18 MOhm, Milli-Q), while NaOH (ACE, SA) and phenolphthalein (Merck, SA) were used to standardise the 80 wt% H_2SO_4 solution The ion exchange capacity was determined by titration using 0.1M HCl (Titrosol® for 1L) and Bromothymol blue as indicator (Merck, SA). Before titration the membranes were submerged in NaCl (ACE, SA).

Table 3.1: The compositions and concentrations of the copolymers and cross-linkers used for the manufacture of the membranes.

No.	Abb.	Copolymers (%)			Cross-linkers (%)	
		1	2	3	1	2
1	N212_A	Nafion®(100)	-	-	-	-
2	N212_B	Nafion®(100)	-	-	-	-
3	N212_C	Nafion®(100)	-	-	-	-
4	NB1	PSU-SCl(56.1)[a]	-	-	PSU-S(33.2)[k]	BFO(10.7)[n]
5	NB2	PSU-SCl(56.1)	-	-	PSU-S(33.2)	BFO(10.7)
6	NB3	PSU-SCl(49.5)	-	-	PSU-S(39.8)	DFBP(10.7)[o]
7	NB4	PEEK-SCl(49.5)[b]	-	-	PSU-S(39.6)	BNFPS(10.9)[p]
8	NB5	PEEK-SCl(49.5)	-	-	PSU-S(39.6)	BNFPS(10.9)
9	NB6	PEEK-SCl(49.5)	-	-	PSU-S(38.2)	BFO(12.3)
10	NB7	sPSU(80)[c]	PFS(20)[g]	-	-	-
11	NB8	sPSU(70)	PFS(30)	-	-	-
12	PB1	sPEEK(63.2)[d]	PBIOO(32.2)[h]	-	Bis-A(4.6)[l]	-
13	PB2	sPEEK(63.2)	PBIOO(32.2)	-	Bis-A(4.6)	-
14	PB3	sPEEK(66.3)	PBIOO(33.7)	-	-	-
15	PB4	sPSU(94)	PBIOO(6)	-	-	-
16	PB5	sPSU(95.6)	PBIOO(4.4)	-	-	-
17	PB6	sPSU(30)	PBIOO(70)	-	-	-
18	PB7	PKA(8)[e]	PBIOO(92)	-	-	-
19	PB8	PKA(30)	PBIOO(70)	-	-	-
20	FPB1	sFS(89.7)[f]	F_6-PBI(10.3)[i]	-	-	-
21	FPB2	sFS(30)	F_6-PBI(70)	-	-	-
22	FPB3	sFS(82)	F_6-PBI(8.9)	PFS(9.1)	-	-
23	FPB4	sFS(73.6)	F_6-PBI(8)	PFS(18.4)	-	-
24	FPB5	sFS(65.1)	F_6-PBI(7)	PFS(27.9)	-	-
25	FPB6	sFS(56.3)	F_6-PBI(6.1)	PFS(37.6)	-	-
26	FPB7	sFS(47.4)	F_6-PBI(5.1)	PFS(47.4)	-	-
27	FPB8	sFS(85.3)	F_6-PBI(11.3)	-	Bis-A(3.4)	-
28	FPB9	sFS(89.7)	F_6-PBI(10.3)	-	DIB(0.1)[m]	-
29	FPB10	sFS(81.3)	F_6-PBI(8.7)	A095(6.7)[j]	Bis-A(3.3)	-
30	FPB11	sPSU(92)	F_6-PBI(8)	-	-	-

a) Poly(phenyl sulfone)-sulfochloride
b) Poly(ether ether ketone)-sulfochloride
c) Sulfonated poly(phenyl sulfone)
d) Sulfonated poly(ether ether ketone)
e) Sulfonated-phosphonated arylene
f) Sulfonated partially fluorinated polymer
g) Partially fluorinated polymer
h) Polybenzimidazole
i) Fluorinated polybenzimidazole
j) Poly(phenyl sulfone)-derivate with groups $–C(OCH_3)(4\text{-diethylaminophenyl})_2$
k) Poly(phenyl sulfone)- sulfinate
l) Bisphenol A-diglycidylether
m) Diiodobutane
n) Bis(pentafluorophenyl)-2,5-oxadiazole
o) Decafluorobiphenyl
p) Bis(3-nitro-4-fluorophenyl)sulfone

3.3 Membrane H_2SO_4 treatment

3.3.1 Pre-treatment

Before the acid treatment, the membranes were washed in deionized water for two hours at 80 °C. Subsequently, they were dried in a vacuum oven (over silica gel), again at 80 °C for 12 h and then weighed to determine the weight of the membranes before H_2SO_4 treatment.

3.3.2 H_2SO_4 treatment

A 80 wt% H_2SO_4 solution was prepared from the purchased 96 % solution. The concentration of the prepared acid was determined by titration with 0.1 M NaOH and phenolphthalein as indicator. Each membrane was then submerged in the prepared 80 wt% H_2SO_4 for 120 h at 80 °C.

3.3.3 Post-treatment

After the H_2SO_4 treatment, the membranes were repeatedly rinsed in deionized water at 80 °C until the water in which the membranes had been washed remained at a neutral pH (approximately three hours), to ensure that any residual H_2SO_4 that could compromise the results of the characterisation of the membranes, had been removed. Subsequently, the membranes were dried and weighed as described before in Section 3.3.1.

3.4 Characterisation

The choice of specifically Nafion®212 for the stability studies was based on the fact that its thickness (50 μm) was comparable to the thickness (ranging from 25-80 μm with an average of 42.5 μm) of the PEM materials under investigation. By repeating both acid treatment and characterisation of Nafion®212 in triplicate for many of the mentioned characterisation studies, it was possible to determine both the experimental error due to the H_2SO_4 treatment of the membrane, and the experimental error of the analytical technique (experimental procedure) applied for characterisation.

3.4.1 Weight change

The weight change of each membrane sample was determined by obtaining the dry weight of the PEM material before and after the H_2SO_4 treatment.

3.4.2 Thickness change

The swelling of the membrane was determined in terms of the change in thickness of the membrane (y-dimension). The thickness before and after H_2SO_4 treatment was measured in mm to the third decimal using a Digimatic Micrometer. Five measurements at different locations across the membrane's surface were taken to determine the average change in thickness. From the average change in thickness the percentage thickness change due to H_2SO_4 treatment was calculated.

3.4.3 IEC

The IEC was determined by acid-base titrations as adapted from Kerres *et al*. [1]. The dry membranes were weighed and immersed in saturated sodium chloride solution (NaCl) for 24 h to replace the protons of the sulfonic acid groups with sodium ions. To the solution bromothymol blue was then added as indicator. The exchanged protons were then determined by titration with 0.1 M NaOH to the equivalent point (IEC_{direct}). The equivalent point is shown by a colour change from yellow to green. Subsequently 3 ml excess of 0.1 M NaOH was added and stirred for 24 h. This solution was back-titrated with 0.1 M HCl to get the IEC_{total}, where the equivalent point is shown by a colour change from blue to green. The IEC values were calculated using the following equations:

$$IEC_{direct} = V*0.1/m \quad (3.1)$$

$$IEC_{total} = (V+R)*0.1/m \quad (3.2)$$

where V is the volume of titration solution used (L), R is the additional volume not needed by back-titration, taking into account a 3 ml NaOH excess, m is the weight of the membrane and 0.1 represents the molarity of the solution. From these calculations an IEC measured in milli-equivalents per gram of membrane is obtained.

3.4.4 SEM and EDX

A FEI Quanta 250 FEG with ESEM capabilities was used to visually investigate the PEM material before and after H_2SO_4 treatment for possible mechanical degradation present on the membrane's cross-sections. An energy-dispersive X-ray spectroscopy (EDX) analysis with the Oxford system using INCA software, coupled with the SEM, provided an elemental analysis of each membrane sample before and after treatment.

3.4.5 FTIR

FTIR spectra of the membrane's surfaces were recorded with a Bruker Alpha-P spectrometer in ATR (attenuated total reflection) mode at a resolution of 4 cm^{-1} measuring in the ranges 4000-550 cm^{-1}. The FTIR spectra obtained for each membrane before and after treatment were investigated to determine whether the membrane underwent a change in chemical structure based on the possible changes in peak positions and intensities.

3.4.6 TGA

The thermal stability of the membranes was determined by thermogravimetry (TGA, Netzsch, model STA 449C) with a heating rate of 20 °C/ min under an atmosphere enriched with oxygen (65 – 70 % O_2, 35 – 30 % N_2) [2].

3.5 References

[1] J. Kerres, D. Xing, F. Schönberger, Comparative Investigation of Novel PBI Blend Ionomer Membranes from Nonfluorinated and Partially Fluorinated Poly Arylene Ethers., Journal of Polymer Science: Part B: Polymer Physics, 44 (2006) 2311-2326.

[2] J. Kerres, A. Ulrich, M. Hein, V. Gogel, K.A. Friedrich, L. Jörissen, Cross-linked polyaryl blend membranes for polymer electrolyte fuel cells., Fuel Cells, 4 (2004) 105-112.

Chapter 4: Results and Discussion

Contents

4.1 Introduction 45

4.2 Nafion®212 45

4.2.1 Physical changes 45

4.2.2 Chemical changes 47

4.3 Non-PBI based membranes 54

4.3.1 Physical changes 54

4.3.2 Chemical changes 58

4.4 PBIOO based membranes 64

4.4.1 Physical changes 64

4.4.2 Chemical changes 67

4.5 F_6-PBI based membranes 73

4.5.1 Physical changes 73

4.5.2 Chemical changes 77

4.6 Conclusion 81

4.7 References 82

4.1 Introduction

In this chapter the results of the characterisation techniques described in Chapter 3, which were used to determine the H_2SO_4 stability of the various PEM materials, are presented. The detailed discussion based on the results from the physical observations supported by the chemical changes observed was compiled for the various membrane groups. Nafion®212 was included in the H_2SO_4 stability study (Section 4.2) both as reference membrane for the novel membranes presented as well as being used to determine the experimental and analytical error margins for this study. To facilitate the discussion of the novel membranes manufactured in the group of Dr. Kerres (Stuttgart, Germany), their discussion is grouped according to the PBI-type base component within the blend membrane. Accordingly (see Table 3.1), first the non-PBI based membranes will be discussed in Section 4.3, followed by the PBIOO based membranes in Section 4.4 and finally the F_6-PBI based membranes in Section 4.5. To further facilitate the discussion, the characterisation in each Section will be sub-divided into physical (weight change and swelling) and chemical (SEM-EDX, IEC, FTIR, TGA) changes that might have occurred due to the H_2SO_4 treatment.

4.2 Nafion®212

As mentioned previously Nafion®212 was included in the H_2SO_4 stability study as reference as its thickness (50 µm) was comparable to the thickness of the novel PEM materials which varied between 25-80 µm with an average of 42.5 µm. By repeating both the acid treatment and the characterisation of Nafion®212 in triplicate (three different membrane samples), it was possible to determine both the experimental error due to the H_2SO_4 treatment of the membrane, as well as the experimental error of the analytical technique (experimental procedure) applied for characterisation.

4.2.1 Physical changes

The % weight change due to the acid treatment of Nafion®212 is presented in Figure 4.1. As mentioned previously, three Nafion®212 membranes were treated with H_2SO_4 and the average standard deviations obtained from these repeats were included Figure 4.1

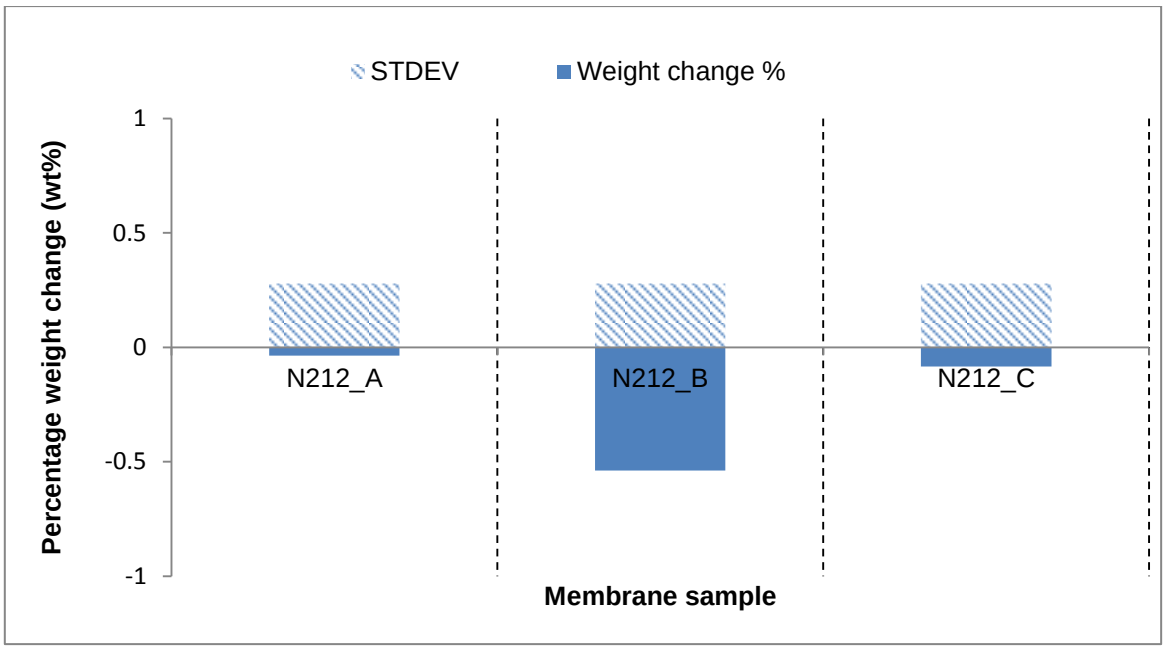

Figure 4.1: Weight changes of the three different Nafion®212 samples (A, B and C) due to H_2SO_4 treatment.

According to Figure 4.1, Nafion®212 was stable in H_2SO_4 with less than 1 % weight loss. The deviation in the weight change measurements was less than 0.5 %, while the difference between the three membranes was also less than 0.5 %. This is further supported by the insignificant change in thickness measured for Nafion®212 as presented in Figure 4.2, with the included average standard deviations obtained from the repeated thickness measurements (5 x before and after treatment) which for each set of Nafion®212 membranes was approximately 2 % independent of the Nafion® sample. It is interesting to note that the variation in thickness change between the three membranes (A, B and C) was significantly more (>4 %) than the difference observed for the weight changes (<0.5 %) for the same three membranes. This could partially be explained by the increased error observed for the thickness measurements (±2 %) compared to the error observed for the weight changes (<0.5 %) suggesting that the weight change measurements gave a more accurate indication of the changes that might have occurred due to the H_2SO_4 treatment. It should also be mentioned that the swelling and drying the membranes underwent during the H_2SO_4 treatment may have changed the morphology and could subsequently have led to a change in thickness as observed for Nafion®212.

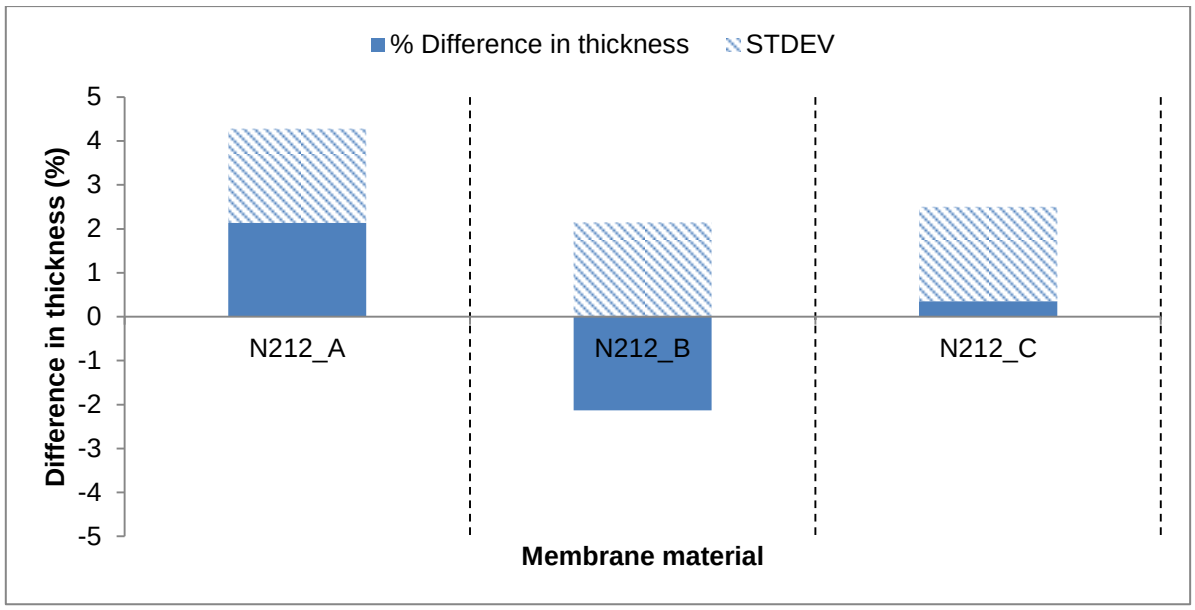

Figure 4.2: Percentage difference in thickness (%) of the three different Nafion®212 samples (A, B and C) due to H_2SO_4 treatment.

4.2.2 Chemical changes

4.2.2.1 SEM-EDX and IEC

The SEM-micrographs of the Nafion®212 membrane cross-sections (data not shown) presented no significant visual changes in the membrane's morphology after the H_2SO_4 treatment. The EDX analysis results of the sulfur done for all three Nafion®212 membrane surfaces before and after the H_2SO_4 treatment are listed in Table 4.1. In view of the focus on the H_2SO_4 treatment, only the sulfur (S) values before and changes due to H_2SO_4 treatment are summarised in Table 4.1.

Table 4.1: IEC values and sulfur content (SEM-EDX) determined for the three different Nafion®212 samples (A, B and C) before treatment and the difference after treatment.

Membrane	IEC (total, exp.)*		EDX: S-content	
	Before [meq SO_3H/g]	Change (%)	Before (%)	Change (%)
N212_A	1.16	8.3	3.60	-28.9
N212_B	1.40	7.2	3.96	-33.6
N212_C	1.07	7.8	0.38	13.2

*The total IEC was determined experimentally as described in Section 3.4.3.

In Table 4.1 only the IEC_{total} was presented as it accounts for all -SO_3H groups within the membrane, i.e. both free and those involved in the cross-linking (ionical) of polymer chains [1] thereby providing a more complete picture by determining the total effect of the H_2SO_4 on the membrane, whether it is due to the sulfonation of polymer components or the promotion of cross-linking between the polymer components (increased thermal stability).

It is clear that the EDX data obtained from various sections of the membrane showed significant variation not only after H_2SO_4 treatment but even for the three identical Nafion® samples before acid treatment confirmed by the standard deviation of 25 % (in terms of the S-content). It is well known that EDX provides only a semi-quantitative analysis of the chemical composition of the membrane sample studied, as the content values given are relative to the amount of the other elements detected within the area of the sample analysed. Hence it has been proposed that the accuracy of the EDX-analysis is limited to ±2 % for the major components within the samples measured [2], which is, however, significantly less than the error observed in this study. What might have aggravated the accuracy is the fact that the area analysed only presents a fraction of the actual membrane material and the data only provides an estimate average, assuming that the polymers are homogeneously distributed throughout the matrix.

Therefore, to ensure an accurate representation of the effect of the H_2SO_4 treatment on the PEM material, the other analytical techniques (IEC, FTIR and TGA) were included in this discussion. According to the IEC data also presented in Table 4.1, the -SO_3H content for the Nafion®212 samples varied <10 % (average = 7.8 %) due to the H_2SO_4 treatment, which confirms the stability according to the weight and thickness changes. Since the IEC is indicative

of the -SO_3H groups within the PEM sample, it is clear that Nafion®212 did not significantly sulfonate during the H_2SO_4 treatment. The standard deviation of 0.6 %, determined for the changes in IEC measurements between the three Nafion®212 samples, confirms the accuracy of the IEC measurements as opposed to the SEM-EDX data.

4.2.2.2 FTIR

For each of the three Nafion®212 membrane samples, a FTIR spectrum was obtained before and after treatment and the average of the three spectra is presented in Figure 4.3. The spectra are comparable to literature with the characteristic doublet peaks at 970 and 981 cm^{-1} assigned to the symmetric vibrations of C-O-C bonds located on the side chains of Nafion® [3]. Similarly, the peak at 1056 cm^{-1} is due to S-O stretching, while the peaks at 1144 and 1203 cm^{-1} can be attributed to the anti-symmetric vibrations of Nafion's C-F bonds [4,5]. The before and after spectra again confirm that the Nafion®212 material remained unaffected by the H_2SO_4 treatment.

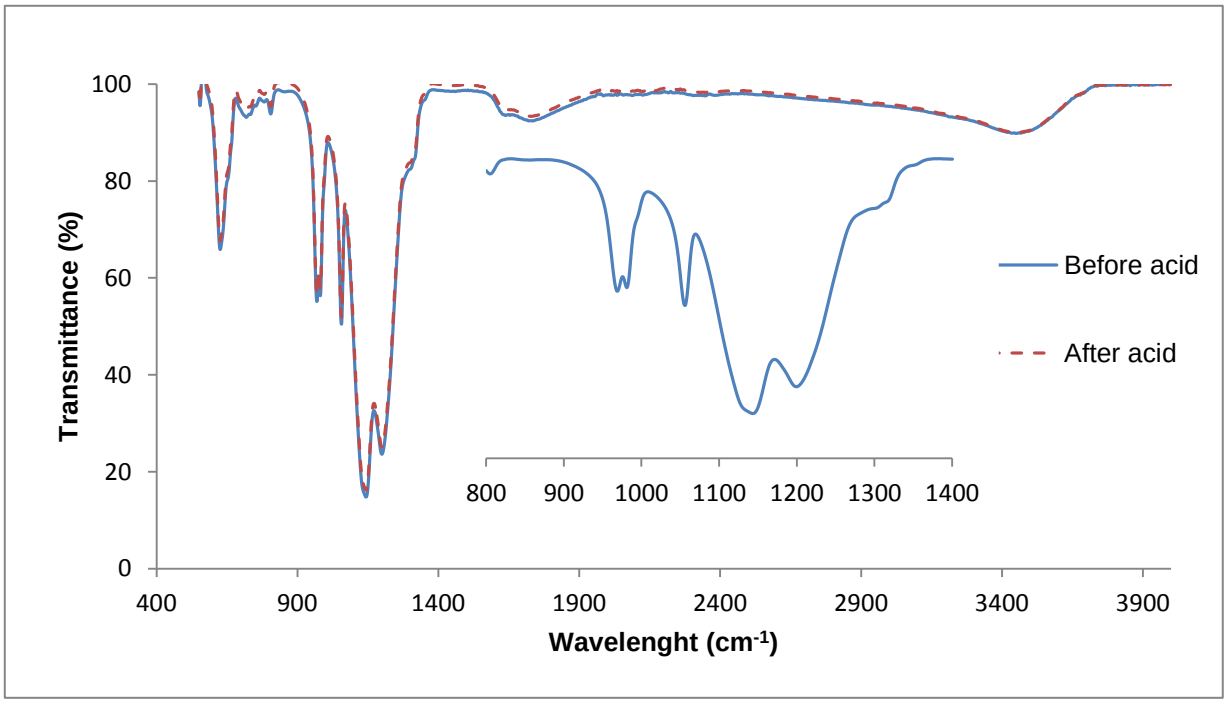

Figure 4.3: Average FTIR spectra of the three Nafion®212 samples before and after H_2SO_4 treatment.

When considering the repeatability obtained with the FTIR measurements before and after H_2SO_4 treatment obtained by plotting the average standard deviation from the three different Nafion®212 spectra (Figure 4.4), it is clear that the standard deviation of the FTIR technique is insignificantly small, where the similarity of the before and after standard deviations again confirm the stability of Nafion®212 in an H_2SO_4 environment.

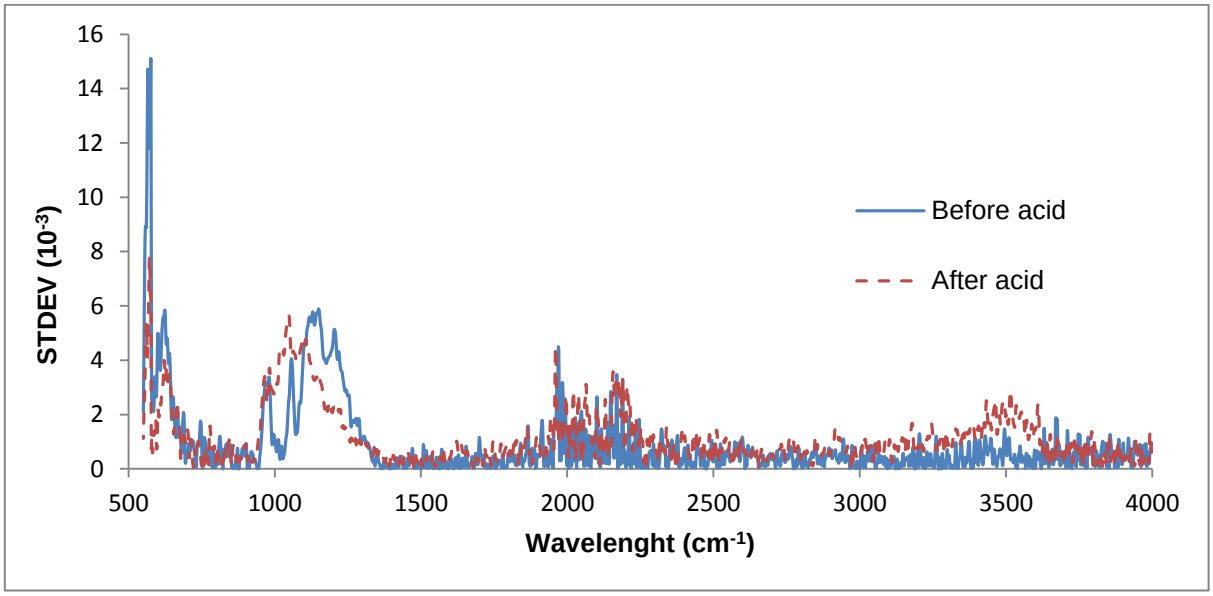

Figure 4.4: Standard deviation of FTIR spectra determined for Nafion®212 before and after H_2SO_4 treatment from the three different Nafion®212 samples.

4.2.2.3 TGA

The TGA-curves for the three Nafion®212 samples before and after H_2SO_4 treatment are presented in Figure 4.5, showing the repeatability attainable with the TGA technique. The results confirm that the thermal degradation behaviour after the H_2SO_4 treatment did not differ from the before data as there is only minimal deviation visible from the Nafion®212 before treatment, especially at temperatures below 400°C.

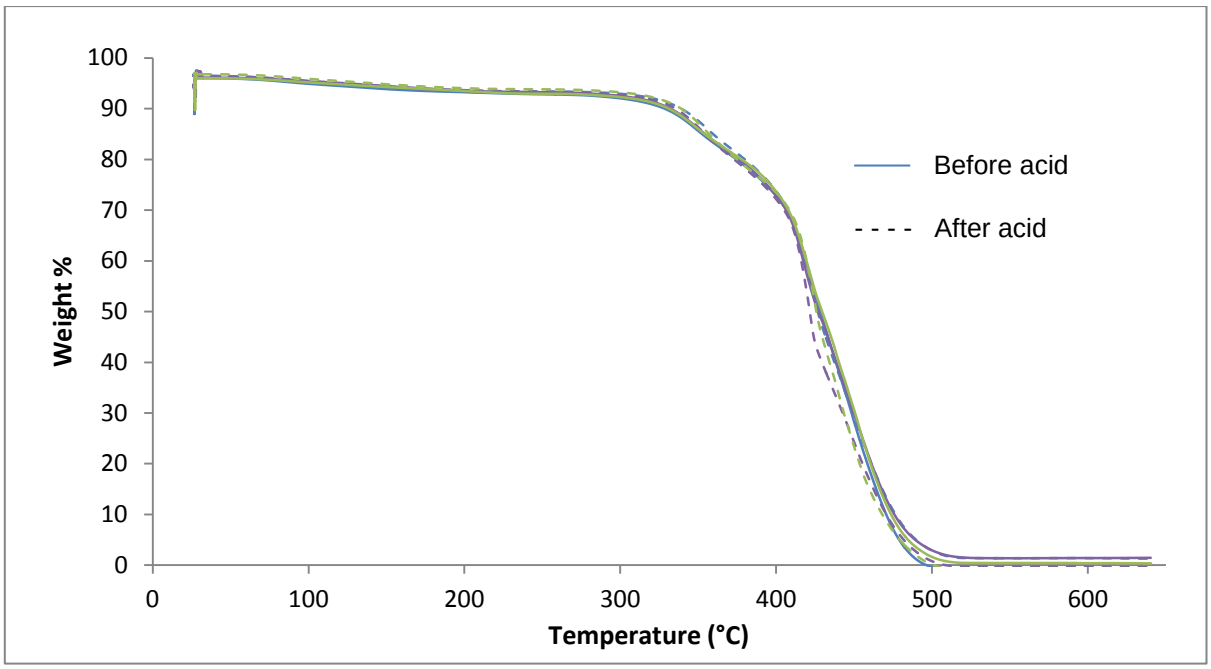

Figure 4.5: Thermal degradation for the in triplicate analysis of Nafion®212 both before and after 80 wt% H_2SO_4.

The average standard deviation of the TGA analysis of the different Nafion®212 membranes presented in Figure 4.5 was determined and is presented in Figure 4.6, showing the repeatability of the TGA method using the three untreated Nafion®212 membranes (before acid treatment) and the error obtained with a triplicate repetition of the H_2SO_4 treatment (after acid treatment). As expected, the error from the TGA of the untreated membranes, i.e. the error due to the TGA analysis alone, remained below 1 %, increasing slightly in the 400-500 °C region. In spite of the addition of the experimental error due to the acid treatment, the total error (TGA and acid treatment) remained below 1 % at temperatures below 300 °C. Above 400 °C, the total error reached a peak of 5 % at just above 400 °C, which clearly shows both the repeatability of the TGA analysis and the acid treatment.

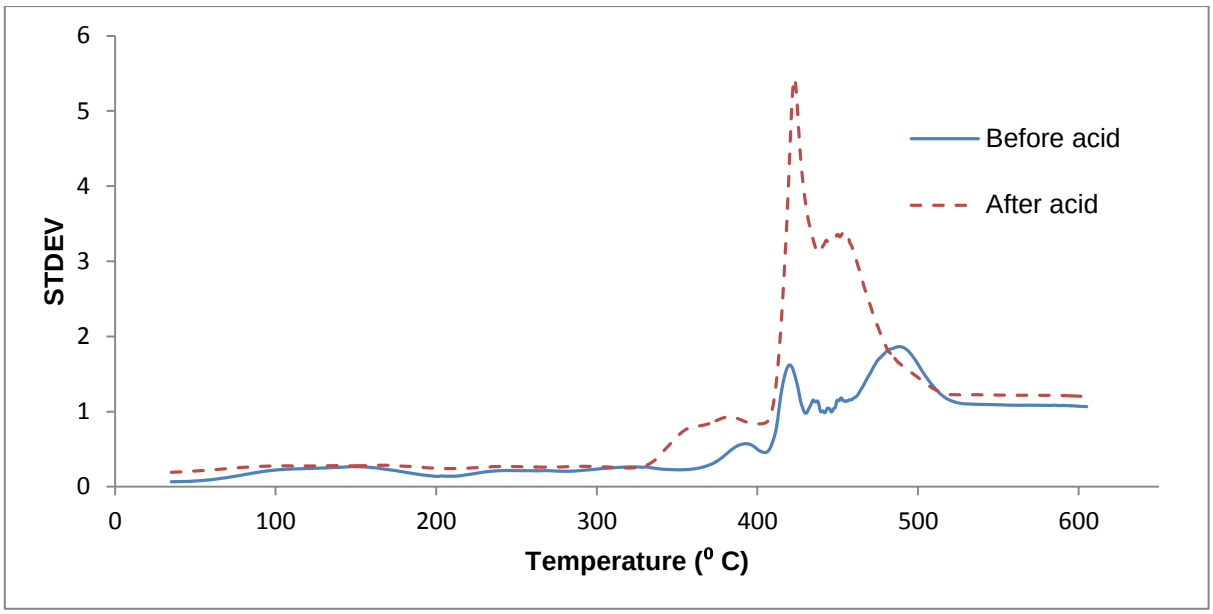

Figure 4.6: Standard deviation comparison of TGA data obtained Nafion®212 repeats before and after H_2SO_4treatment.

To further elucidate the TGA data, the temperature regions where the largest weight losses were observed for the TGA signals were determined by calculating the first derivative of the TGA signals for each Nafion® sample before and after acid treatment. According to Figure 4.7, there were 3 regions where weight changes occurred, i.e. 86-100 °C, ±350 °C and 400–450 °C. An account of these maximum weight loss regions will follow in Section 4.3.2. The identified temperatures of maximum weight loss before and after acid treatment in these regions are summarised in Table 4.2, showing that a minimal deviation (0–5 ^{0}C) was observed for the 1st and 2nd maxima points, while a larger deviation was noted by the decrease in temperature of the maximum weight change point above 400 ^{0}C.

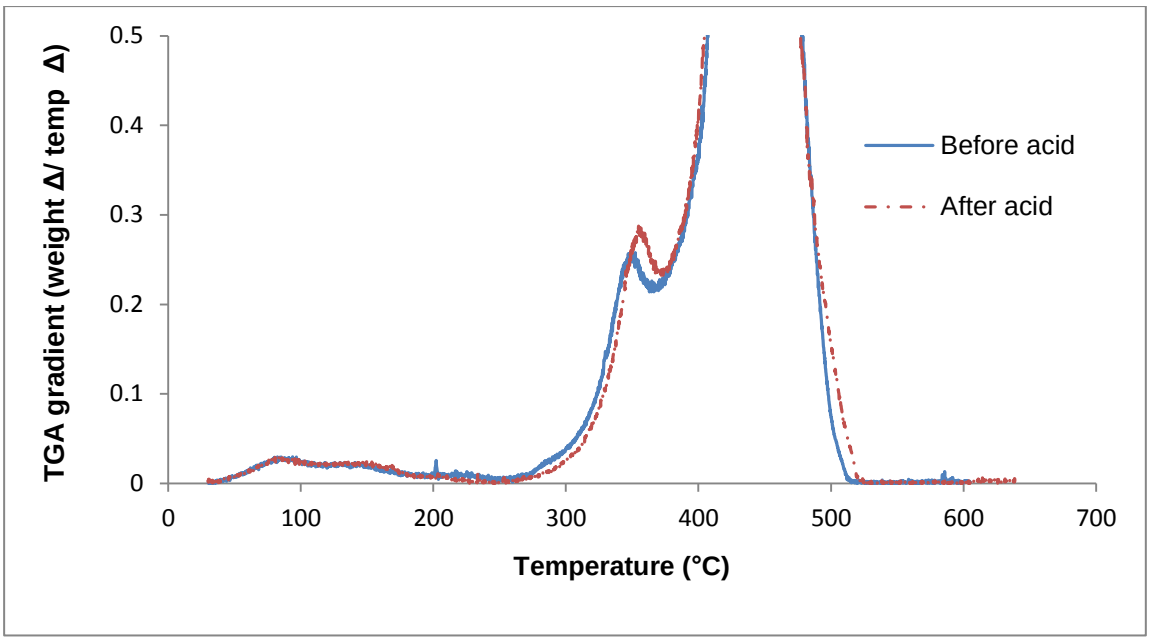

Figure 4.7: Differential TGA signal reported for Nafion®212_A before and after H_2SO_4treatment.

Table 4.2: Temperatures of maximum weight loss determined from the first derivative of the TGA data for Nafion®212 before and after H_2SO_4 treatment.

Membrane	Temperature of weight change maxima (°C)		
N212_A	94	352	450
N212_Aa*	97	355	423
N212_B	86	350	417
N212_Ba	91	353	422
N212_C	100	349	453
N212_Ca	100	354	425

* -a- refers to membrane after H_2SO_4 treatment.

From the Nafion®212 data, which had been obtained in triplicate, it is clear that the experimental error of both the analytical and H_2SO_4 treatment remained below 10 %, except for the SEM-EDX sulfur-content where significantly larger errors were observed.

4.3 Non-PBI based membranes

4.3.1 Physical changes

The weight changes for the non-PBI based membranes containing either PSU or PEEK with or without PFS and various cross-linkers are summarised in Figure 4.8. To simplify the discussion, the non-PBI based membranes will be divided into three groups according to their acid copolymers and cross-linkers. With reference to Table 3.1, we can hence distinguish between those groups containing PSU-SCl (NB1-3), PEEK-SCl (NB4-6) or sPSU (NB7 and 8).

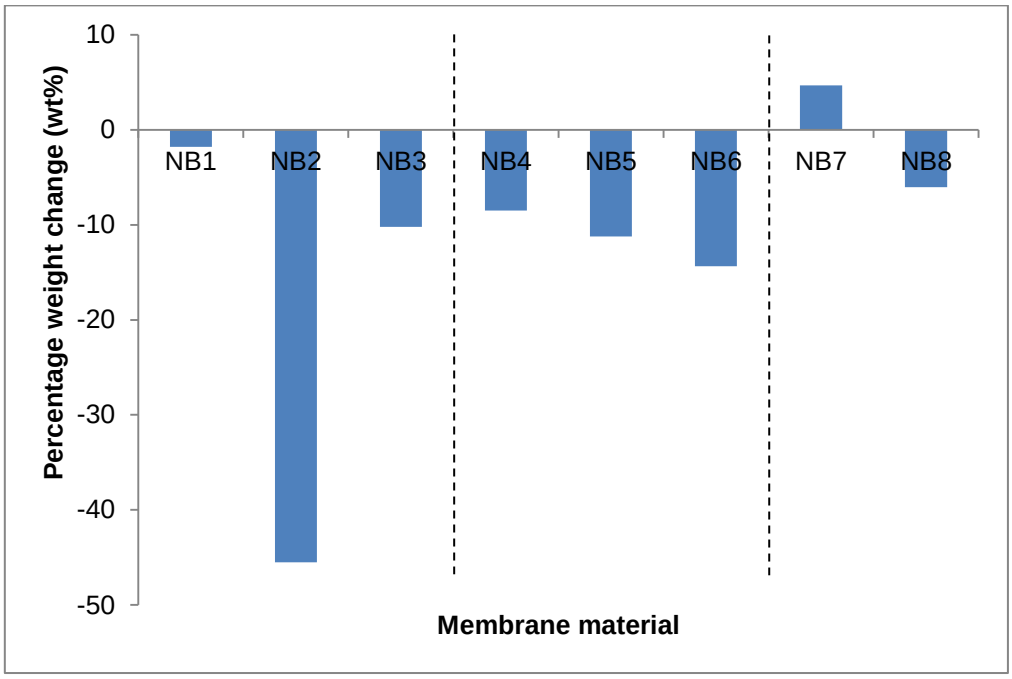

Figure 4.8: Weight change of the non-PBI based membranes due to H_2SO_4 treatment.

The overall tendency of weight decrease observed in Figure 4.8 can partially be ascribed to the PSU-component present either as copolymer or cross-linker (see Appendix A for polymer structures) within the non-PBI based blend membranes. It is known that sulfonation of the polyethersulfone at the *ortho*- position to the ether bridge within the biarylene ether portion of the PSU repeat unit is possible due to the electrophilic sulfonation properties of H_2SO_4 [6,7]. The sulfonation followed by the dissolution of molecular fragments during the post treatment washing can account for further weight decreases and corresponding thickness changes observed for most of the non-PBI based membranes. The significant weight loss noted for NB2 is possibly due to incomplete cross-linking and will further be discussed in Section 4.3.1(a).

In the absence of a basic-copolymer, this group is characteristically covalently cross-linked and can in some cases become brittle when dried out, limiting their flexibility due to the inflexibility of the covalent networks [8]. Significant weight losses could suggest a covalent network where some polysulfonated macromolecules are only physically cross-linked by entanglement and not participating in the cross-linked network [9], which can then subsequently diffuse from the network [10].

a) The PSU-SCl blends (NB1-3)

Although NB1 and 2 consist of the same acidic polymer and cross-linkers in concurring ratios, the significant difference in the weight changes (Figure 4.8) and the brittleness noted for NB2 after treatment shown in Figure 4.9 confirms the instability of NB2. This is likely due to incomplete cross-linking during synthesis, followed by the diffusion of macromolecules from the blended membrane that were probably rinsed out during the post-treatment wash.

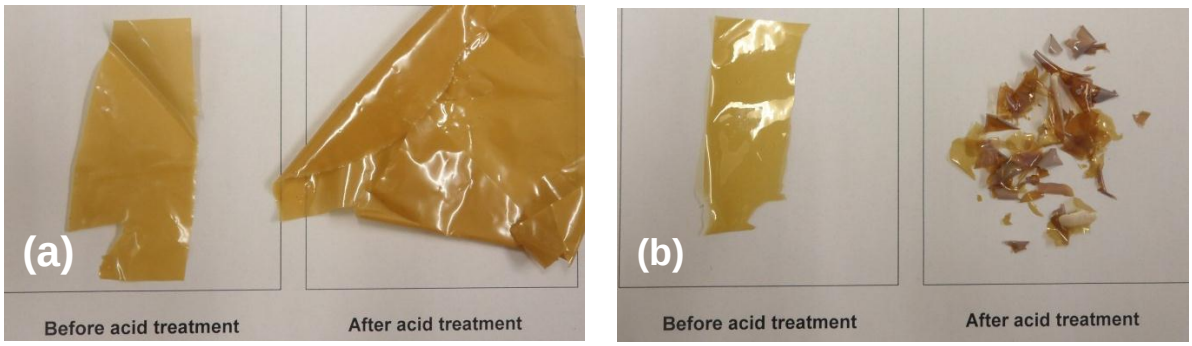

Figure 4.9: Photographs of PSU-SCl membranes (a) NB1 and (b) NB2 before and after H_2SO_4 treatment.

The suggested incomplete cross-linking is further supported by the difference in morphology noted in the SEM micrographs (Figure 4.10) taken of the membranes' cross-sections after treatment clearly showing the increased inhomogeneity.

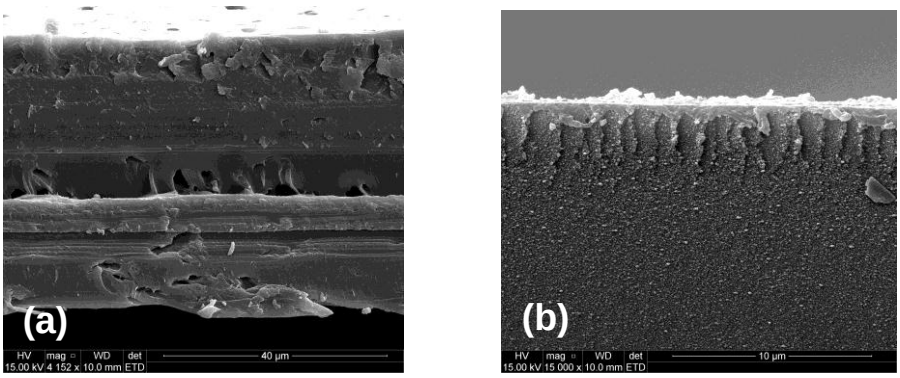

Figure 4.10: SEM micrographs of membranes NB1 (a) and NB2 (b) after H_2SO_4 treatment.

The 10 % weight loss and 40 % decrease in thickness (Figure 4.11, due to shrinkage) reported for membrane NB3 in comparison with the 3 % and <20 % decrease for membrane NB1, respectively, are most likely due to the difference in the second cross-linker (Table 3.1), where BFO was used for NB1 and DFBP for NB3. It was shown in a previous study, where only DFBP was included as aromatic cross-linker, that different aromatic cross-linkers do not necessarily have an influence on the properties of covalently cross-linked blend membranes [9]. The decrease in weight of NB3 could again be attributed to some of the sulfonated polymer chains that had only been entangled in the covalent network being washed from the network [10], supporting the weight loss observed for membrane NB3. Due to the brittleness of NB2, visible in Figure 4.9, a measurement of its thickness was not possible and thus no swelling data was presented for NB2 as indicated by the X in Figure 4.11.

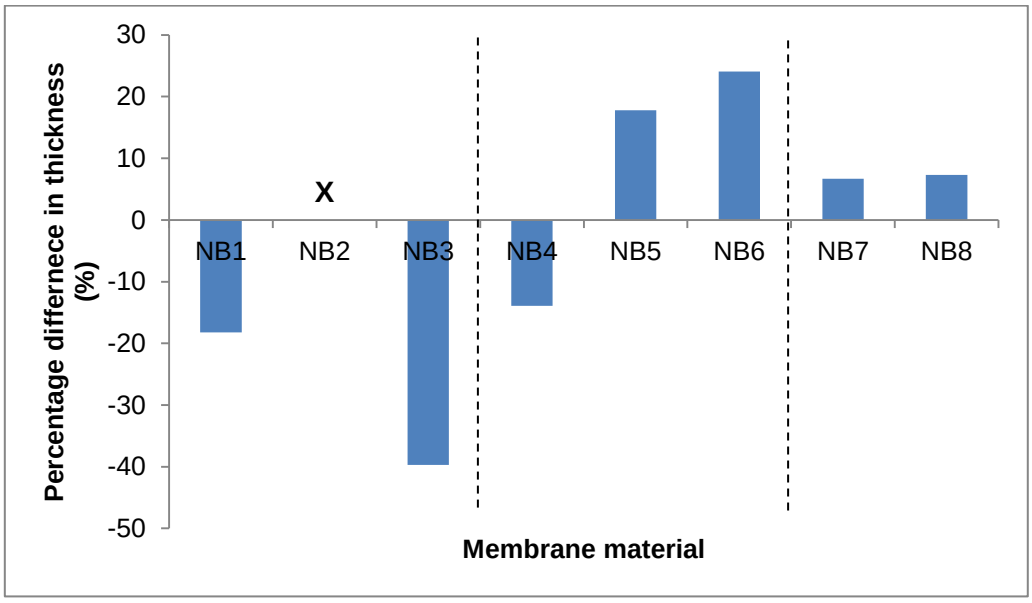

Figure 4.11: Percentage difference in thickness reported for the non-PBI based membranes after treatment.

b) PEEK-SCl blends (NB4-6)

The decrease in weight noted for the PEEK-SCl membranes is most likely due to the partial sulfonation of the PEEK polymer (see sPEEK Section 4.4.1) and PSU components, as mentioned previously for the PSU-SCl blends, followed by the dissolution of blend membrane constituents during the repeated washing of the membranes after treatment. The PEEK-SCl membranes appeared slightly darker and more brittle after treatment as is visible from the photos of membrane NB4 before and after treatment shown in Figure 4.12, which supports the proposed loss of membrane fragments as discussed for the PSU-SCl blends in Section 4.3.1(a).

Figure 4.12: Visual of PEEK-SCl membranes NB4 before and after H_2SO_4 treatment.

While, according to Table 3.1, membranes NB4 and 5 had identical compositions, the thickness changes varied according to Figure 4.11, which could be attributed to the difference in the initial thicknesses measured for the membranes (NB4 = 85 µm and NB5 = 47 µm). Membrane NB6 also reported an increased thickness, with an initial thickness of 48 µm, corresponding to the thickness change of NB5. While we cannot say for certain why the thicker NB4 membrane shrunk and the thinner NB5 swelled, it could be that there was more complete penetration of the thinner membrane by the H_2SO_4 resulting in more sulfonation and swelling.

Irrespective of the cause of the thickness change observed for the PEEK-SCl membranes and the difference in aromatic cross-linker noted, the results confirm their unstable character and unsuitability as membranes to be applied in SO_2 electrolysis due to their poor mechanical stability (brittleness).

c) sPSU-blends (NB7 and 8)

Membranes NB7 and 8 consist of a blend containing sPSU and PFS copolymers in the absence of a cross-linker. The insignificant weight and thickness changes reported for the sPSU-PFS blend membranes indicate that this combination provides a stable type blend compared to some of the other non-PBI based membranes.

The weight and thickness changes reported for membranes NB7 and 8 are likely due to the sulfonation of the sPSU-polymer as suggested in Section 4.3.1, supporting the mass increase of NB7. The bisphenol A unit present within the PFS polymer is known to be potentially acid sensitive [11] and the weight loss of membrane NB8 can be attributed to the 10 % higher PFS content compared to NB7. NB8 was also more wrinkled after treatment when compared to NB7, suggesting the dissolution of low molecular fractions during the post treatment washing of the membrane known to be present in polyarylene condensation polymers [12].

4.3.2 Chemical changes

The data obtained from SEM-EDX analysis, IEC measurements, FTIR and TGA for the non-PBI based membranes will be presented and compared to further clarify the different acid stabilities observed. While the IEC_{total} gives an indication of the total amount of $–SO_3H$ groups present in the sample, the S-content determined by SEM-EDX could relate to any S-containing groups within or on the surface of the sample. To compare these two variables both the IEC and EDX data is presented in Table 4.3.

Table 4.3: IEC values and sulfur content (SEM-EDX) of the non-PBI based membranes measured before treatment and the difference determined after treatment.

Membrane	IEC (total, exp.)		EDX: S-content	
	Before [meq SO_3H/g]	Change (%)	Before (%)	Change (%)
NB1	1.07	5.0	8.30	8.0
NB2	3.44	-69	10.20	-8.0
NB3	1.69	8.0	6.66	10
NB4	1.49	-1.0	7.40	102
NB5	2.06	-20	7.62	58
NB6	1.70	-5.0	9.90	4.0
NB7	1.17	28	14.84	-41
NB8	0.99	52	11.11	-19

The contradiction between the EDX:S-content and IEC data reported for some of the non-PBI based membranes (NB4, 5, 7 and 8) can be attributed to the precision limit of the EDX-data as discussed previously (Section 4.2.2.1), which is related to the fact that the elemental composition determined is a function of the type and amount of accompanying elements present in the sample analysed. As a result, the S-content due to the EDX technique may vary considerably between samples as was shown in Section 4.2.2.1. It can be assumed that the loss of membrane constituents, as indicated by the weight change, would result in an elemental decrease of some components which would in turn result in an increase of the sulfur content. It should also not be excluded that residual unreacted H_2SO_4 could have remained on, or within the membrane after treatment in spite of the washing, which could account for the S-content increases reported. In view of the uncertainties pertaining to the EDX-data, the further discussion will focus on the IEC results.

Since NB1 and 2 have the same composition, it is interesting to note the difference in IEC values obtained for these two membranes. The high IEC value reported for NB2 before treatment in comparison with NB1 (Table 4.3) supports the poor stability witnessed in the presence of additional $-SO_3H$ groups that most likely did not cross-link completely within the covalent network [13]. The negative IEC change and corresponding decrease in S-content reported for NB2 supports the loss of polysulfonate macromolecules from the entangled network as was suggested in view of the decrease in weight discussed in Section 4.3.1. The same initial difference in IEC measured for the similar membranes NB4 and 5 also suggest less efficient

cross-linking and additional -SO_3H groups present in the covalent network of membrane NB5 before treatment, explaining the increase in thickness observed for NB5. The difference in initial IEC values reported could also be due to the difference in thicknesses (Section 4.3.1) reported for membranes NB4 and 5.

The decreased IEC reported for the PEEK-SCl blends (NB4-6) is in agreement with the weight losses reported from entangled macromolecules. However, the increased S-content reported for NB4, 5 and 6 suggests an increase in the hydrophilicity of membrane components and supports the increase observed in membrane thickness (swelling) for membranes NB5 and 6 [14]. The increased IEC values reported for the sPSU-PFS-membranes (NB7 and 8) further support the argument of sulfonation of the sPSU-component as proposed by the physical changes in Section 4.3.1(c).

The FTIR spectra recorded before and after treatment for each of the investigated membranes correspond to the changes noted for the IEC values (Table 4.3) and weight losses (Figure 4.8) reported for the non-PBI based membranes due to the H_2SO_4 treatment. Before and after treatment the same peaks were observed within the spectra suggesting no significant change in the chemical structure of the membrane, but reduced intensities were observed for some membranes. As an example, the reduced peak intensity observed for NB2 after treatment is presented in Figure 4.13. Since the intensity of an absorption band is directly related to the number of specific bonds present [15,16], the decreased intensity observed is likely due to the loss of membrane fragments (macromolecules), confirming the weight losses presented in Section 4.3.1.

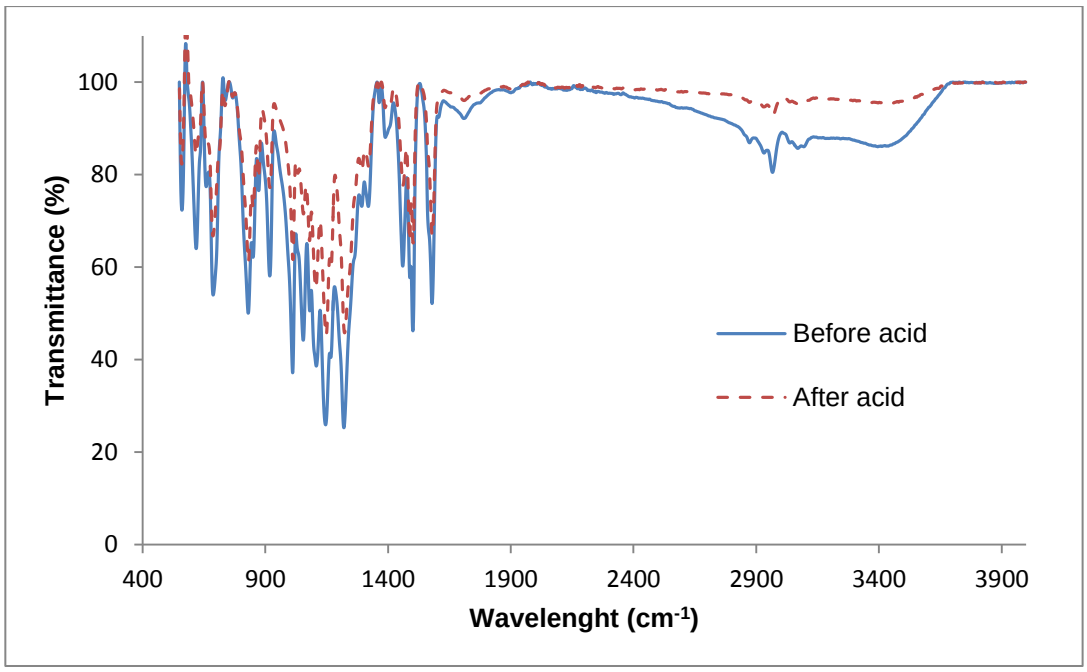

Figure 4.13: FTIR spectra of membrane NB2 before and after H_2SO_4 treatment.

The less significant IEC-changes of NB3, 4 and 6 of the non-PBI based membranes corresponded with the deviation noted for the broad band around 3200-3600 cm^{-1} of the O-H stretching vibration characteristic of $–SO_3H$, associated with acids [17] as can be seen in Appendix B. The slightly higher spectra intensities reported after treatment for membrane NB5 (Appendix B), also confirmed by the increased S-content, can be attributed to the partial sulfonation of the PEEK-component.

For each non-PBI based membrane, TGA data for the before and after treatment membranes were obtained to determine whether a change in the thermal stability occurred due to the H_2SO_4 treatment. Variation in the TGA signals would serve as an indication of an altered membrane composition and structure due to the H_2SO_4 treatment. The TGA signal for membrane NB2, shown in Figure 4.14, serves as an example of the visible deviation in the thermal stability due to the 80 wt% H_2SO_4 exposure of the membrane material. The TGA data for all the other non-PBI based membrane series is presented in Appendix B.

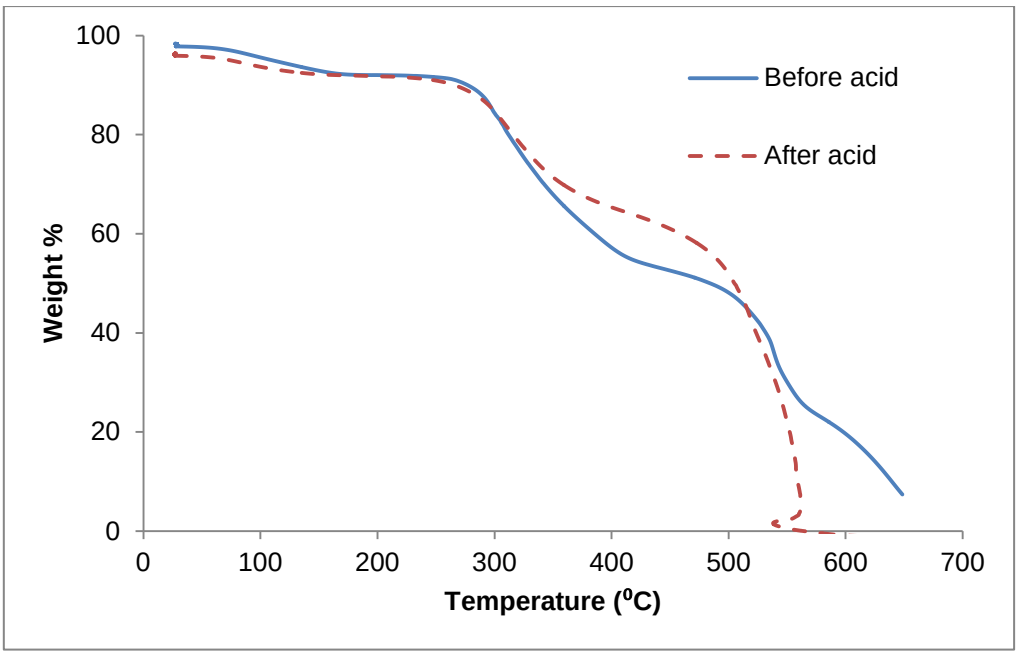

Figure 4.14: TGA signal recorded for membrane NB2 before and after acid treatment.

From the TGA studies that were done in triplicate for Nafion®212 (Section 4.2), the regions of maximum weight loss were identified by calculating the first derivative of the TGA signals recorded (Figure 4.7). Similarly, the first derivative of the data presented in Figure 4.14 for NB2 and Appendix B for all the other non-PBI based membranes was plotted (data not shown) and the regions of maximum change identified. For NB2, the regions (both before and after acid treatment) were in the ranges of 30-200, 250-400 and 450-600 °C, with the maximum changes in weight (chosen) at 80, 300 and 500 °C. According to literature these temperatures can generally be attributed to the following:

- 80 °C: Water evaporation [18,19]
- 300 °C: Thermal sulfonic acid splitting-off [18,19]
- 500 °C: Thermal degradation of the polymer backbones [18,19]

The difference in weight changes (%) before and after H_2SO_4 treatment at 80, 300 and 500 °C, according to the TGA graphs (Figure 4.14 and Appendix B), is summarised in Figure 4.15. The increased thermal stability noted for NB2 after the acid treatment (Figure 4.14) in the 300 to 550 ^{0}C region can be ascribed to the loss of shorter membrane chain constituents during the post treatment wash (weight loss, IEC, S-content). With these fragments already removed from the blend, backbone degradation of the polymer only occurs later at higher temperatures, but ultimately degrades quicker after treatment (470 ^{0}C) than before treatment (520 ^{0}C). This

increase can also be attributed to sulfonation of the blend membrane and the subsequent stabilisation of the polymer backbone (320 – 470 ^{0}C).

In terms of the other non-PBI based membranes, a negligible deviation in TGA signals was observed except for membranes NB7 and 8 in the 500 ^{0}C region. Since this region is associated with the degradation of the polymer backbone, it confirms that the sPSU-membrane's thermal stability is affected by the absence of a partially fluorinated cross-linker [9] in an H_2SO_4 environment.

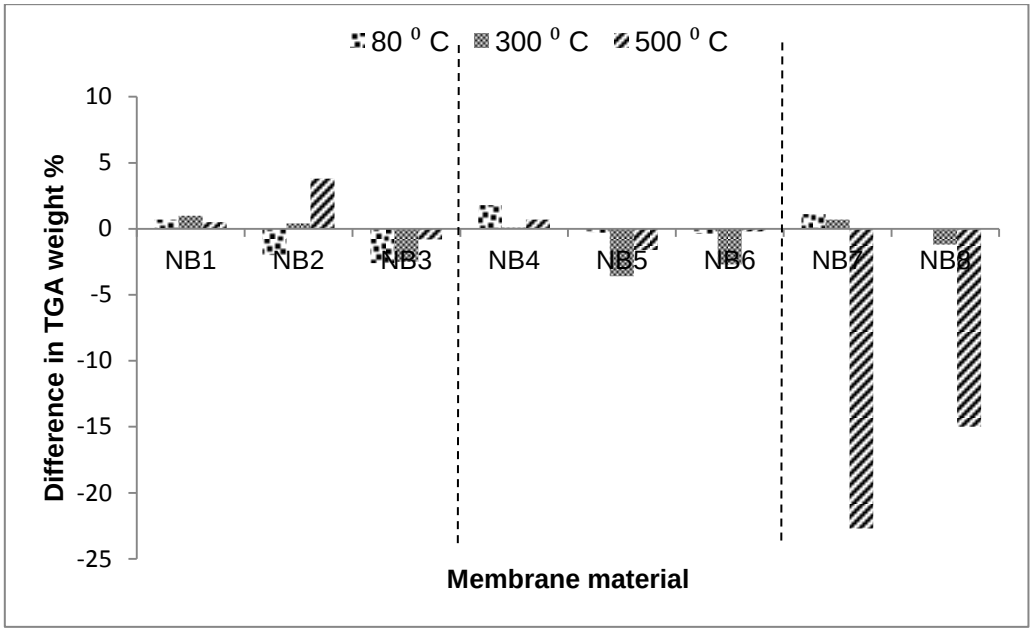

Figure 4.15: Change in weight % determined from TGA-curves for non-PBI based membranes before and after treatment.

4.4 PBIOO based membranes

4.4.1 Physical changes

The weight changes for all PBIOO based membranes evaluated are shown in Figure 4.16. For the discussion on the physical changes, the three PBIOO based groups will be divided according to their acid copolymer, which according to Table 3.1 include sPEEK (PB1-3), sPSU (PB4-6) and PKA9l (PB7 and 8) type membranes.

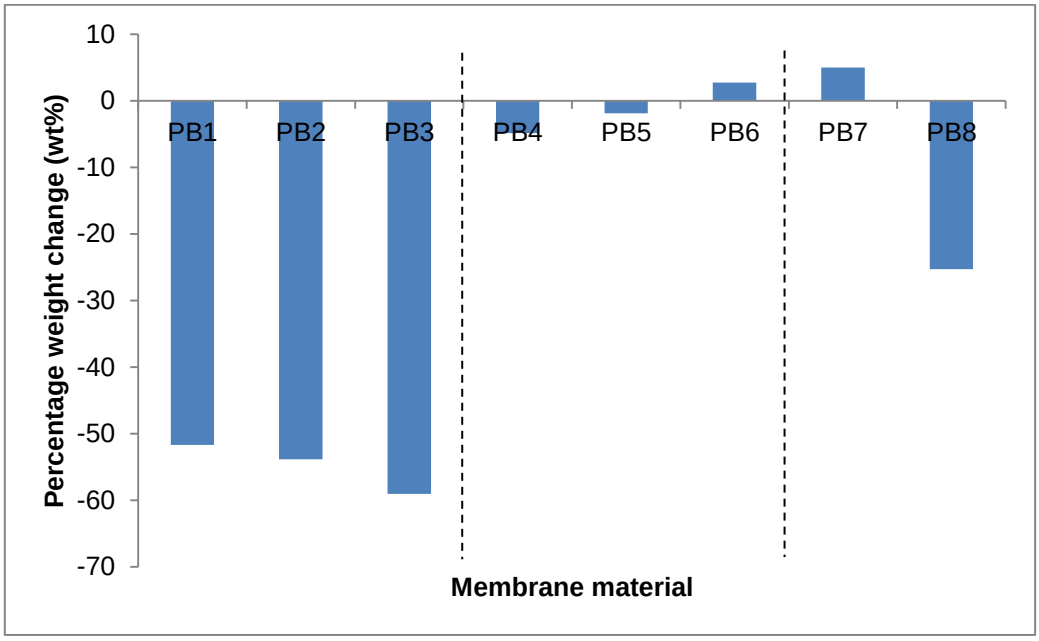

Figure 4.16: Weight change of PBIOO based membranes due to H_2SO_4 treatment.

a) The sPEEK-PBIOO blend (PB1-3)

It is clear from Figure 4.16 that the presence of the sPEEK resulted in a significant weight loss not observed when either sPSU or PKA9l were present. This significant weight loss noted for the sPEEK-PBIOO blended membranes is most likely due to sulfonation of the sPEEK component followed by the dissolution of blend membrane constituents during the repeated washing of the membranes after treatment. Furthermore, the sPEEK membranes appeared wrinkled and less transparent (opaque) after treatment with the addition of colour change as can be seen in Figure 4.17, supporting the partial dissolution of blend membrane constituents.

It seems that the sPEEK polymer is susceptible to hydrolysis when exposed to such harsh conditions as were used in this study (80 wt% H_2SO_4 at 80 ^{0}C) [9,20]. According to Schuster *et al*. [21], the hydrolysis reaction is greatly affected by the kind of substitution of the aromatic ring

containing the sulfonic acid (-SO_3H). Therefore, in the presence of the electron withdrawing carbonyl (-CO-) group present on the backbone of the sPEEK polymer, the formation of the aromatic sulfonic acid intermediate complex is destabilised, influencing the rate-determining step in favour of the back-reaction, i.e. hydrolysis [21].

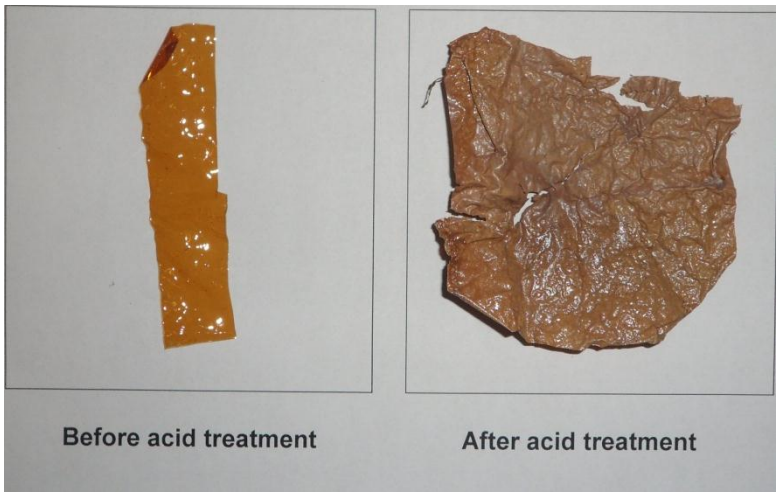

Figure 4.17: Visual of sPEEK membranes (PB2) before and after H_2SO_4 treatment.

Possible sulfonation of the PBIOO component [22], which comprises 33.7 % of the sPEEK containing membrane, resulting in its dissolution from the blend could also have contributed to the weight loss observed, as it has previously been shown that the backbone of the PBIOO membrane can be directly sulfonated (see Equation 4.1) in the presence of a strong electrophile as is the case in 80 wt% H_2SO_4 [23]. However, its contribution was probably smaller than that of the sPEEK when considering that no significant weight loss was observed (Figure 4.16) when no sPEEK was present (BP4-8).

Basic polymer-Im + H_2SO_4 → [Basic polymer-ImH]$^{+}$[HO_3S] (4.1)

In addition, the bisphenol A unit present in the low-molecular cross-linker (Table 3.1) of Bis-A within membranes PB1 and 2 is known to be potentially acid sensitive [11] (Section 4.3.1). Hence, it would seem that the presence of the additional covalent cross-linker within membrane PB1 and 2 did not significantly contribute to the stability of the membrane when comparing to PB3, which did not contain Bis-A. In addition to the acid sensitivity, the ineffective covalent cross-linking could also have been caused by the low PBIOO content present (<34 %, Table 3.1) within the blends in relation to the acid polymer content.

When considering the change in thickness (Figure 4.18), it is clear that PB1 and 3 nearly doubled in thickness, which is interesting compared to the significant reduction in weight

observed. The PB2 membrane became brittle after treatment and crumbled when touched. Therefore, no change in thickness was measureable for PB2 indicated by the X in Figure 4.18. While it is not clear what the origin of the significant swelling is, the results confirm the unstable character of the sPEEK containing PBIOO membranes in a harsh H_2SO_4 environment.

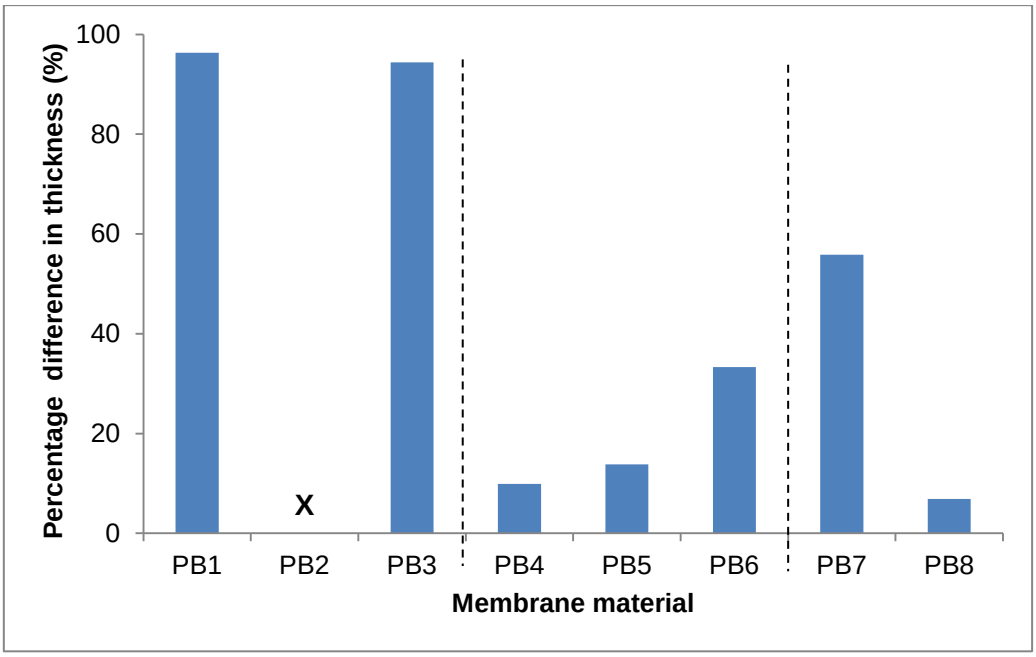

Figure 4.18: Percentage difference in thickness reported for the PBIOO based membrane after treatment.

b) The sPSU-PBIOO blend (PB4-6)

When replacing the sPEEK with sPSU, a significant increase in stability was observed. According to Figure 4.16, only a slight weight change due to the H_2SO_4 treatment occurred. This increased stability is understandable in view of the electron-donor ether group present in the sPSU polymer resisting hydrolysis due to the stabilisation of the intermediate complex [21] in contrast to the -CO- group of sPEEK (Section 4.4.1(a)). In addition, the aromatic sulfone group oriented *meta*- in terms of the substituted sulfonic group ($-SO_3H$) of sPSU (Appendix A), will most likely sterically hinder further sulfonation at the *ortho*-position.

When considering the small weight changes observed in Figure 4.16, it is interesting that the sPSU blends PB4 and 5, which are acid excess blends (Table 3.1), displayed a decrease in weight, while the base excess blend PB6 showed a slight increase in weight. This slight increase observed for PB6 could possibly be attributed to a partial splitting-off of the ionical cross-links by the attack of the strongly acidic sulfuric acid, leading to the formation of

imidazolium hydrogen sulfate salt groups from the PBIOO as shown in the following reaction equation [23]:

Basic polymer-$ImH^{+-}O_3S$-acidic polymer + H_2SO_4→
Basic polymer-$ImH^{+-}HO_3S$ + HO_3S-acidic polymer (4.2)

The difference between PB4, 5 and 6 can also be seen when considering the % difference in thickness (swelling) results (Figure 4.18), where the change in thickness of PB4 and 5 was less than 20 %, while the thickness change of PB6 was close to 40 %, confirming the breakage of the ionical cross-linking due to the H_2SO_4 treatment and the improved stability (Figure 4.16) attainable when using PBIOO to a lesser extent (lower content) (<6 %) in sPSU-PBIOO blends.

c) The PKA-PBIOO blends (PB7 and 8)

While PB7 displayed a slight increase in weight, PB8 showed a significant decrease in weight after H_2SO_4 treatment (Figure 4.16). The cause for this variation can only be ascribed to their different acid:base ratios present within the blends (Table 3.1) as this was the only difference between the membranes. The decrease in weight as noted for PB8 (acid:base = 30:70) can be attributed to the sulfonation of the PBIOO backbone, as suggested in Equation 4.1, accompanied by the partial dissolution from the blend, as further sulfonation of the PKA acid polymer seems unlikely.

As can be seen from Figure 4.18, there is a definite correlation between the high PBIOO-content membranes (base excess, Table 3.1) and the increased swelling reported for PB6 and 7, suggesting a breakage of the ionical cross-links and formation of imidazolium hydrogen sulfate salt groups as demonstrated in Equation 4.2. Due to the lower acid polymer (PKA) content of PB7 (acid:base = 8:92), limited cross-linking is possible in this membrane. A further splitting-off of the (ionical) cross-links by the attack of the strongly acidic sulfuric acid during treatment could further help explain the increased thickness change measured for the membrane.

4.4.2 Chemical changes

The data obtained from SEM-EDS analysis, IEC measurements, FTIR and TGA for the PBIOO based membranes will be presented and compared to further clarify the different acid stabilities observed.

The relatively high decrease in IEC values and S-contents noted for the sPEEK membranes (PB1-3) in Table 4.4 further support the assumption that sulfur containing membrane constituents were washed from the membrane during the acid treatment and subsequent washing (see Section 4.4.1(a)). Results from the physical changes discussed for the sPSU blends (PB4 and 6) correlate to the insignificant changes listed in Table 4.4, with the exception of PB5.

Table 4.4: IEC values and sulfur content (SEM-EDX) of the PBIOO based membranes measured before treatment and the difference determined after treatment.

Membrane	IEC (total, exp.)		EDX: S-content	
	Before [meq SO_3H/g]	Change (%)	Before (%)	Change (%)
PB1	2.90	-17	11.9	-46
PB2	2.40	-74	13.6	-63
PB3	3.40	-31	11.9	-65
PB4	1.80	2.0	18.7	-25
PB5	1.30	35	7.5	122
PB6	n.a.	n.a.	7.2	-28
PB7	n.a.	n.a.	2.4	-25
PB8	n.a.	n.a.	5.45	-63

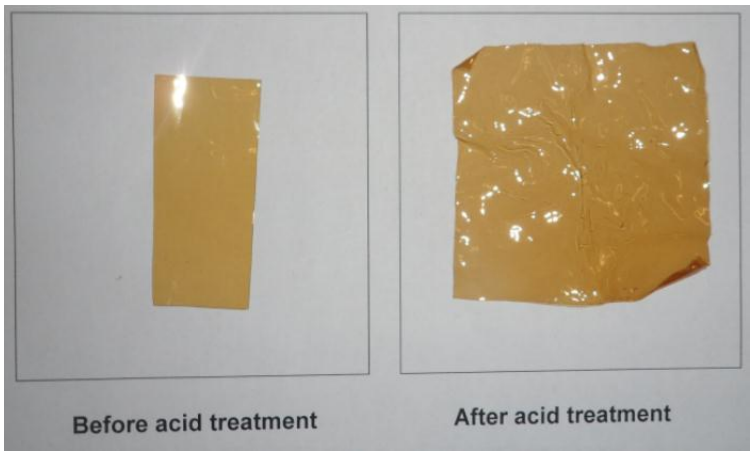

Figure 4.19: Visual of PB5 membrane before and after H_2SO_4 treatment.

While both the weight changes (Figure 4.16) and the visual appearance (Figure 4.19) suggest that PB5 remained stable after treatment, the results from Table 4.4 indicate that sulfonation of the blend and possible dissolution of shorter chains (oligomers), as discussed previously, might

have occurred. This is in line with literature where it has been shown that the sulfonation of both i) the PBIOO components, as illustrated in Equation 4.1, and ii) the polyethersulfones present within the sPSU polymer is possible in the presence of H_2SO_4 [6,7]. The possible sulfonation of the polyethersulfone at the *ortho*-position to the ether bridge within the sPSU polymer is shown in Figure 4.20 *(adapted from [23])*.

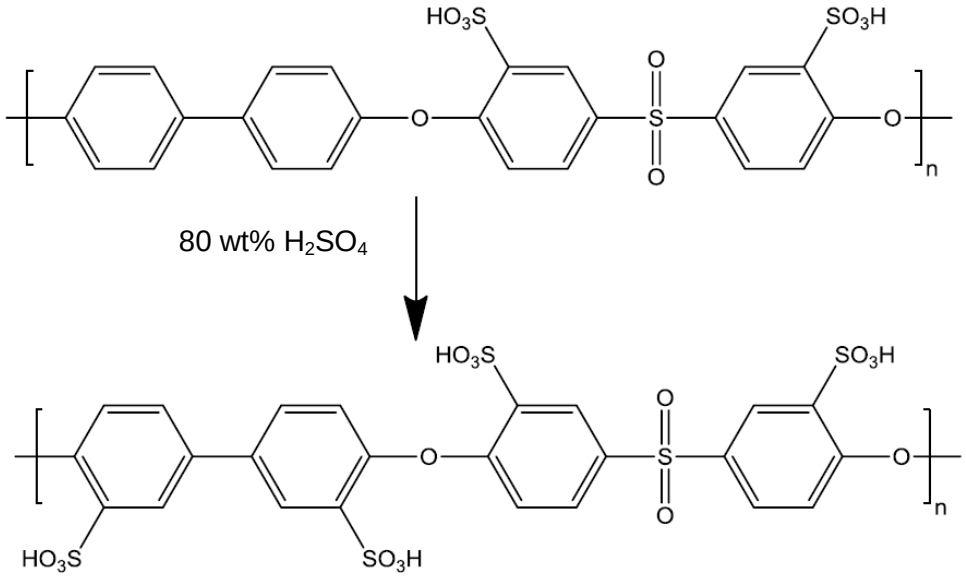

Figure 4.20: Possible sulfonation of the sPSU polymer's backbone during H_2SO_4 treatment *(adapted from [23]).*

No IEC measurements were measurable and hence reported (Table 4.4) for the base excess membranes (PB6-8) due to the sulfonic acid (–SO_3H) groups of the acidic blend component being bound to PBIOO through acid-base bonds, resulting in negligible amounts of free –SO_3H groups [23] leading to IEC values that were too low to measure.

The lower S-content measured for PKA blends PB7 compared to PB8 is attributable to the acid:base ratio (refer to Table 3.1) as sulfur is only present as –SO_3H groups within the acid component of the membrane. The decrease noted in S-content after treatment corresponds to the suggested dissolution of membrane constituents following the sulfonation of the PBIOO backbone bonded to the –SO_3H groups of the acidic blend component confirming the observations made for the physical changes (Section 4.4.1(c)).

The FTIR spectra recorded before and after treatment for most of the PBIOO blended membranes (Appendix C) correspond to the changes noted in Table 4.4 for the S-content measured. The EDX reported a decrease in S-content for all PBIOO based membranes (except

for PB5) and is supported by the reduced intensity observed in the FTIR spectra for the membranes after treatment, indicating a reduction in the number of bonds or groups present within the blend membrane (Section 4.3.2). When considering the FTIR spectra of PB2 (Figure 4.21) for example, the reduced intensity observed for the O-H stretching vibration, associated with acids, as the broad band around 3200-3600 cm^{-1} [17], suggests a reduction in the number of -OH groups [24] present within the blend membrane, further confirming the partial dissolution of blend membrane constituents. Other than the O-H stretching vibration characteristic of $–SO_3H$, further changes associated with the sulfonic acid group correspond to S=O and S-O stretches [17] located within the "fingerprint" region from 1500 to 400 cm^{-1}. Similar tendencies were observed for all the membranes where a decrease in the S-content was observed (Appendix C).

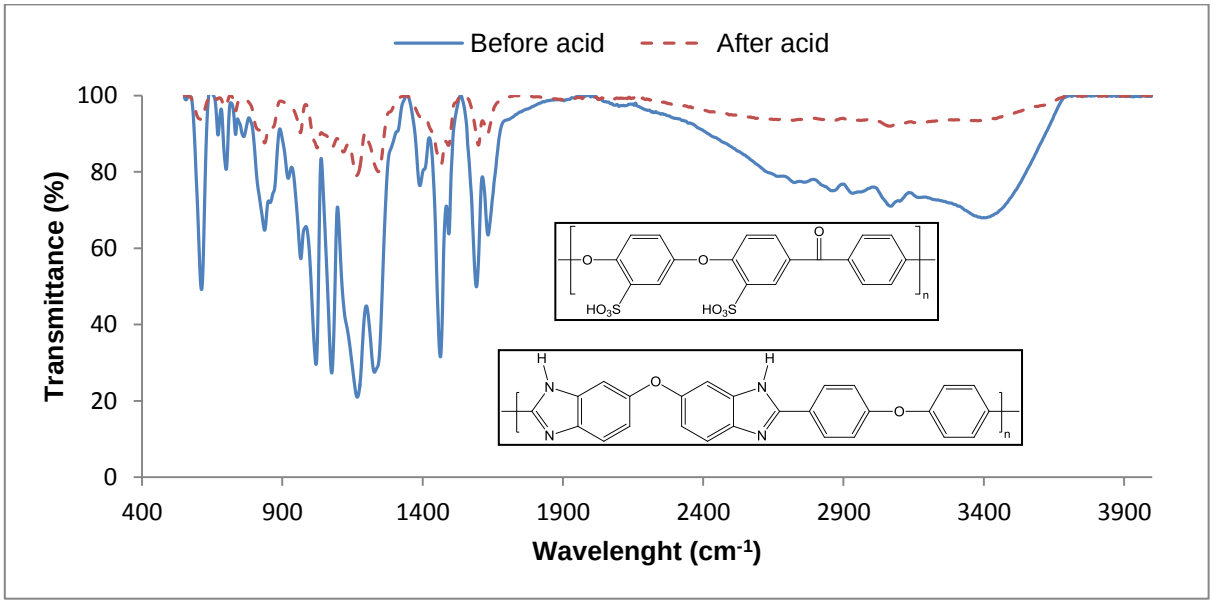

Figure 4.21: FTIR spectra of PB2 before and after H_2SO_4 treatment.

The only membrane showing an increase in the S-content, however, without showing a weight change, was PB5. The near identical before and after acid treated FTIR-spectra, shown in Figure 4.22, support the assumed stability of the sPSU-membrane (PB5) in an 80 wt% H_2SO_4 environment. It should, however, be noted that the SEM-EDX analysis was completed on the cross-section of the membrane (IEC measurements on a 24h immersed membrane), while for the FTIR no sample preparation was required and the membrane was analysed perpendicular to the surface. The mentioned differences (surface area of investigation and sample preparation) can possibly account for the contradictions in the data and should further be investigated for the different analytical techniques.

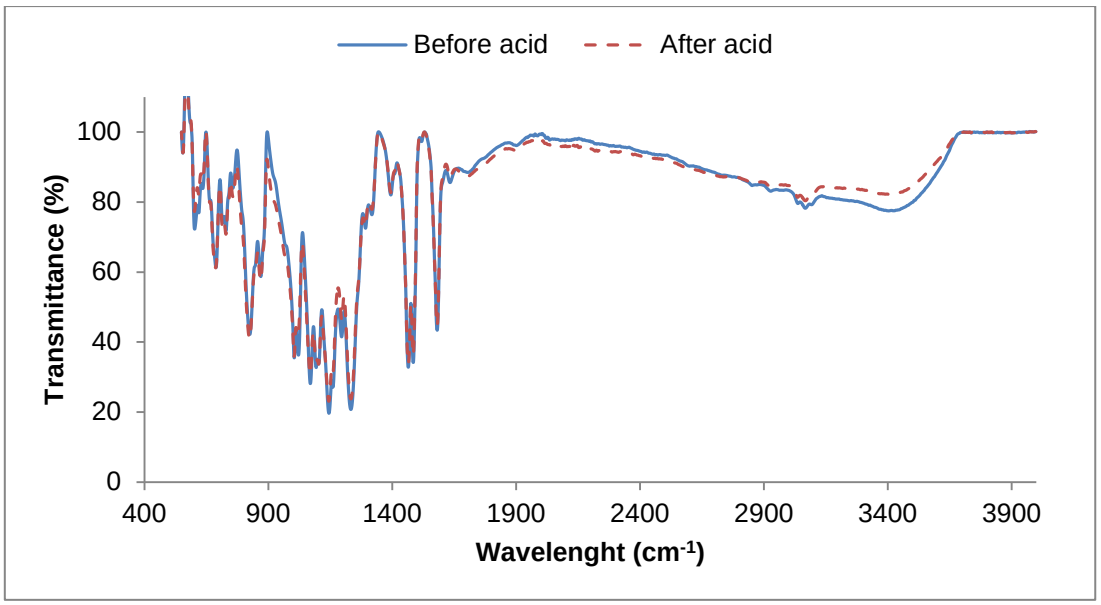

Figure 4.22: FTIR spectra of PB5 blend before and after H_2SO_4 treatment.

The TGA data obtained for the PBIOO blended membranes (Appendix C) was investigated at the identified maximum weight loss regions (Section 4.3.2) and the change in weight (%) before and after H_2SO_4 treatment at 80, 300 and 500 °C is summarised in Figure 4.23.

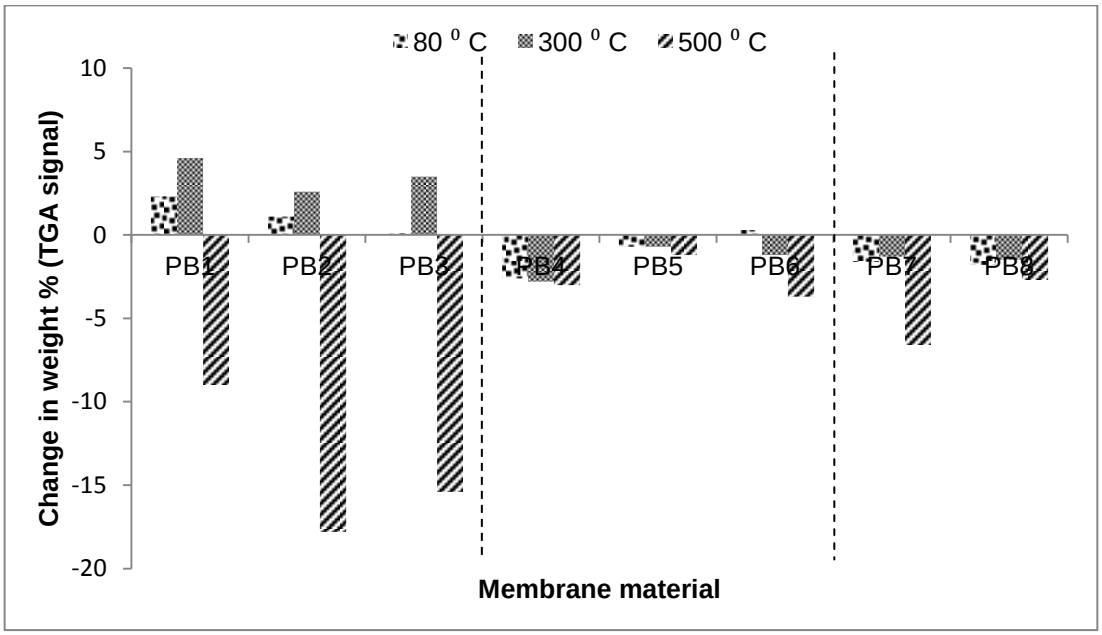

Figure 4.23: Change in weight % determined from TGA for PBIOO based membranes before and after treatment.

According to Figure 4.23, the TGA signals of the sPEEK blended membranes (PB1-3) deviate significantly more, especially at 500 °C, than the minimal deviation in thermal stability noted for the sPSU and PKA blended membranes. This supports and confirms the decreased stability of the sPEEK blended membranes as indicated by the characterisation data previously discussed.

The deviation in weight % noted for membrane PB1 is captured in Figure 4.24, indicating an altered membrane structure (sulfur protected) where degradation of the polymer backbone starts later, but proceeds quicker above 400 ºC when compared to the before treatment. A similar pattern was observed for PB2 and PB3 (Appendix C), while PB4-6 showed no significant change in the TGA data. For PB7 and 8, a slight decrease in stability above 500 ºC was observed after H_2SO_4 treatment, likely due to sulfonation of the PBIOO backbone and the splitting-off of ionic cross-links followed by the dissolution of blend components as suggested by the physical changes in Section 4.3.1(c).

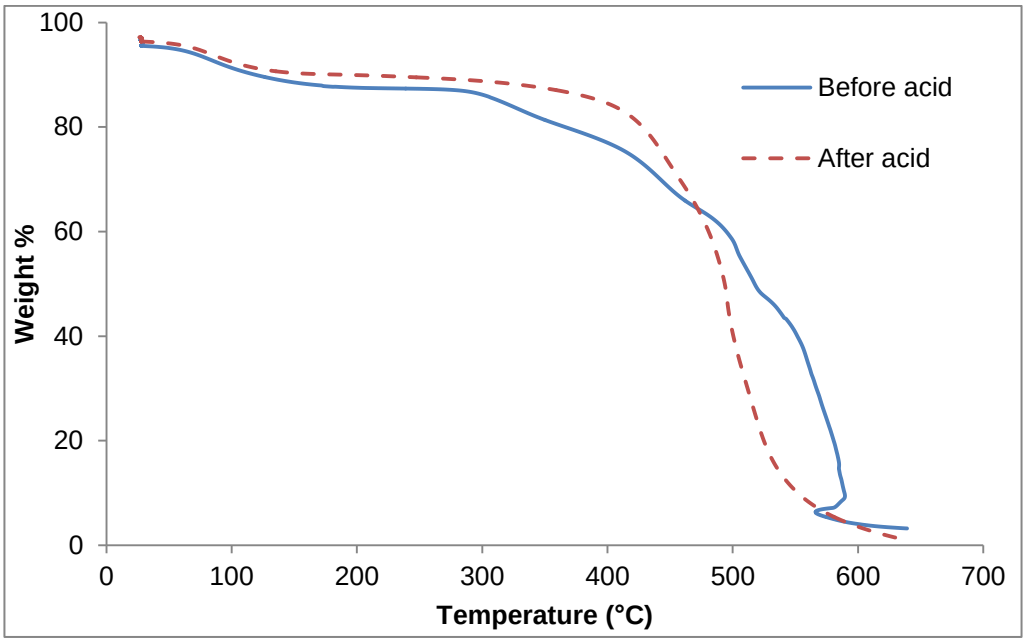

Figure 4.24: TGA signal recorded for membrane PB1 before and after acid treatment.

4.5 F_6-PBI based membranes

4.5.1 Physical changes

As was done for the previous two membrane groups, the F_6-PBI blended membranes will also be discussed in terms of their acid copolymer(s) as well as the addition and possible difference of cross-linkers. Discussion on the physical changes of the F_6-PBI based group is divided as follows: FPB1 and 2 consisting of sFS-F_6-PBI blend; FPB3-7, where PFS was added as a third copolymer to the sFS-F_6-PBI blend; FPB8-10, where either a cross-linker (Bis-A or DIB) or a third copolymer (A095) was added to the sFS-F_6-PBI blend; and finally FPB11, consisting of a sPSU-F_6-PBI blend.

From the y-axis of Figure 4.25 it is clear that the weight changes determined for all the F_6-PBI based membranes were insignificant, suggesting that overall stable blend membranes were obtained irrespective whether the acidic sFS- or sPSU-components were blended with the basic F_6-PBI component. However, upon closer inspection, with accompanying characterisation techniques, to be discussed subsequently, slight differences in stability become more evident. The general weight losses observed for the sFS blend membranes (FPB1-10) can partially be traced back to the acidic sFS component. The loss of low molecular fractions of the sulfonated polymer, (oligomers) is characteristic of polyarylene condensation polymers, where upon polycondensation reactions, not only macromolecules, but also oligomeric chains are formed [12].

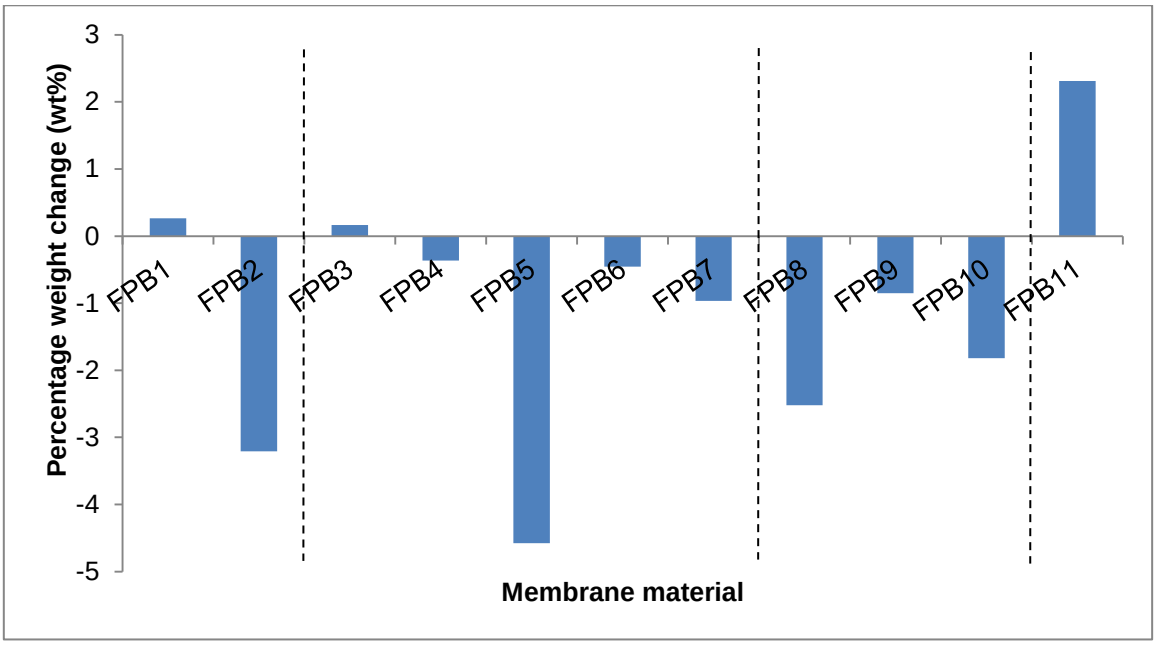

Figure 4.25: Weight changes of the F_6-PBI based membranes due to H_2SO_4 treatment.

a) The sFS blend (FPB1 and 2)

While the blend membranes FPB1 and 2 only consist of the copolymers sFS and F_6-PBI, their different acid:base ratios (see Table 3.1) seem to be the cause for the different weight changes observed after H_2SO_4 treatment. As discussed in Section 4.4.1 for the base excess membrane PB8, the weight loss reported for the base excess membrane FPB2 (acid:base = 30:70) can be attributed to the sulfonation of the basic polymer (PBIOO backbone) accompanied by its partial dissolution from the blend, as well as partial sulfonation of the sFS and/ or oligomer dissolution. The slight increase observed for FPB1 is possibly due to the formation of imidazolium hydrogen sulfate salt groups of the PBI component as discussed in Section 4.4.1(b). The corresponding increased thickness reported for the acid-excess blend (FPB1, Table 3.1) in Figure 4.26 could be due to limited cross-linking possibilities in view of the small base polymer content, or the subsequent splitting-off of ionical cross-links in the strongly acidic H_2SO_4 environment.

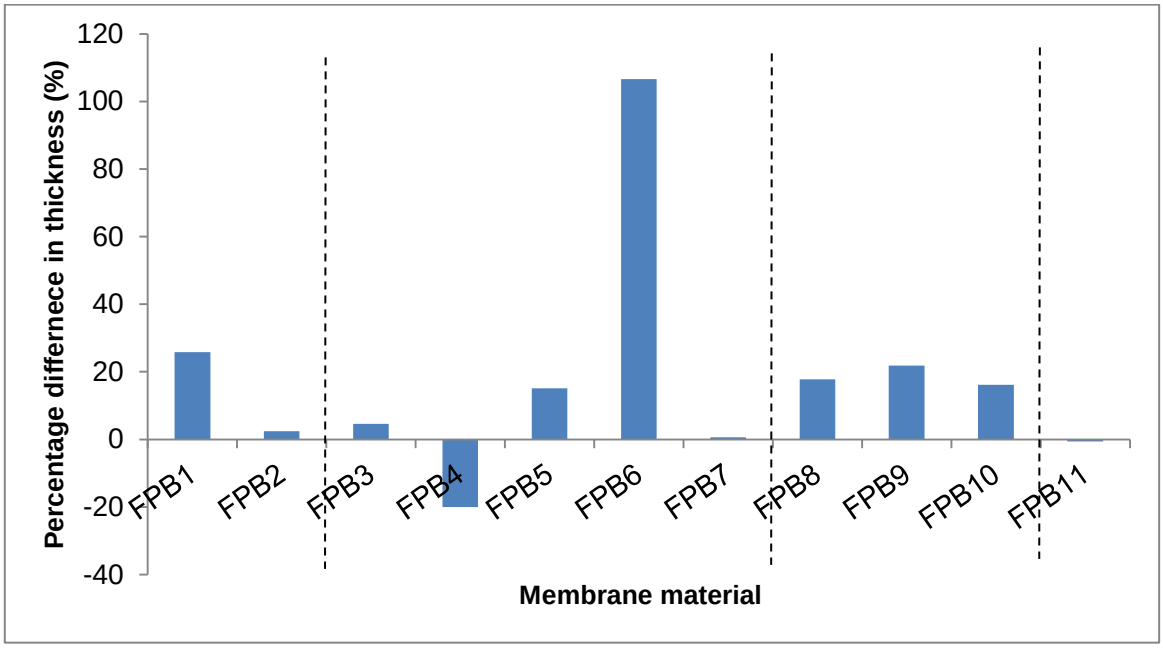

Figure 4.26: Percentage difference in thickness reported for the F_6-PBI based membranes after treatment.

b) sFS-PFS additive blend (FPB3-7)

The strong swelling associated with ionically cross-linked membranes (typically acid-base blend membranes) due to the splitting-off of ionical cross-links at temperatures above 70 ^{0}C is known [8,12]. The swelling effect was also observed in this study as illustrated in Figure 4.26. In an attempt to elucidate the cause of the swelling, the concentrations (expressed as % of the total weight) of the various copolymers in this group of membranes are presented in Figure 4.27.

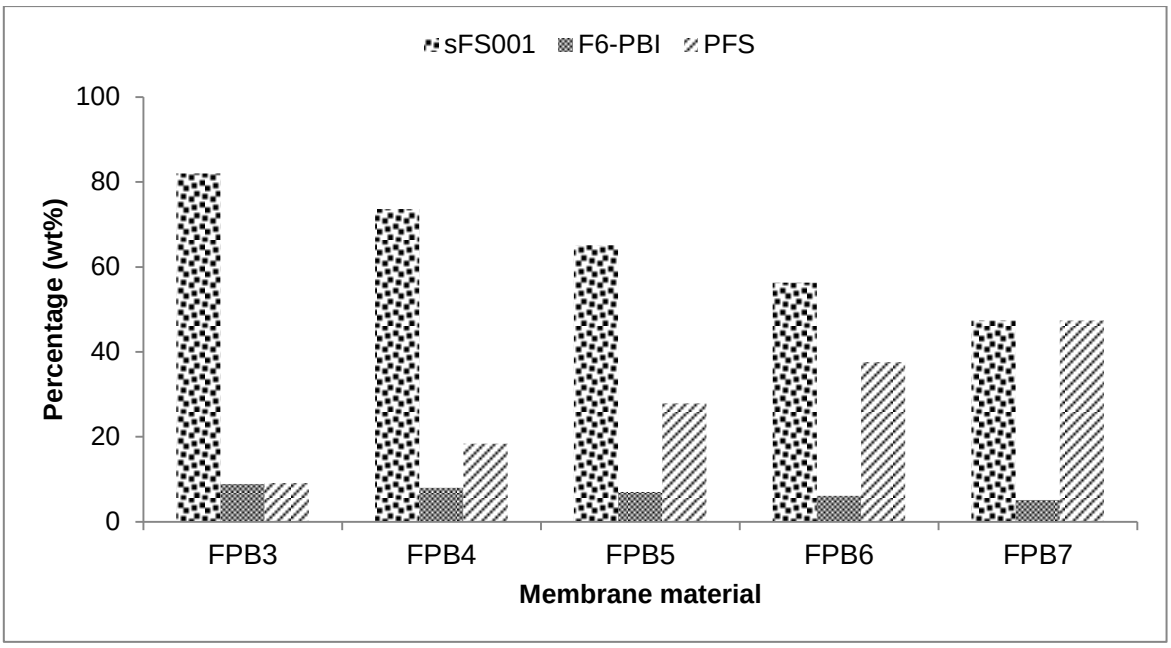

Figure 4.27: The concentrations of the copolymers present in the acid-base membranes FPB3-7.

The decrease in F_6-PBI and sFS content and corresponding PFS content increase clearly influences the stability of the sFS-PFS blend when considering the weight changes (Figure 4.25) and thickness changes (Figure 4.26) reported for the sFS-PFS additives. According to Figure 4.27, it seems that either an excess of sFS (FPB3) or equal quantities of sFS and PFS (FBP7) is favourable.

Weight loss can be attributed to sulfonation of the sFS and/ or the F_6-PBI polymer components as discussed before, followed by dissolution of those components during the washing of the membrane material after treatment. It is likely that the PFS component is sulfonated in the 80 wt% environment as it is a precursor of sFS and the bisphenol A unit present in the PFS polymer is known to be acid sensitive [11]. Ultimately the weight and thickness changes reported indicate that the polymer concentrations of membrane FPB5 (weight loss) and FPB6 (thickness increase) are not favourable, which is further supported by the chemical changes noted by IEC measurements and SEM:EDX analysis (see Section 4.5.2).

Besides the possible influence of the difference in initial (before treatment) thickness measured for FPB6 and 7 (58 and 65 µm), which was approximately double the thickness of FPB3, 4 and 5 (average of 30 µm), the membrane structure of both FPB6 and 7 should also be included in the discussion of the observed change in thickness. The poor mechanical stability of FPB6 became evident when the membrane layers separated during the post-treatment handling of the membranes, suggesting partial immiscibility of the polymers [25] in membrane FPB6. In support

of the physical results presented, the SEM micrographs of FPB6 before and after acid treatment (Figure 4.28) support the unstable character of the blend membrane (a) by the dissolution of membrane fragments after treatment (b) due to splitting-off of cross-links leading to the observed 102 % change in thickness.

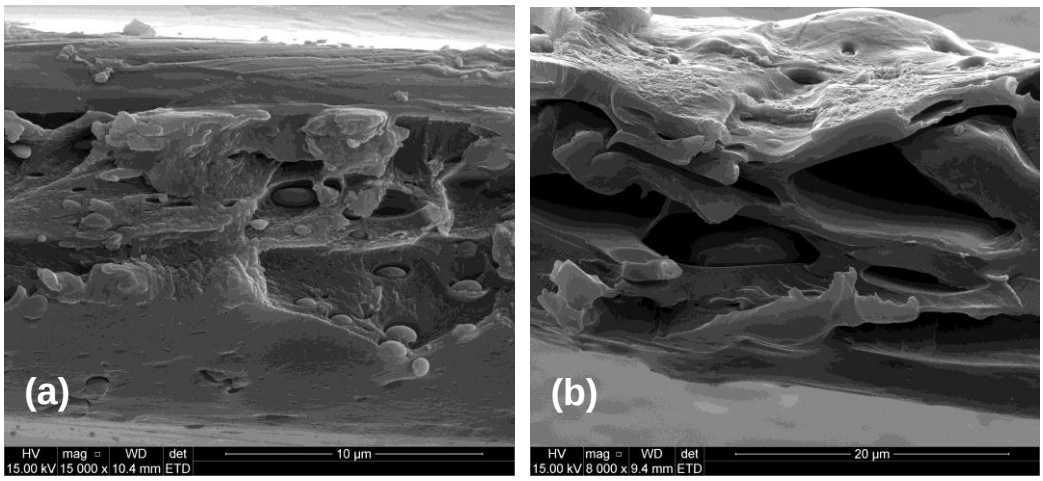

Figure 4.28: SEM micrographs of the cross-section of membrane FPB6 before (a) and after (b) the H_2SO_4 treatment.

c) sFS-cross-linker blend (FPB8-10)

For membrane FPB9, a smaller weight loss was observed when compared to FPB8 and 10 containing the cross-linker DIB. The weight loss can be attributed to the bisphenol A unit of the sFS membrane, which is known to be potentially acid sensitive [11]. The washing of the membrane material could also have contributed to the weight loss as the membranes were wrinkled after the acid treatment and a significant change in colour was noted for the FPB10, which is an indication of the partial dissolution of blend membrane constituents [14].

It is clear that by the addition of a covalent cross-linker, stable membranes were obtained, displaying a similar change in thickness (Figure 4.26). The change in thickness reported was slightly higher for membrane FPB9, likely due to the weaker cross-linking of DIB in comparison with Bis-A related to their difference in acid sensitivity. The significantly higher thickness change observed for example for FPB1 was therefore probably due to the absence of any covalently bound cross-linking. The increased thickness change observed for the covalent-ionically cross-linked membranes (FPB8-10), could be ascribed to a slight sulfonation leading to an increase in the hydrophilicity and hence an increase in the thickness [14].

d) sPSU-blend (FPB11)

The inclusion of the sPSU-component as acidic polymer resulted in more stability than when sFS was incorporated in terms of the physical changes observed (Figure 4.25 and 4.26). This is probably due to the acid sensitive bispenol A unit present within the sFS polymer, in comparison to the supposed hydrolysis resistant sulfon and ether functions of the sPSU polymer, as was discussed in Section 4.4.1(b) [21]. The slight increase in weight observed for FPB11 can possibly be attributed to the formation of imidazolium hydrogen sulfate salt groups from the PBI component as discussed in Section 4.4.1(b).

4.5.2 Chemical changes

The data obtained from SEM-EDS analysis, IEC measurements, FTIR and TGA for the F_6-PBI based membranes will be presented and compared to further clarify the different acid stabilities observed.

The increased IEC values measured after treatment for FPB1 (Table 4.5) confirms the partial splitting-off of the ionical cross-linking in the presence of the concentrated H_2SO_4 solution and the subsequent formation of imidazolium hydrogen sulfate groups in the PBI portion of the blend, supported by the weight increase observed. Similar to the base-excess membranes described in Section 4.4.2, no IEC values were measurable for FPB2 due to the negligible amount of free $–SO_3H$ groups [23]. The noted increase in S-content for FPB2, however, supports the possible sulfonation of the PBI-backbone, followed by dissolution of membrane fragments, as proposed by the weight change (Section 4.5.1(a)).

Table 4.5: IEC values and sulfur content (SEM-EDX) of the F_6-PBI based membranes measured before treatment and the difference determined after treatment.

Membrane	IEC (total, exp.)		S-content	
	Before [meq SO_3H/g]	Change (%)	Before (%)	Change (%)
FPB1	1.68	19.0	6.1	1.2
FPB2	n.a.	n.a	2.3	81.6
FPB3	1.91	10.5	7.4	32.4
FPB4	1.45	57.9	5.4	-10.1
FPB5	1.42	-4.2	6.7	-36.7
FPB6	1.42	-29.6	6.7	-42.6
FPB7	0.87	49.4	4.7	65.7
FPB8	1.98	8.6	11.2	-59.6
FPB9	1.77	9.6	8.7	-8.5
FPB10	1.65	13.3	3.5	20.4
FPB11	1.60	16.3	8.9	60.1

When considering the IEC values of the FPB3-7 series, the splitting-off of ionical cross-links is evident in membranes FPB3, 4 and 7, with the accompanying sulfonation of the PBI portion of the blend visible in the increased S-content reported for FPB7. The decreased S-content of FPB4 suggests the dissolution of membrane fragments during the post treatment wash due to the mentioned splitting-off of cross-links. The decrease in IEC measurements and S-content for FPB5 and 6 supports the dissolution of low molecular fractions (oligomeric chains) of the sFS-polymer as discussed in Section 4.5.1(a). This further confirms the swelling and weight loss reported for the mentioned membranes.

For membranes FPB8 and 9, the increased IEC measurements can be accounted for by the splitting-off of ionical cross-links as mentioned before (Section 4.5.1(c)). The accompanying decrease in S-content suggests the dissolution of membrane fragments (FPB8 and 9), while the increase noted for FPB10 indicates the possible sulfonation of the additional basic component (A095) present. The increased IEC measurements and S-content of membrane FPB10 further support the possible sulfonation of the sPSU polymer discussed in Sections 4.3.1 and 4.4.2 for sPSU-containing membrane blends.

As before, FTIR was used to determine whether a change in the chemical structure of the membrane took place due to the H_2SO_4 treatment. For the F_6-PBI based membranes (Appendix

D) visible deviations in the FTIR spectra were noted for FPB2 and to a lesser extent for membranes FPB9 and 10. An increased intensity in the FTIR spectra after treatment is noted for membrane FPB2, shown in Figure 4.29. This supports the previous discussion regarding the dissolution of the PBI-component for the base-excess blend membranes after sulfonation of the polymer backbone. The increased intensities observed are associated with the sulfonic acid group present at the wavelengths as discussed in Section 4.4.2, and corresponds to the increased sFS content in relation to the basic polymer after treatment which was confirmed by the increased S-content measured.

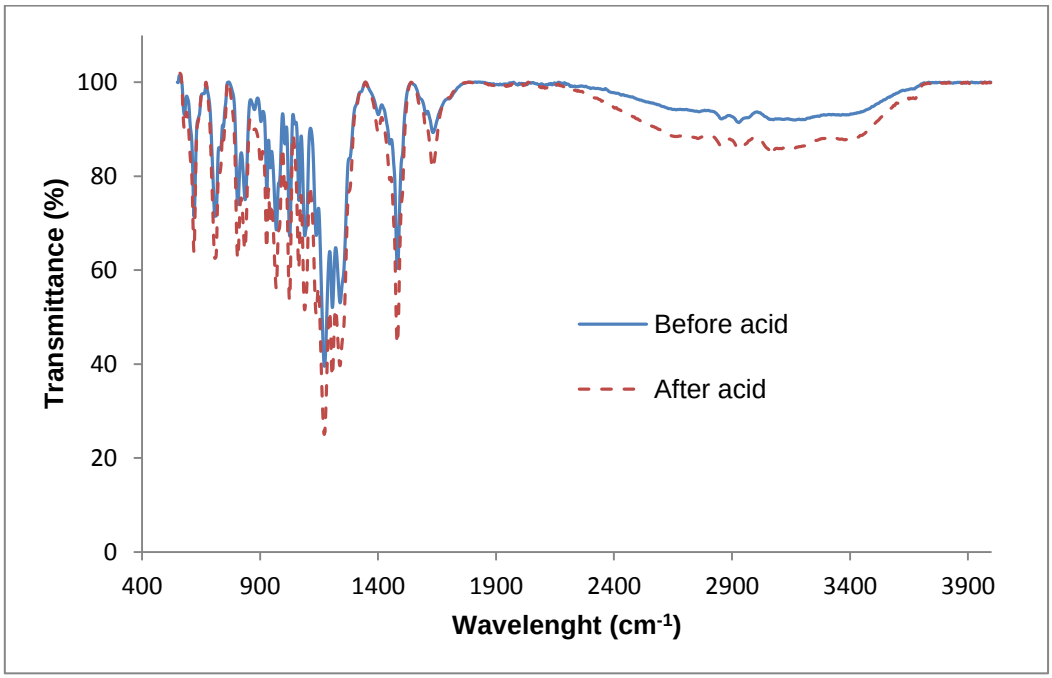

Figure 4.29: FTIR spectra of membrane FPB2 before and after H_2SO_4 treatment.

The slight decrease in FTIR spectra intensities noted for membrane FPB9 (Appendix D) is possibly due to the loss of membrane fragments from the post treatment wash as supported by the decrease in weight change. The slightly higher intensities noted after treatment for membrane FPB10 (Appendix D) with the accompanying increased S-content and IEC measurements can likely be attributed to the sulfonation in the electron-rich part of the A095´s polyethersulfone backbone, leading to an increased water-solubility, which could have led to the partial or superficial washing of the A095 component from the blend during the H_2SO_4 treatment [14].

Most of the partially fluorinated PBI (F_6-PBI) blend membranes showed small deviations in their TGA signals before and after treatment (Figure 4.30, Appendix D) confirming their stability under the investigated conditions. Only membranes FPB6 and 7 displayed a larger deviation in

the 500 ^{0}C region, suggesting that after treatment polymer backbone degradation, associated with weight changes at this temperature region (Section 4.3.2.), proceeds faster at a lower temperature. This is in support of the mechanical instability noticed from the SEM photos of the partial immiscible (inhomogeneous) membranes.

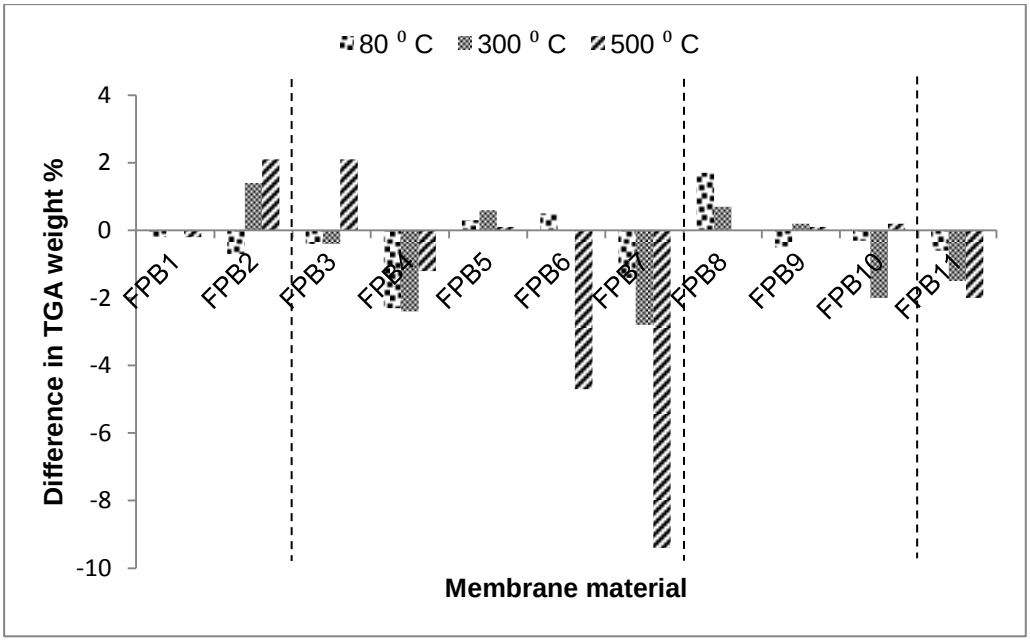

Figure 4.30: Change in weight % determined from TGA-curves for the F_6-PBI based membranes before and after treatment.

4.6 Conclusion

In this study, three groups of membranes, i.e. those not containing PBI, those containing PBIOO and those containing F_6-PBI, were subjected to H_2SO_4 treatment in order to determine their acid stability for future application in an SO_2 electrolyser.

After the 80 wt% H_2SO_4 treatment, large weight losses were reported within the non-PBI based and PBIOO based membrane groups in comparison with the minimal changes noted for the F_6-PBI based group. This is evidence of the improved stability in an H_2SO_4 environment due to the partially fluorinated basic polymer. The accompanying acid polymers within these groups were compared and the sPEEK/PEEK-containing blends displayed poor stability due to sulfonation resulting in the dissolution of membrane constituents and fragments. It was also shown that the addition of partially fluorinated non-functionalized polymers (cross-linkers) only marginally improved the stability of the membranes.

Additionally, it was shown that the type of cross-linking between blend components also influenced the stability of the membrane, where covalent cross-linking, as in the case of the non-PBI based membranes, was less effective than the ionical cross-linking present within the PBIOO and F_6-PBI based blend membranes.

4.7 References

[1] J. Kerres, D. Xing, F. Schönberger, Comparative Investigation of Novel PBI Blend Ionomer Membranes from Nonfluorinated and Partially Fluorinated Poly Arylene Ethers., Journal of Polymer Science: Part B: Polymer Physics, 44 (2006) 2311-2326.

[2] Ammrf, EDS Precision, In: Australian Microscopy and Microanalysis Research Facility. My scope training for advanced research., 2012. http://www.ammrf.org.au/myscope/analysis/eds/accuracy/

[3] A.C. Fernandes, E.A. Ticianelli, A performance and degradation study of Nafion 212 membrane for proton exchange membrane fuel cells., Journal of Power Sources, 193 (2009) 547-554.

[4] T. Kinumoto, M. Inaba, Y. Nakayama, K. Ogata, R. Umebayashi, A. Tasaka, Y. Iriyama, T. Abe, Z. Ogumi, Durability of perfluorinated ionomer membrane against hydrogen peroxide., Journal of Power Sources, 158 (2006) 1222-1228.

[5] S. Kundu, L.C. Simon, M.W. Fowler, Comparison of two accelerated Nafion™ degradation experiments., Polymer Degradation and Stability, 93 (2008) 214-224.

[6] A. Noshay, L.M. Robenson, Sulphonated polysulphone., Journal Of Applied Polymer Science, 20 (1976) 1885-1903.

[7] D. Xing, J. Kerres, Improved performance of sulphonated polyarylene ethers for proton exchange membrane fuel cells., Polymers For Advanced Technologies, 17 (2006) 591-597.

[8] J. Kerres, Development of ionomer membranes for fuel cells., Journal of Membrane Science, 185 (2001) 3-27.

[9] J. Kerres, Blended and Cross-Linked Ionimer Membrane for Appliction in Membrane Fuel Cells., Fuel Cells, 2 (2005) 230-247.

[10] J. Kerres, W. Zhang, W. Cui, New Sulfonated Engineering Polymers via the Metalation Route. II. Sulfinated/Sulfonated Poly (ether sulfone) PSU Udel and Its Crosslinking., Journal of Polymer Science: Part A: Polymer Chemistry, 36 (1998) 1411-1448.

[11] B.C. Johnson, İ. Yilgör, C. Tran, M. Iqbal, J.P. Wightman, D.R. Lloyd, J.E. McGrath, Synthesis and characterisation of sulphonated poly(acrylene ether sulphones)., Journal of polymer science: Polymer chemistry edition, (1984) 22721-22737

[12] J. Kerres, F. Schönberger, A. Chromik, T. Häring, Q. Li, J.O. Jensen, C. Pan, P. Noyé, N.J. Bjerrum, Partially Fluorinated Arylene Polyethers and Their Ternary Blend Membranes with PBI and H3PO4. Part I. Synthesis and Characterisation of Polymers and Binary Blend Membranes., Fuel Cells, 8 (2008) 175-187.

[13] J. Kerres, W. Zhang, T. Haering, Covalently Cross-Linked Ionomer (Blend) Membranes for Fuel Cells., Journal of New Materials for Electrochemical Systems, 7 (2004) 299-309.

[14] R. Peach, H.M. Krieg, A.J. Krüger, D. van der Westhuizen, D. Bessarabov, J. Kerres, Comparison of ionically and ionical-covalently cross-linked polyaromatic membranes for SO2 electrolysis., International Journal of Hydrogen Energy, 39 (2014) 28-40.
[15] H.J. Sloane, P.R. Griffiths, Fourier Transform Infrared Spectroscopy., John Wiley & Sons, 1986, p. 83.
[16] J. Coats, Interpretation of Infrared Spectra, A Practical Approach., John Wiley & Sons Ltd, Chichester, 2000, p. 10815-10837.
[17] D.S. Kim, M.D. Guiver, S.J. Nam, T.I. Yun, M.Y. Seo, S.J. Kim, H.S. Hwang, J.W. Rhim, Preparation of ion exchange membranes for fuel cell based on crosslinked poly(vinyl alcohol) with poly(styrene sulfonic acid- *co*-maleic acid)., Journal of Membrane Science, 281 (2006) 156-162.
[18] W. Zhang, V. Gogel, K.A. Friedrich, J. Kerres, Novel covalently cross-linked poly(etheretherketone) ionomer membranes., Journal of Power Sources, 155 (2006) 3-12.
[19] J. Kerres, A. Ulrich, M. Hein, V. Gogel, K.A. Friedrich, L. Jörissen, Cross-linked polyaryl blend membranes for polymer electrolyte fuel cells., Fuel Cells, 4 (2004) 105-112.
[20] V. Atanasov, Personal correspondation via e-mail., (September 2013).
[21] M. Schuster, K.D. Kreuer, H.T. Andersen, J. Maier, Sulfonated Poly(phenylene sulfone) Polymers as Hydrolitically and Thermooxidatively Stable Proton Conducting Ionomers., Macromolecules, 40 (2006) 598-607.
[22] H. Schoeman, H.M. Krieg, A.J. Kruger, A. Chromik, K. Krajinovic, J. Kerres, H2SO4 stability of PBI-blend membranes for SO2 electrolysis., International Journal of Hydrogen Energy, 37 (2012) 603-614.
[23] H. Schoeman, H2SO4 stability of PBI-blend membranes for SO2 electrolysis, MSc dissertation, Faculty of Natural Science, Focus Area: Chemical Resource Beneficiation, North-West University, Potchefstroom 2520, South Africa, 2011.
[24] H. Beydaghi, M. Javanbakht, H.S. Amoli, A. Badiei, Y. Khaniani, M.R. Ganjali, P. Norouzi, M. Abdouss, Synthesis and characterization of new proton conducting hybrid membranes for PEM fuel cells based on poly(vinyl alcohol) and nanoporous silica containing phenyl sulfonic acid., International Journal of Hydrogen Energy, (2011) 13310-13316.
[25] M.H. Jeong, K.S. Lee, J.S. Lee, Cross-Linking Density Effect of Fluorinated Aromatic Polyethers on Transport Properties., Macromolecules, 42 (2009) 1652-1658.

Chapter 5: Evaluation and recommendations

Contents

5.1 Introduction 85

5.2 Evaluation of analytical techniques 85

5.3 Stability of PEMs 87

5.3.1 Non-PBI based blend membranes 91

5.3.2 PBIOO based blend membranes 91

5.3.3 F_6-PBI blend membranes 92

5.4 H_2SO_4 effect on polymer structures 92

5.5 Recommendation 97

5.6 References 99

5.1 Introduction

The purpose of this study was to determine the H_2SO_4 stability of various different blended membranes with the objective to identify other suitable membranes, as possible alternatives to the widely used Nafion® membranes, for future application in SO_2 electrolysis. To evaluate the different PBI-based blend membranes' stability in an H_2SO_4 environment, as found in the SO_2 electrolyser during operation, various characterisation techniques were applied, including weight and thickness changes, SEM-EDX, IEC, FTIR and TGA. The investigated membrane materials were characterised before and after an 80 wt% H_2SO_4 treatment of 120 h at 80 ^{0}C.

In this chapter the various analytical techniques that were used will be evaluated. To facilitate this discussion in terms of H_2SO_4 stability, cut-off values were chosen specifically for the weight and thickness changes, thereby creating a distinction between generally stable and unstable membranes. A comparison between the membrane groups in terms of the physical changes will guide the further evaluation of polymer structures and the determination of the most common H_2SO_4 effects influencing the polymer's chemical stability. This chapter will conclude with recommendations for the future development of blended membranes in terms of components which proved chemically and mechanically stable in the investigated H_2SO_4 environment and candidates to be considered for further application in an SO_2 electrolyser. Additional analytical techniques considered valuable for the characterisation of the membranes' H_2SO_4 stability will also be included in the recommendations.

5.2 Evaluation of analytical techniques

The analytical techniques on the three different Nafion®212 membrane samples were performed in triplicate, providing insight into the errors associated with the various analytical techniques that were used to characterise the membranes before and after H_2SO_4 treatment. This made it possible to determine the accuracy with which the analytical techniques were able to indicate possible changes caused by the H_2SO_4 treatment of the membrane material.

It was shown that the weight change is an effective screening technique to evaluate whether the membrane exhibited the required stability within an H_2SO_4 environment. This type of physical characterisation technique allows for a simple evaluation of the studied membrane's stability, either by degradation and dissolution (weight loss), sulfonation or salt formation (weight gain) due to the H_2SO_4 treatment. The difference in thickness (swelling) can subsequently be used to support the weight change as it measures the changes in the y-dimension of the membrane, giving further information on the mechanical integrity of the treated membrane. Where

significant changes in weight or thickness had been observed, SEM analysis was suitable in showing any visual degradation of the membrane. However, it has been determined for the different Nafion®212 samples characterised that the error associated with the thickness change (±2 %) is slightly higher than the observed error of the weight change (<0.5 %), and therefore slightly less accurate in determining the changes that might have occurred due to the H_2SO_4 treatment.

In an attempt to elucidate the physical changes (visual) observed for the membranes due to the H_2SO_4 treatment, further analytical techniques that could help clarify the chemical cause of the physical changes were applied. The techniques used in this study included IEC in support of SEM-EDX, FTIR and TGA analysis. While both the IEC_{direct} or the IEC_{total} could have been used, the IEC_{total} was used as it gives an indication of the changes of all the $-SO_3H$ groups present within the membrane, irrespective of whether those changes were due to sulfonation or further promotion of cross-linking between the polymer components. EDX data was used mainly to confirm the presence of sulfur within the membrane and to report the subsequent increases (sulfonation) or decreases (dissolution of membrane constituents) in S-content due to the H_2SO_4 treatment. However, a significant variation in the S-content was determined between the three Nafion®212 samples with an error of 25 %, which implied that this technique was least suited to show differences due to polymeric differences. Therefore, the SEM-EDX data was used only in support of the interpretation of the IEC data within the study.

FTIR spectra were obtained for each membrane before and after treatment using changes in peak position and intensity to indicate the regions where possible degradation (decrease) could have occurred, which was then related either to sulfonation (IEC measurements) or dissolution of membrane constituents (weight loss). The TGA technique was used to determine the effect of the H_2SO_4 treatment on the thermal stability of the investigated membrane materials. Deviations in weight % at the determined temperatures of maximum weight loss indicated either a degradation or stabilisation of the polymer backbone in correlation with the sulfonation reported by IEC.

Even though some analytical techniques proved more suitable in the characterisation of the H_2SO_4 stability than others, it can be concluded that all techniques were used, in support of each other, to determine the complete effect (both physical and chemical) of H_2SO_4 on the membrane. Therefore, it can be argued that all the analytical techniques used in this study for the characterisation of the PEM materials proved suitable in providing various sets of data, which combined, was valuable and enabled us to evaluate the various blended PEM materials in terms of their H_2SO_4 stability.

5.3 Stability of PEMs

The physical changes (weight and thickness) observed will be used to evaluate the stability of the investigated PEM materials, referring to the chemical changes where necessary. A summary of the weight and thickness changes for all the membranes is given in Figure 5.1 and 5.2, respectively. To facilitate the discussion, the PEMs were divided into the same groups presented in Chapter 4. Following a brief introduction of Figure 5.1 and 5.2, a more detailed evaluation of the various groups' behaviour will be presented.

Both in Figure 5.1 and Figure 5.2, cut-off values (horizontal dashed line) were introduced. These cut-offs (percentage change) were based on the chemical changes presented in Chapter 4 at which significant variations were reported for IEC, FTIR and TGA measurements, either respectively or in all three instances. Accordingly, the weight change cut-off was set at ±10 %. It is clear from Figure 5.1 that, generally, the non-PBI based and PBIOO based membrane groups were less stable in terms of the reported weight changes (2-60 %) in comparison to Nafion®212 and the fluorinated PBI-based membrane group (0.5-5 %). Similarly, according to the results in Chapter 4, the cut-off stability of the membranes in terms of the summarised thickness changes presented in Figure 5.2 was set at ±30 %. In this instance more than 50 % of the studied PBIOO based membranes reported thickness changes breaching the limit, compared to the 12.5 and 9 % of the non-PBI and fluorinated PBI-based membrane groups, respectively.

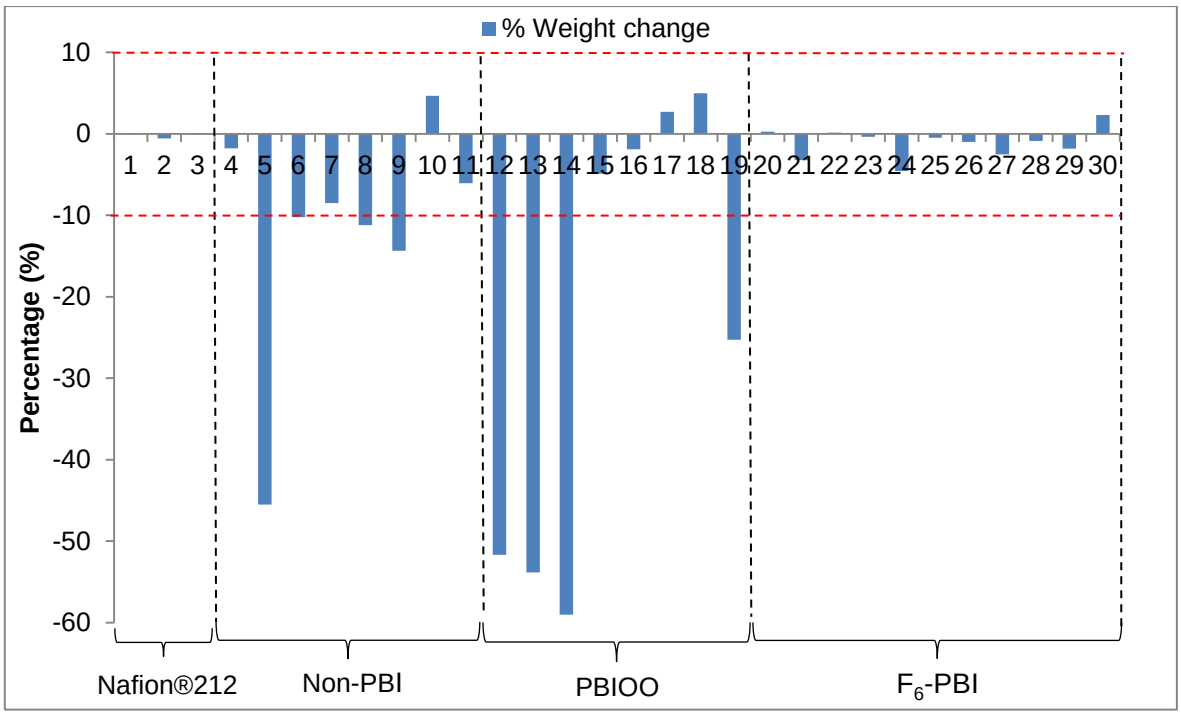

Figure 5.1: Percentage weight change for the studied PEM materials due to H_2SO_4 treatment.

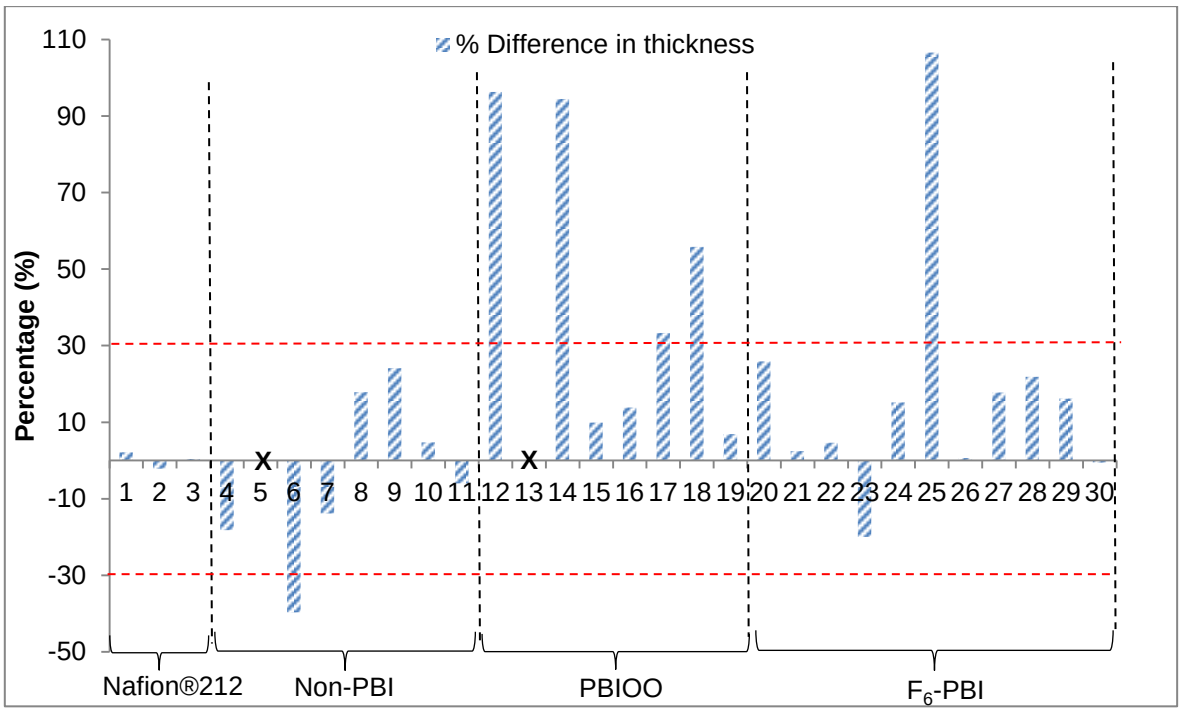

Figure 5.2: Percentage difference in thickness for the studied PEM materials due to H_2SO_4 treatment.

Based on the cut-off values of Figure 5.1 and 5.2, the membranes can be classified according to their stability as has been summarised in Table 5.1. While it was expected that Nafion®212 would be stable within the investigated H_2SO_4 environment, the aim of the study was to evaluate promising candidates to replace Nafion® in view of its high temperature instability. The obtained stability of the three novel groups will be further evaluated according to their composition. Apart from the differences in type and concentration of the basic polymer, the blended PEM materials also varied in terms of the type and concentration of the acid polymer, the presence of additives and low molecular cross-linkers, the type of interactions (cross-linking) present between the blend components and the degree of fluorination of the polymer components (partially and/ or limited to copolymer and/ or cross-linker).

Table 5.1: **Distinction between stable and unstable PEM materials in an H_2SO_4 environment.**

No.	Membrane Abb.	Stable	Unstable
1	N212_A	X	
2	N212_B	X	
3	N212_C	X	
4	NB1	X	
5	NB2		X
6	NB3		X
7	NB4		X
8	NB5		X
9	NB6		X
10	NB7	X	
11	NB8	X	
12	PB1		X
13	PB2		X
14	PB3		X
15	PB4	X	
16	PB5	X	
17	PB6		X
18	PB7		X
19	PB8		X
20	FPB1	X	
21	FPB2	X	
22	FPB3	X	
23	FPB4	X	
24	FPB5	X	
25	FPB6		X
26	FPB7	X	
27	FPB8	X	
28	FPB9	X	
29	FPB10	X	
30	FPB11	X	

5.3.1 Non-PBI based blend membranes

This group of membranes are characterised by the covalent cross-linking of blend components in the absence of a basic PBI polymer. In general, the weight losses reported for this group can be attributed to incomplete (NB2) or ineffective cross-linking (limited to physical entanglement of copolymers in network, not participating in the cross-linked network), likeliness of sulfonation of the PSU-component (See Section 4.3.1) present throughout the non-PBI blended group either as copolymer or cross-linker and the subsequent dissolution of membrane fragments during the post treatment washing.

However, membranes NB1, 7 and 8 were considered stable (Table 5.1). From the discussions in Section 4.3.1(a) it could be concluded that the reported stability of NB1 was likely due the presence of the partially fluorinated low-molecular cross-linker BFO. It is supposed that the strong C-F bonds contributed to the interactions between blend components. In the instance of NB7 and 8, it is believed that strong interactions between the partially fluorinated PFS and sulfonated PSU copolymers within the covalent network were responsible for the stability observed.

5.3.2 PBIOO based blend membranes

The interactions present between the acid-base polymers of the PBIOO based blended membranes include ionical cross-linking, hydrogen bridges and the addition of covalent cross-linking (PB1 and 2). The significant changes in thickness and subsequent unstable character reported for membranes PB1-3, 6 and 7 can be attributed to the known splitting-off of ionic cross-links at temperatures above 70 ^{0}C [1], and the insufficient covalent cross-linking in membranes PB1 and 2. Furthermore, the poor stability of membranes PB1-3 is likely due to the unstable character of the sPEEK copolymer undergoing hydrolysis in an H_2SO_4 environment. It was also shown that the additional cross-linker Bis-A in PB1 and 2 did not contribute to the stability of the blend when compared to PB3.

Acid excess sPSU-PBIOO blended membranes (PB4 and 5) had a stable character in the H_2SO_4 environment, possibly due to the presence of the more stable sulfonated PSU component in comparison with the sPEEK copolymer (PB1-3). However, the base-excess membranes PB6, 7 and 8 were considered unstable due to the significant changes in thickness and weight reported after the treatment of these membranes, showing the importance of the acid:base ratio. These high PBIOO containing membranes did not form stable blends,

irrespective of whether they had been blended with the phosphonated or sulfonated acid polymers, PKA and sPSU.

5.3.3 F_6-PBI blend membranes

This group is considered overall stable due to the minimal % weight changes reported after treatment of the membranes. The observed stability of the F_6-PBI blend membranes can largely be attributed to the presence of the partially fluorinated acid (sFS) and base (F_6-PBI) polymers, limiting the significant thickness changes otherwise associated with ionically cross-linked blended membranes [2].

The exception in the group, FPB6, showed a significant increase in thickness after treatment. It can be concluded that the fluorinated additive (PFS) did not effectively increase the stability of the blended membranes FPB3-7 in comparison to FPB1 and 2, where no PFS was present. It was shown for the membranes FPB8-10 that the different cross-linkers and additive (A095 in FPB10) only had a minor influence on the stability of the F_6-PBI blended membranes. The addition of covalent cross-linking between the acid copolymer and cross-linkers of the membranes, FPB8-10, could have contributed to the reduced thickness changes observed in comparison with the PBIOO based membranes, but otherwise did not substantially contribute to the stability of the membranes. The base-excess blend FPB2 was significantly more stable than the base-excess PBIOO based membranes (PB6, 7 and 8), confirming the increased stability due to the fluorinated character of both the acid (sFS) and base (F_6-PBI) components. The sulfonated PSU polymer was just as stable in the F_6-PBI blend as the partially fluorinated copolymer sFS under the conditions investigated.

5.4 H_2SO_4 effect on polymer structures

According to the results discussed in Chapter 4, it is evident that the H_2SO_4 treatment had a specific effect on specific polymer structures present in the PEM blends investigated. Only those effects that resulted in significant changes supported both by physical and chemical changes will be discussed in this section. The effects, which include sulfonation, salt formation, hydrolysis and the accompanied dissolution of membrane fragments are summarised in Table 5.2. Subsequently, the effect of H_2SO_4 on each of the identified polymers within their blend will be discussed including the analytical techniques in support of the changes observed.

Table 5.2: Effect of H_2SO_4 on polymer structures within the investigated PEM blends.

Polymer	H_2SO_4 effect	Blends affected	Analytical Technique
PSU (sPSU)	Sulfonation, dissolution (membrane fragments)	NB1-8 and PB5	Weight change (decrease), thickness change (NB4-6), IEC and EDX:S-content (NB1-3,6 and PB5), FTIR (decreased intensities) and TGA (NB7 and 8)
PEEK	Sulfonation, dissolution (membrane fragments)	NB4-6	Weight change (decrease), thickness change, IEC, FTIR
sPEEK	Hydrolysis of ether bond, dissolution (membrane fragments)	PB1-3	Weight change (significant decrease), IEC, EDX:S-content, FTIR, TGA
PBIOO	Sulfonation of backbone, dissolution (membrane fragments)	PB1-3 and 8	Weight change (decrease), IEC, EDX:S-content, FTIR, TGA
PBIOO	Salt formation and subsequent splitting-off of ionic cross-links	PB4-8	Thickness change (increase), weight change (PB6 and 7), FTIR and TGA (PB7 and 8)
PFS	Sulfonation, dissolution (membrane fragments)	FPB6	Thickness change (significant increase), SEM, IEC, EDX: S-content, TGA

The base PSU polymer is present in the non-PBI based membranes NB1-8, PBIOO based membranes PB4-6 and in the fluorinated PBI-based membrane FPB11, either in the sulfonated form or by the addition of sulfochloride or sulfinate as copolymer or cross-linker. Sulfonation of the polyethersulfone at the *ortho*-position to the ether bridge within the sPSU polymer in the presence of H_2SO_4 [3,4] shown in Figure 5.3, is well known. The subsequent dissolution of membrane fragments is further confirmed by the decreased weight change, FTIR intensities and in some instances by the IEC, EDX: S-content and TGA as indicated in Table 5.2.

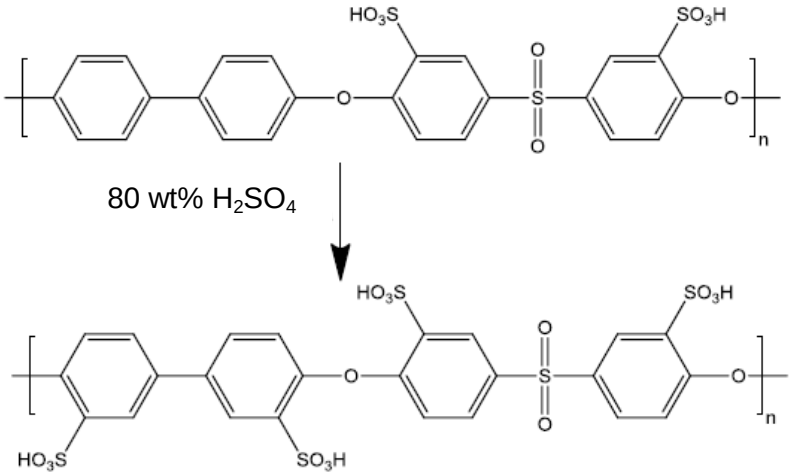

Figure 5.3: Possible sulfonation of the sPSU polymer's backbone during H_2SO_4 treatment *(adapted from [5]).*

Dissolution of membrane fragments due to sulfonation of the PEEK-SCl polymer is considered likely in the changes reported for the non-PBI based membranes NB4-6. This assumption is further supported by the observed weight loss, decreased IEC values and FTIR intensities for the membranes NB4-6. It can also be suggested that the PEEK-SCl polymer is susceptible to hydrolysis as discussed further for sPEEK, but in a slighter degree. The unstable character of the sPEEK polymer was clearly observed in the significant weight loss reported for membranes NB1-3 and the accompanied deviations noted in thickness, FTIR, TGA, IEC and EDX:S-content change after treatment. The changes observed for sPEEK after the H_2SO_4 treatment was most likely due to hydrolysis [2,6] in the harsh conditions of 80 wt% H_2SO_4 at 80 ^{0}C. Hydrolysis of the ether bond [7] in the sPEEK polymer is suggested by the mechanism as shown in Figure 5.4.

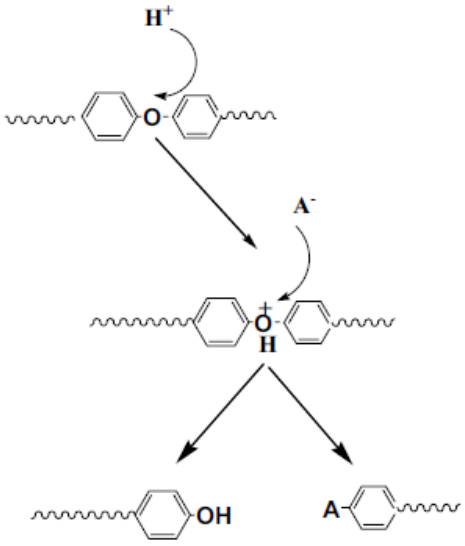

Figure 5.4: Proposed hydrolysis of a sPEEK polymer at the ether bond [7].

Sulfonation of the PBIOO-backbone and its subsequent dissolution from the blend can be associated with the weight losses observed in the PBIOO based membranes PB1-3 and 8 as indicated in Table 5.2. It can be suggested that the strong electrophilic properties of the 80 wt% H_2SO_4 were responsible for the direct sulfonation of the PBIOO backbone, leading to the structure as proposed in Figure 5.5. It could also be proposed that an ether bond cleavage of the PBIOO is possible, adding to the polymers instability in an H_2SO_4 environment. The decreased IEC, EDX:S-content, FTIR intensities and TGA signals further support the dissolution of membrane constituents after sulfonation and/ or the possible ether bond cleavage of PBIOO.

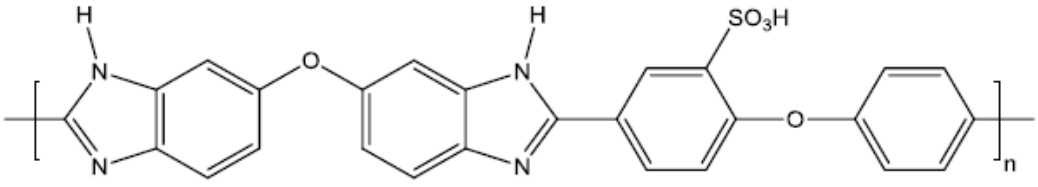

Figure 5.5: Supposed structure of sulfonated PBIOO [5].

PBIOO is also likely to form hydrogen sulfate salts in the 80 wt% H_2SO_4 environment investigated. The increased weight observed in some instances (PB6 and 7) was accompanied by an increase in thickness (PB4-8) after treatment. This is likely due to the splitting-off of ionical

cross-links [8] as the imidazolium hydrogen sulfate salt groups form in the presence of H_2SO_4 as shown in Equation 5.1 [5]:

Basic polymer-Im$H^{+-}O_3S$-acidic polymer + H_2SO_4→

Basic polymer-Im$H^{+-}HO_3S$ + HO_3S-acidic polymer (5.1)

Sulfonation of the PFS polymer in the 80 wt% H_2SO_4 environment is considered likely (precursor of sFS) followed by the dissolution of membrane fragments as reported in the case of FPB6 (which comprised 38 % of the blend membrane). The acid sensitive bisphenol A unit, present within the PFS polymer, could also have contributed to the unstable character of PFS. The dissolution was further supported by a decrease observed in IEC, EDX: S-content and TGA signals after treatment.

From the discussed H_2SO_4 effects on the copolymers (Table 5.2), the membranes NB2-6, PB1-3, 6-8 and FPB6 were considered unstable in an H_2SO_4 environment. The stable membranes from the study included Nafion®212, NB1, 7, 8, PB4, 5, FPB1-5 and 7-11. In summary, the stability of the blended membranes can be controlled by managing the composition (blend components) of the membrane and by ensuring effective cross-linking between the blend components (miscibility), where blend components sFS, PFS and sPSU were more stable than sPEEK and PEEK-SCl. From the discussions in Chapter 4 and Section 5.3, it is clear that the type of cross-linking is also important for ensuring a stable membrane, where ionic and the combined covalent-ionical cross-linking seems more effective than covalent cross-linking. To conclude, the fluorinated PBI-based membranes had the highest acid stability when compared to the non-PBI and PBIOO based membranes, likely due to the protective role of the fluorinated membrane components. In conclusion it can be proposed that most of the F_6-PBI based membranes, along with NB1, 7, 8; PB4 and 5, are suitable for application in an SO_2 electrolyser.

5.5 Recommendation

The recommendations will be subdivided in terms of further PEM material development and analytical techniques for the characterisation of the membranes' H_2SO_4 stability.

Recommendations regarding PEM development.

- Further investigate base-excess type blends with F_6-PBI as basic polymer and determine the influence of the basic polymer's content on the stability of the blend.
- Evaluating the strength of the acid-base interactions in F_6-PBI based membranes in a study where the fluorinated PBI is blended with various suitable stable acidic polymers.
- Further characterisation of phosphonated membranes (PKA) in acid excess type blends to compare with base-excess phosphonated blends in terms of stability.
- Investigate the stability of phosphoric acid doped F_6-PBI membranes as acid-base complex in an attempt to improve the membrane properties desirable for the SO_2 electrolyser application.

Recommendations regarding analytical techniques for characterisation purposes.

- To ensure that the investigated PEM materials are suitable for long term application in an SO_2 electrolyser, it could be considered to expose the membranes to H_2SO_4 for a longer period, for example 10-14 days.
- It is known that higher temperature operations within the electrolyser set-up holds the potential benefit of faster electrode kinetics and simplified water management above 120 °C [9]. PBI membranes have good ionic conductivity and heat resistance making them ideal candidates at these high temperature applications [10]. Therefore, it can be suggested that the fluorinated PBI-based high temperature membrane blends be exposed to H_2SO_4 concentrations, as expected in an SO_2 electrolyser (30-40 wt%), at temperatures up to 120 °C [5].
- Requirements of the PEM material include the ability to act as a barrier to prohibit and limit any SO_2 crossover. Considering the stability of Nafion® compared to the F_6-PBI blended membranes in the same H_2SO_4 environment, SO_2 crossover experiments can be conducted to determine which membrane will ultimately perform better in the SO_2 set-up.
- For a complete understanding of the H_2SO_4 effect on the thermal stability of the membrane, TGA coupled MS could be employed to further provide information on the thermal decomposition of the membrane by monitoring the fragments (functional groups) as a function of the increasing temperature [11].

- Transmission electron microscopy (TEM) could be applied to investigate the micromorphology of the membranes before and after H_2SO_4 treatment. The microphase-separation between blend components present in the micromorphology of the membrane could be used to determine the miscibility of different blend components and give some insight into the transport properties associated with certain types of blends [12].
- Differential scanning calorimetry (DSC) could be included in the thermal analysis of the membrane materials to determine possible structural changes of the membranes after the H_2SO_4 treatment and its effect on the thermal stability of the membrane as indicated by a deviation in the glass transition temperature (T_g) [13]. It could serve to compare the thermal stability of the PEM materials with the profile determined by the TGA analysis of the membrane.

5.6 References

[1] J. Kerres, W. Zhang, A. Ullrich, C.M. Tang, M. Hein, V. Gogel, T. Frey, L. Jörissen, Synthesis and characterization of polyaryl blend membranes having different composition, different covalent and/or ionical cross-linking density, and their application to DMFC., Desalination, 147 (2002) 173-178.

[2] J. Kerres, Blended and Cross-Linked Ionimer Membrane for Appliction in Membrane Fuel Cells., Fuel Cells, 2 (2005) 230-247.

[3] A. Noshay, L.M. Robenson, Sulphonated polysulphone., Journal Of Applied Polymer Science, 20 (1976) 1885-1903.

[4] D. Xing, J. Kerres, Improved performance of sulphonated polyarylene ethers for proton exchange membrane fuel cells., Polymers For Advanced Technologies, (2006) 591-597.

[5] H. Schoeman, H2SO4 stability of PBI-blend membranes for SO2 electrolysis, MSc dissertation, Faculty of Natural Science, Focus Area: Chemical Resource Beneficiation, North-West University, Potchefstroom 2520, South Africa, 2011.

[6] V. Atanasov, Personal correspondation via e-mail., (September 2013).

[7] C. Iojoiu, M. Marechal, F. Chabert, J.Y. Sanchez, Mastering Sulfonation of Aromatic Polysulfones: Crucial for Membranes for Fuel Cell Application., Fuel Cells, 5 (2005) 344-354.

[8] R. Peach, H.M. Krieg, A.J. Krüger, D. van der Westhuizen, D. Bessarabov, J. Kerres, Comparison of ionically and ionical-covalently cross-linked polyaromatic membranes for SO_2 electrolysis., International Journal of Hydrogen Energy, 39 (2014) 28-40.

[9] P. Jannasch, Recent developments in high-temperature proton conducting polymer electrolyte membranes., Current Opinion in Colloid and Interface Science, 8 (2003) 96-102.

[10] R. Savinell, E. Yeager, D. Tryk, U. Landau, J. Wainright, D. Weng, K. Lux, M. Litt, C. Rogers, A Polymer Electrolyte for Operation at Temperatures up to 200°C., Electrochemical Society, 141 (1994) L46-L48.

[11] S.D. Mikhailenko, G.P. Robertson, M.D. Guiver, S. Kaliaguine, Properties of PEMs based on cross-linked sulfonated poly(ether ether ketone)., Journal of Membrane Science, 285 (2006) 306-316.

[12] J. Kerres, Development of ionomer membranes for fuel cells., Journal of Membrane Science, 185 (2001) 3-27.

[13] B. Smitha, S. Sridhar, A.A. Khan, Synthesis and characterization of proton conducting polymer membranes for fuel cells., Journal of Membrane Science, 225 (2003) 63-76.

Appendix A: Structure of the copolymers and cross-linkers

A-1: Basic-component polymers

PBIOO

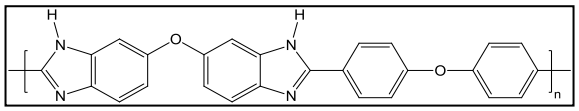

F_6-PBI

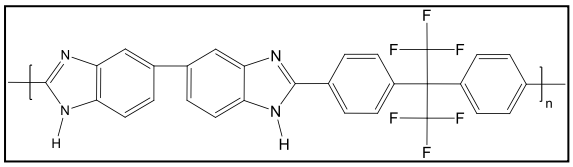

A095

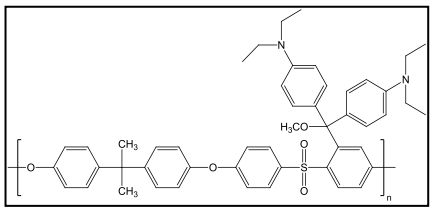

A-2: Acid-component polymers

PSU-Sulfochloride

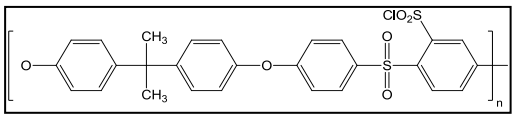

PSU-Sulfinate

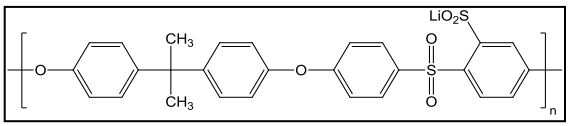

PEEK-Sulfochloride

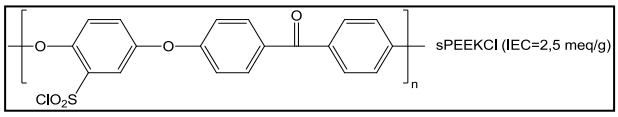

sPSU

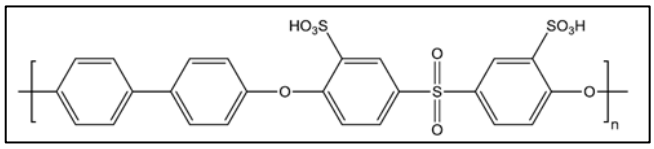

PFS

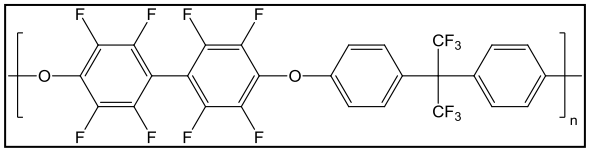

sPEEK

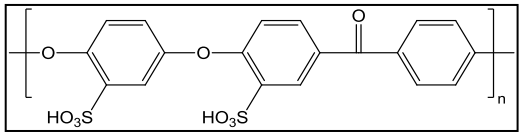

PKA

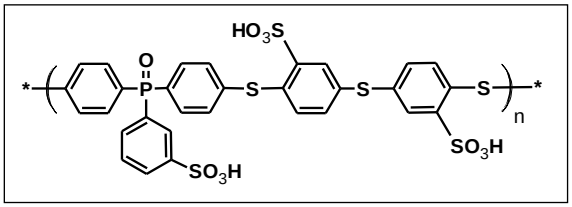

sFS

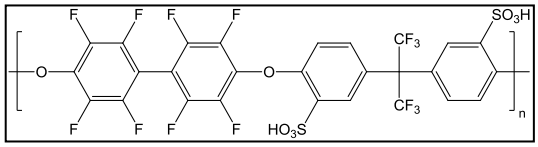

A-3:Low molecular weight cross-linkers

Bisphenol A-Diglycidylether

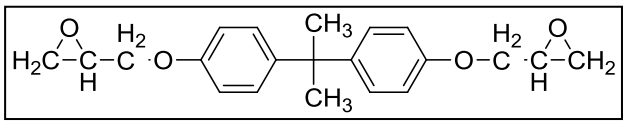

Diiodobutane

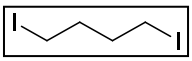

Bis(pentafluorophenyl)2,5-oxadiazole

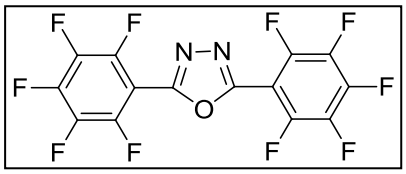

Decafluorobiphenyl

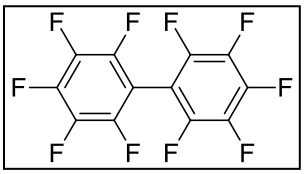

Bis(3-nitro-4-fluorophenyl)sulfone

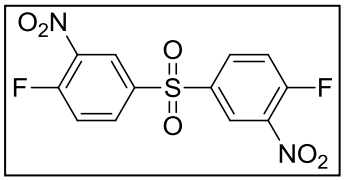

A-4: Nafion®

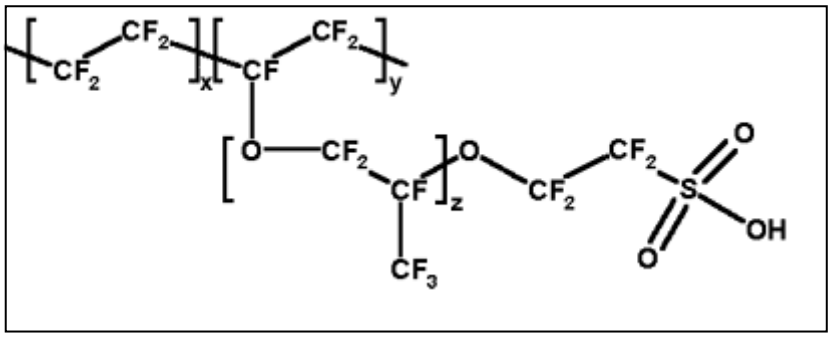

Appendix B: FTIR and TGA data of non-PBI based membranes

B-1: FTIR

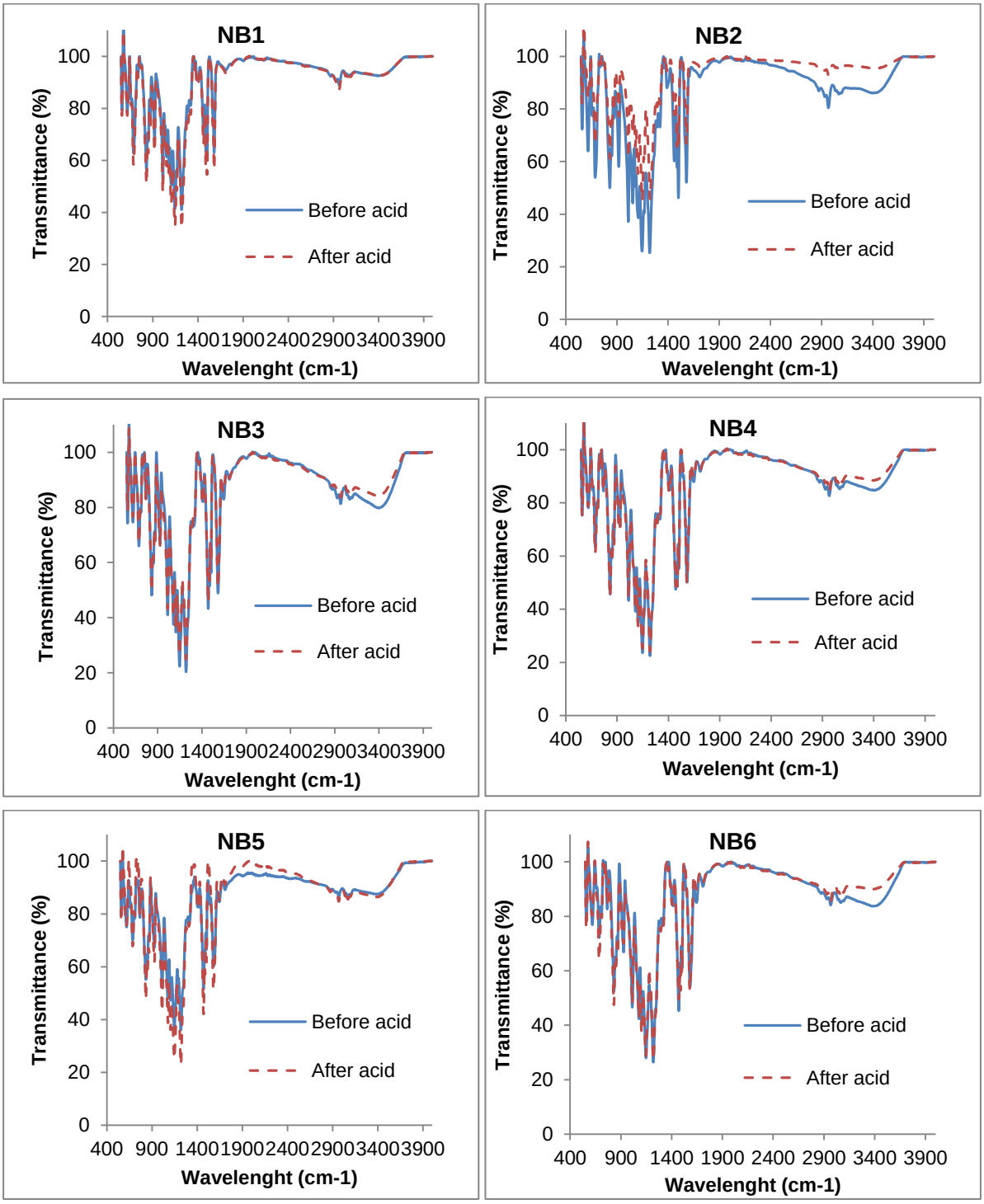

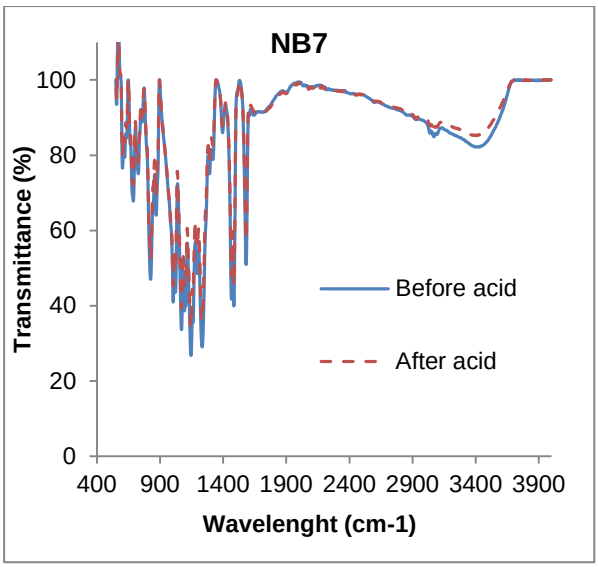
NB7
Transmittance (%)
100
80
60
40
20
0
400 900 1400 1900 2400 2900 3400 3900
Wavelenght (cm-1)
Before acid
After acid

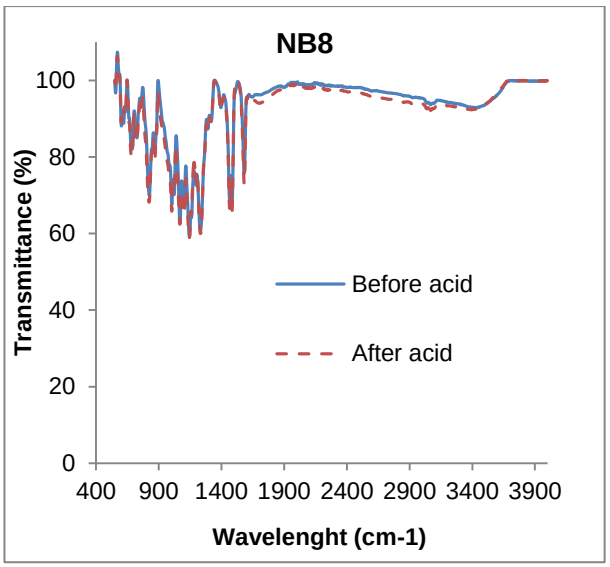
NB8
Transmittance (%)
100
80
60
40
20
0
400 900 1400 1900 2400 2900 3400 3900
Wavelenght (cm-1)
Before acid
After acid

B-2: TGA

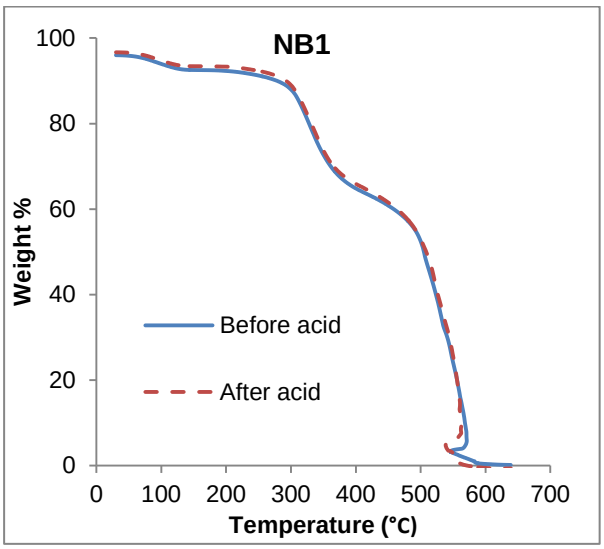
NB1
Weight %
100
80
60
40
20
0
0 100 200 300 400 500 600 700
Temperature (°C)
Before acid
After acid

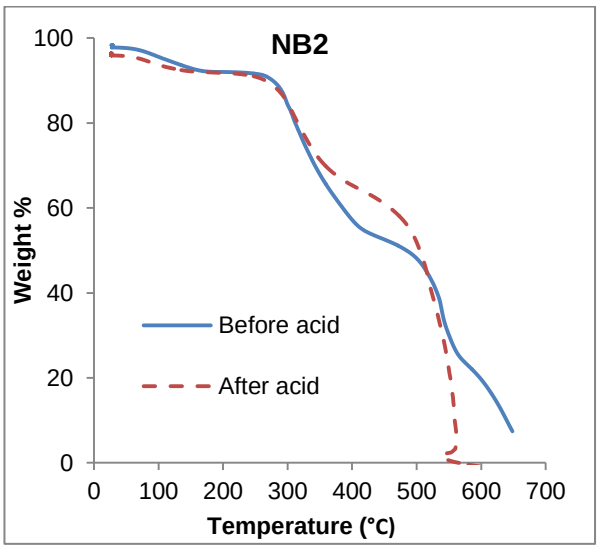
NB2
Weight %
100
80
60
40
20
0
0 100 200 300 400 500 600 700
Temperature (°C)
Before acid
After acid

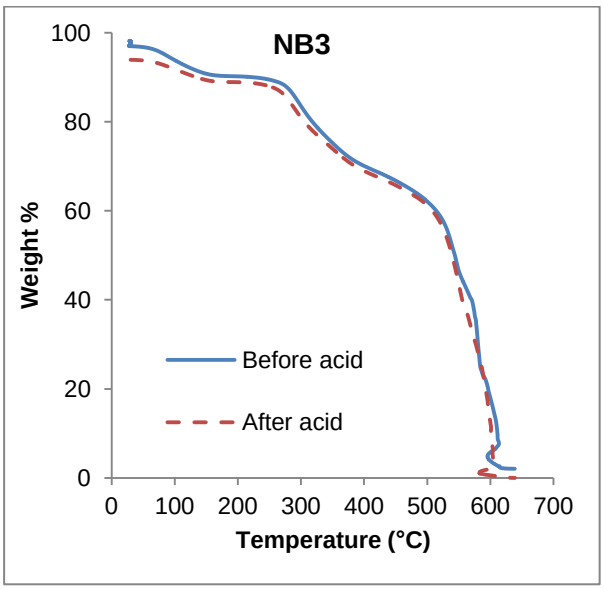
NB3
Weight %
100
80
60
40
20
0
0 100 200 300 400 500 600 700
Temperature (°C)
Before acid
After acid

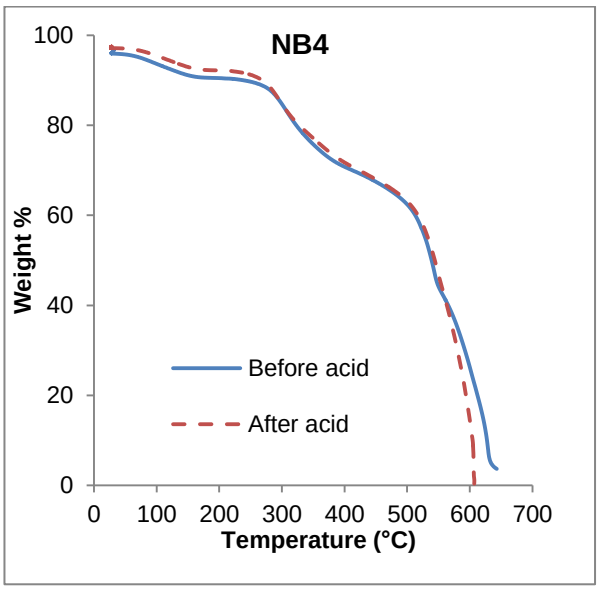
NB4
Weight %
100
80
60
40
20
0
0 100 200 300 400 500 600 700
Temperature (°C)
Before acid
After acid

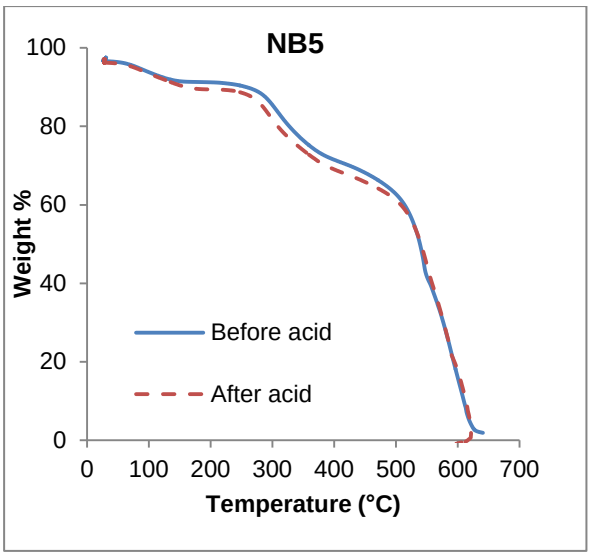
NB5
Weight %
Temperature (°C)
Before acid
After acid
100
80
60
40
20
0
0 100 200 300 400 500 600 700

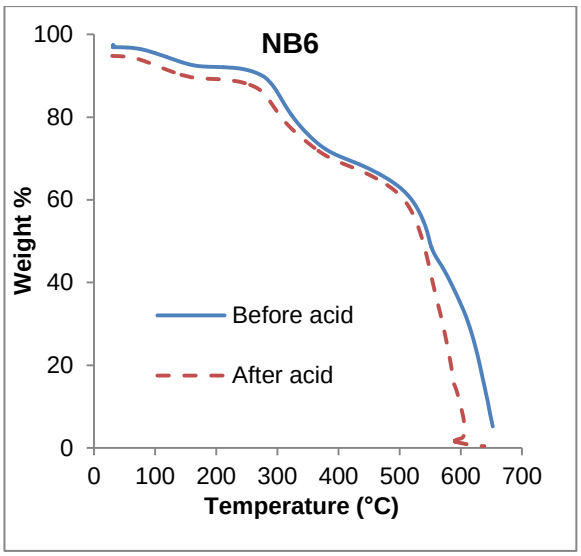
NB6
Weight %
Temperature (°C)
Before acid
After acid
100
80
60
40
20
0
0 100 200 300 400 500 600 700

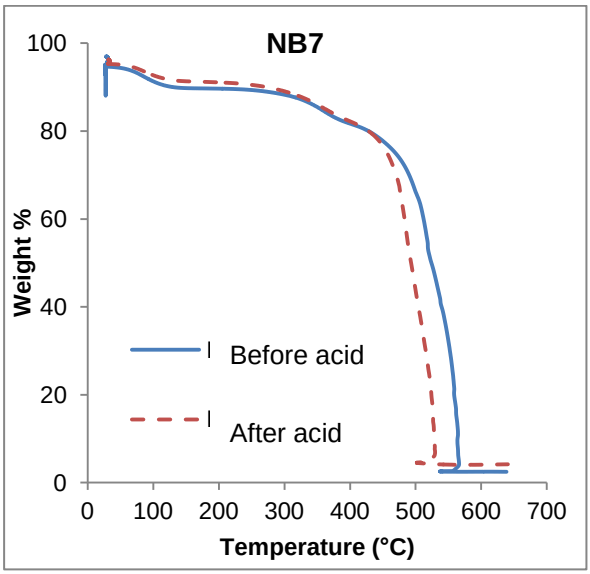
NB7
Weight %
Temperature (°C)
Before acid
After acid
100
80
60
40
20
0
0 100 200 300 400 500 600 700

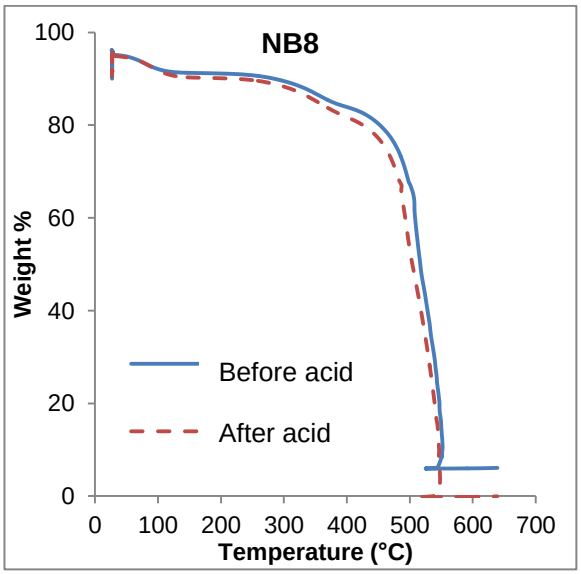
NB8
Weight %
Temperature (°C)
Before acid
After acid
100
80
60
40
20
0
0 100 200 300 400 500 600 700

Appendix C: FTIR and TGA data of PBIOO based membranes

C-1: FTIR

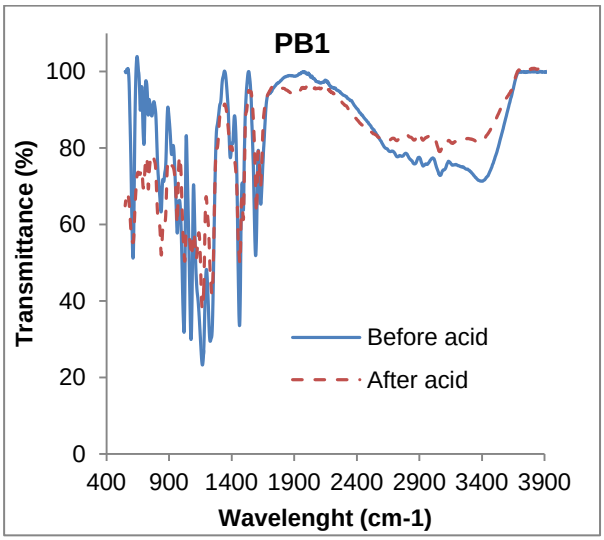

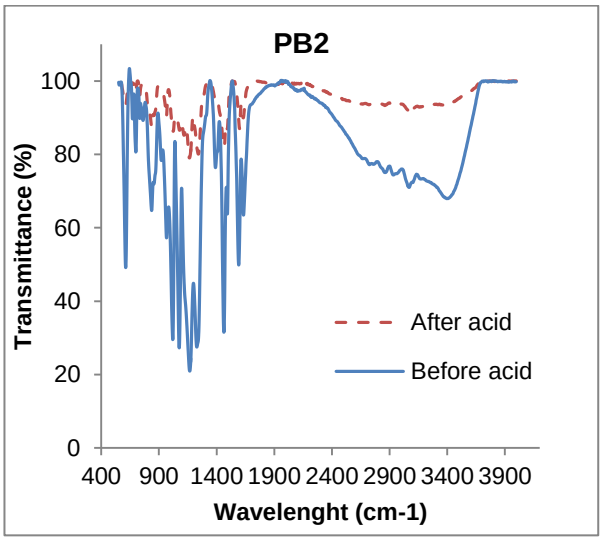

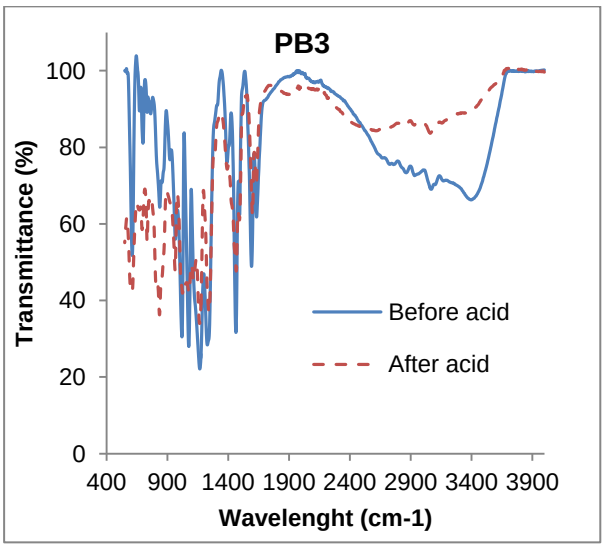

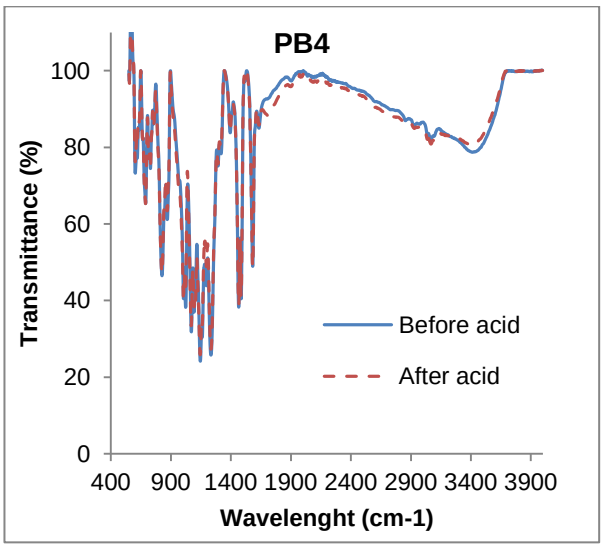

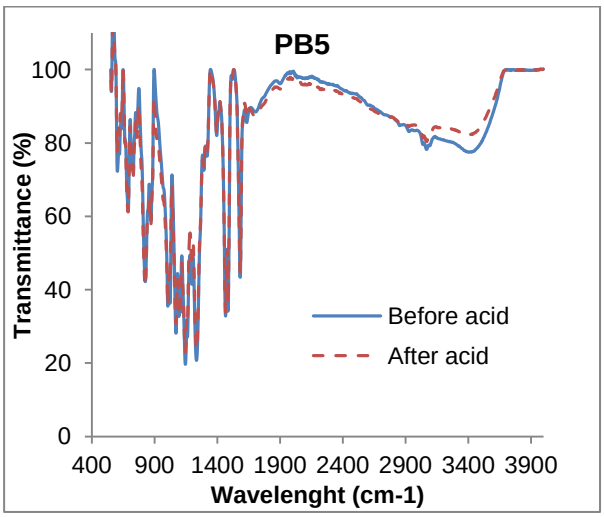

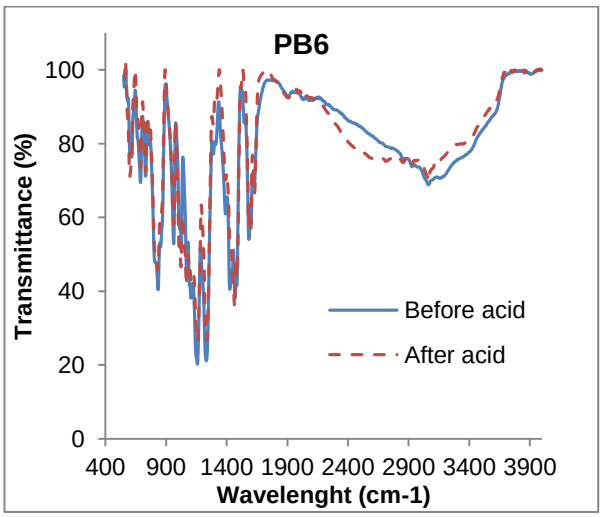

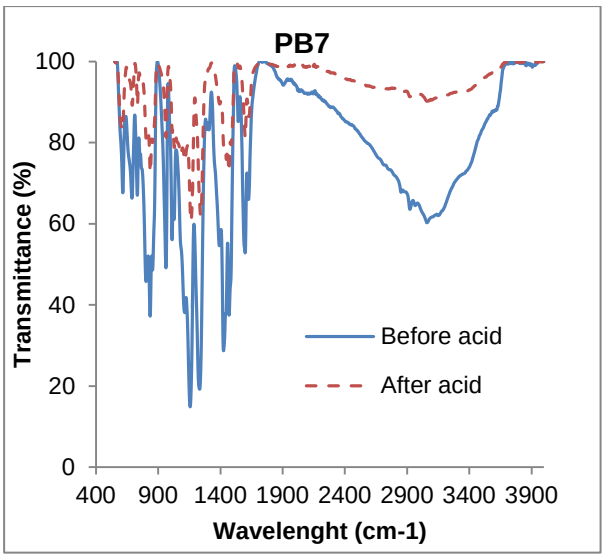
PB7
Transmittance (%)
100
80
60
40
20
0
400 900 1400 1900 2400 2900 3400 3900
Wavelenght (cm-1)
Before acid
After acid

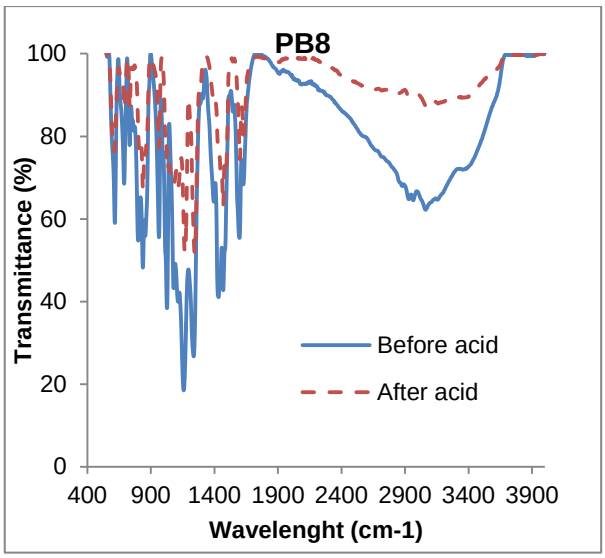
PB8
Transmittance (%)
100
80
60
40
20
0
400 900 1400 1900 2400 2900 3400 3900
Wavelenght (cm-1)
Before acid
After acid

C-2: TGA

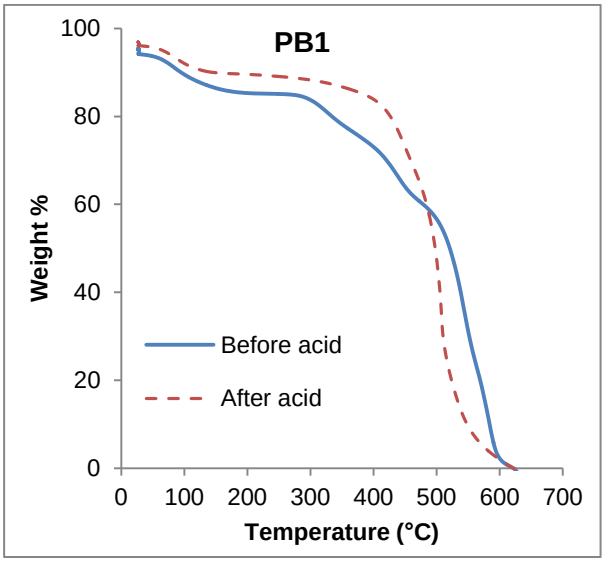
PB1
Weight %
100
80
60
40
20
0
0 100 200 300 400 500 600 700
Temperature (°C)
Before acid
After acid

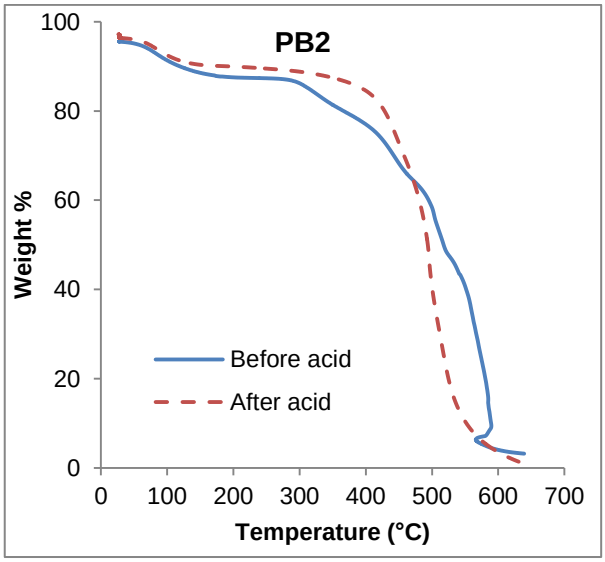
PB2
Weight %
100
80
60
40
20
0
0 100 200 300 400 500 600 700
Temperature (°C)
Before acid
After acid

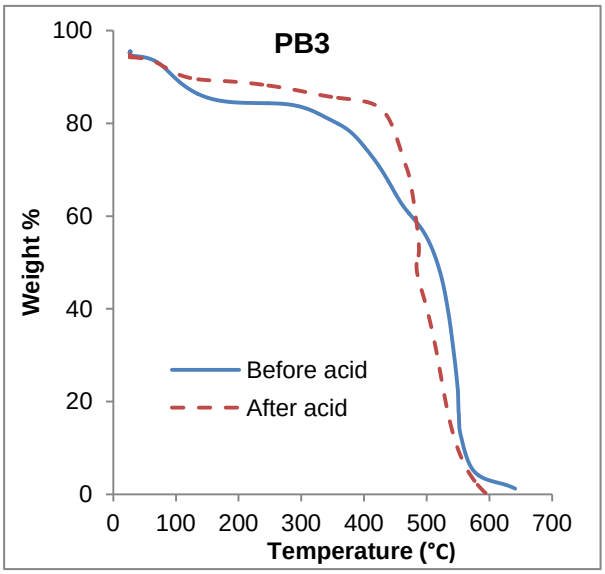
PB3
Weight %
100
80
60
40
20
0
0 100 200 300 400 500 600 700
Temperature (°C)
Before acid
After acid

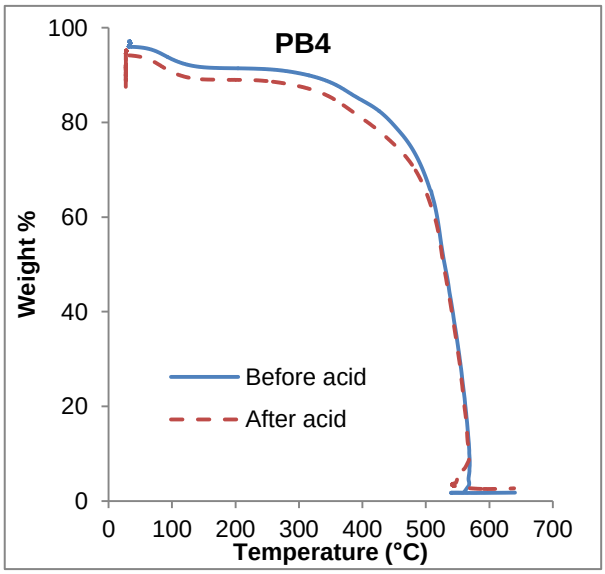
PB4
Weight %
100
80
60
40
20
0
0 100 200 300 400 500 600 700
Temperature (°C)
Before acid
After acid

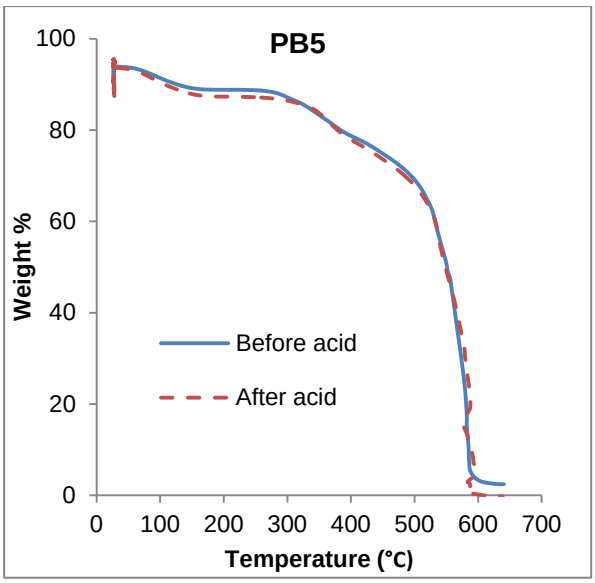
PB5
Weight %
Temperature (°C)
Before acid
After acid
100
80
60
40
20
0
0 100 200 300 400 500 600 700

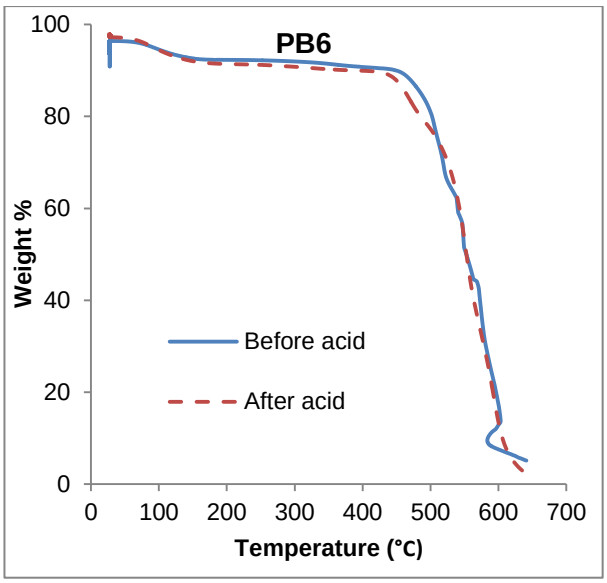
PB6
Weight %
Temperature (°C)
Before acid
After acid
100
80
60
40
20
0
0 100 200 300 400 500 600 700

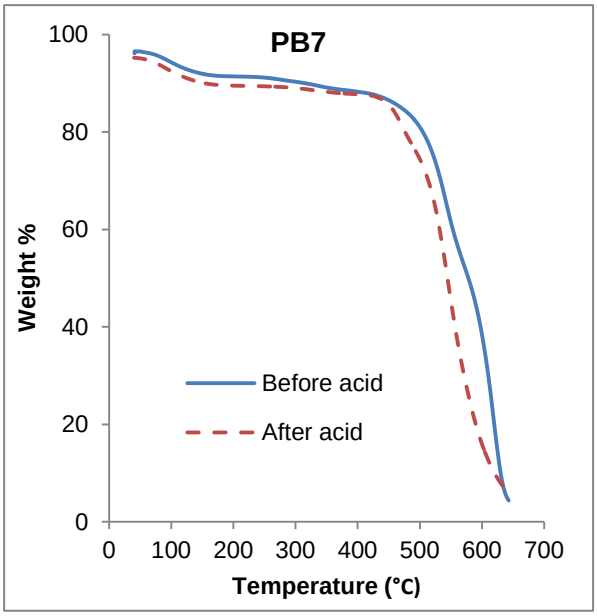
PB7
Weight %
Temperature (°C)
Before acid
After acid
100
80
60
40
20
0
0 100 200 300 400 500 600 700

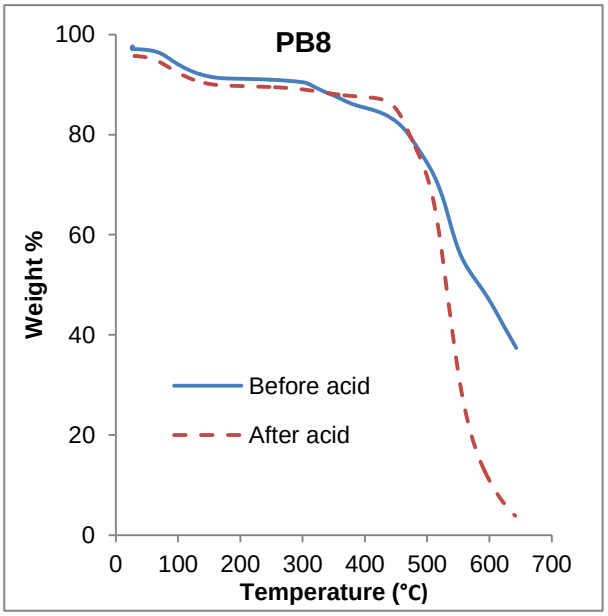
PB8
Weight %
Temperature (°C)
Before acid
After acid
100
80
60
40
20
0
0 100 200 300 400 500 600 700

Appendix D: FTIR and TGA data of F_6-PBI based membranes

D-1: FTIR

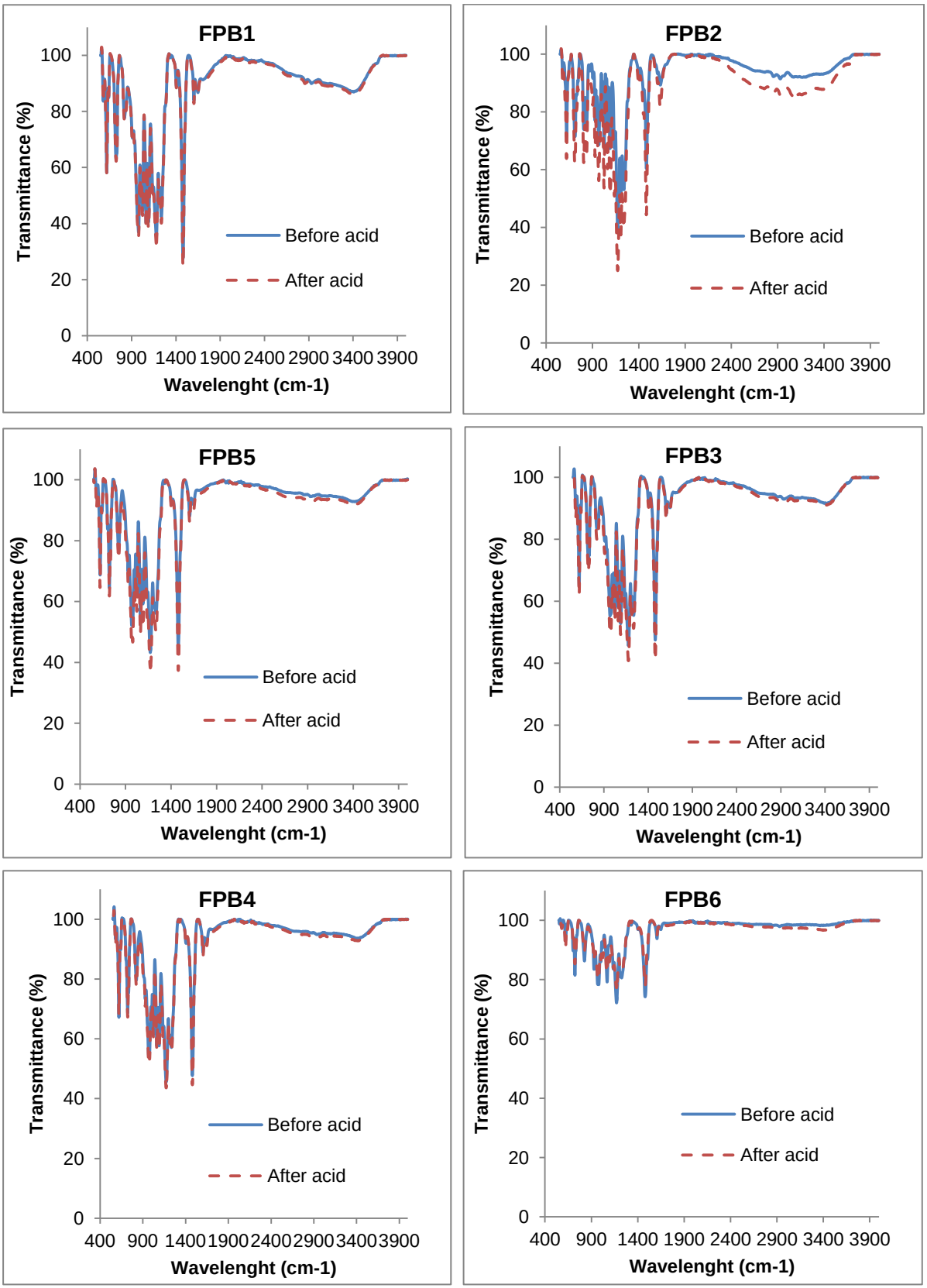

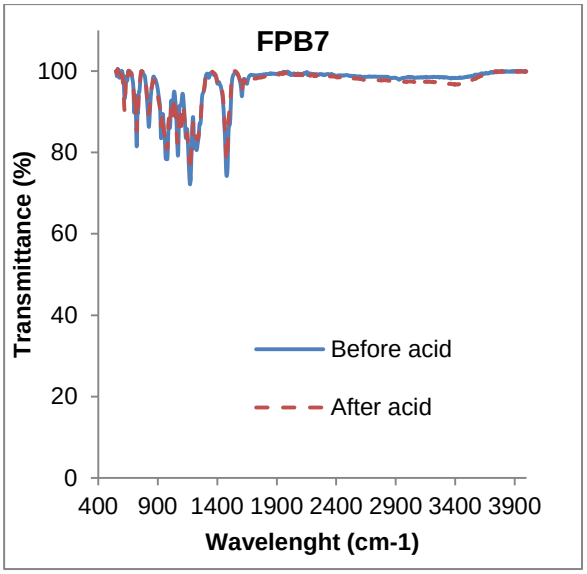
FPB7
Transmittance (%)
100
80
60
40
20
0
Before acid
After acid
400 900 1400 1900 2400 2900 3400 3900
Wavelenght (cm-1)

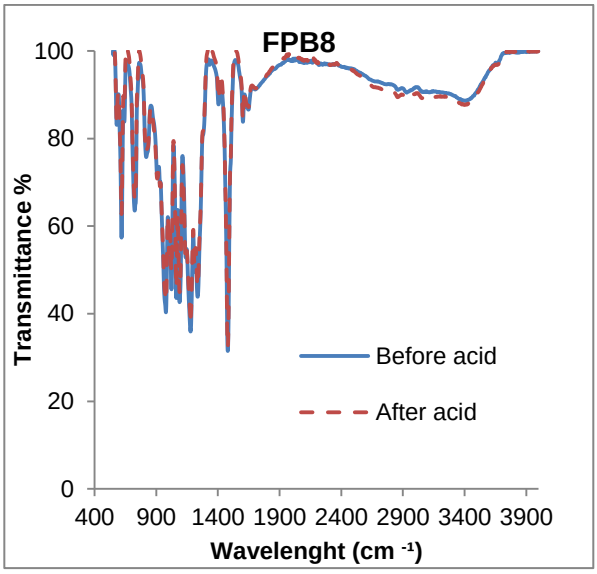
FPB8
Transmittance %
100
80
60
40
20
0
Before acid
After acid
400 900 1400 1900 2400 2900 3400 3900
Wavelenght (cm -1)

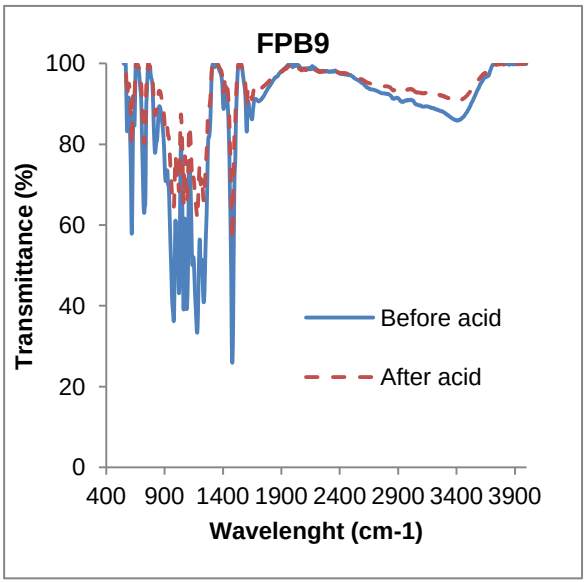
FPB9
Transmittance (%)
100
80
60
40
20
0
Before acid
After acid
400 900 1400 1900 2400 2900 3400 3900
Wavelenght (cm-1)

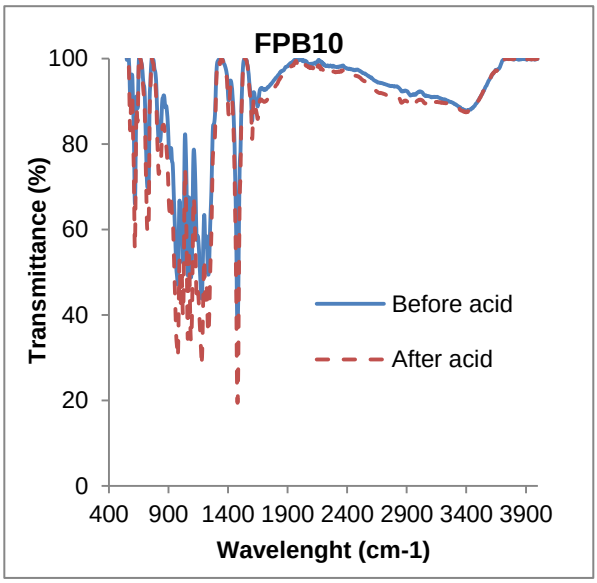
FPB10
Transmittance (%)
100
80
60
40
20
0
Before acid
After acid
400 900 1400 1900 2400 2900 3400 3900
Wavelenght (cm-1)

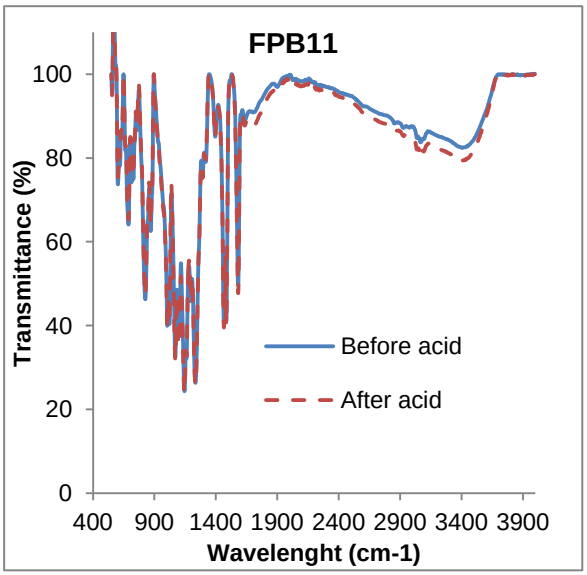
FPB11
Transmittance (%)
100
80
60
40
20
0
Before acid
After acid
400 900 1400 1900 2400 2900 3400 3900
Wavelenght (cm-1)

D-2: TGA

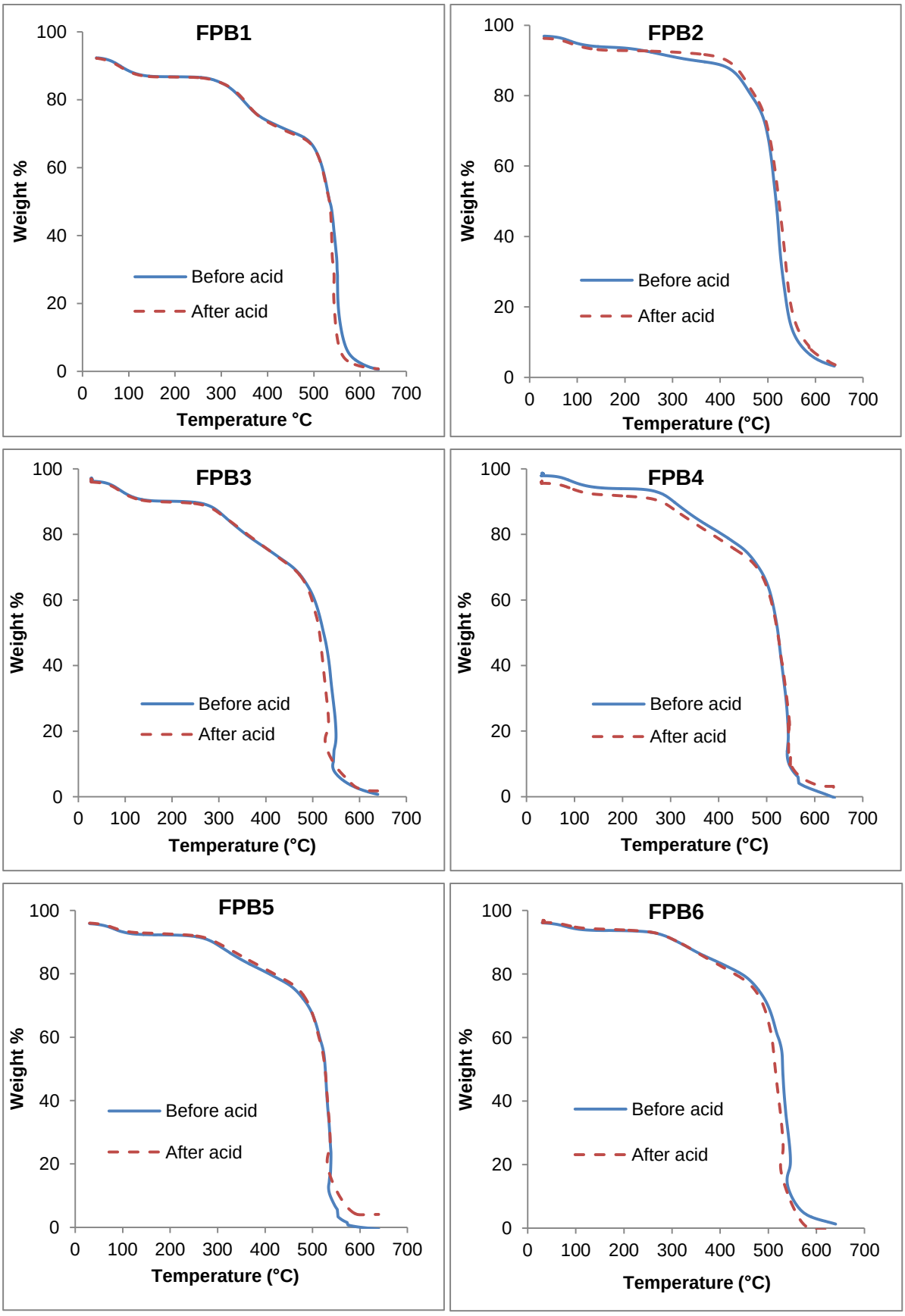
FPB1
Weight %
Temperature °C
Before acid
After acid
FPB2
Weight %
Temperature (°C)
Before acid
After acid
FPB3
Weight %
Temperature (°C)
Before acid
After acid
FPB4
Weight %
Temperature (°C)
Before acid
After acid
FPB5
Weight %
Temperature (°C)
Before acid
After acid
FPB6
Weight %
Temperature (°C)
Before acid
After acid

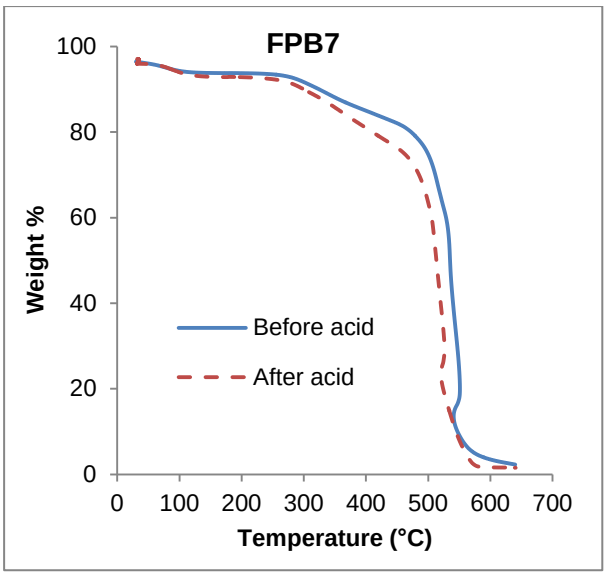
FPB7
Weight %
Temperature (°C)
Before acid
After acid
0
20
40
60
80
100
0
100
200
300
400
500
600
700

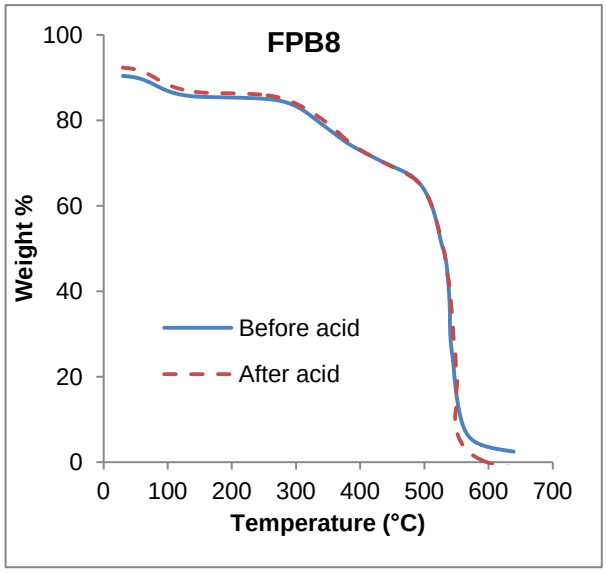
FPB8
Weight %
Temperature (°C)
Before acid
After acid
0
20
40
60
80
100
0
100
200
300
400
500
600
700

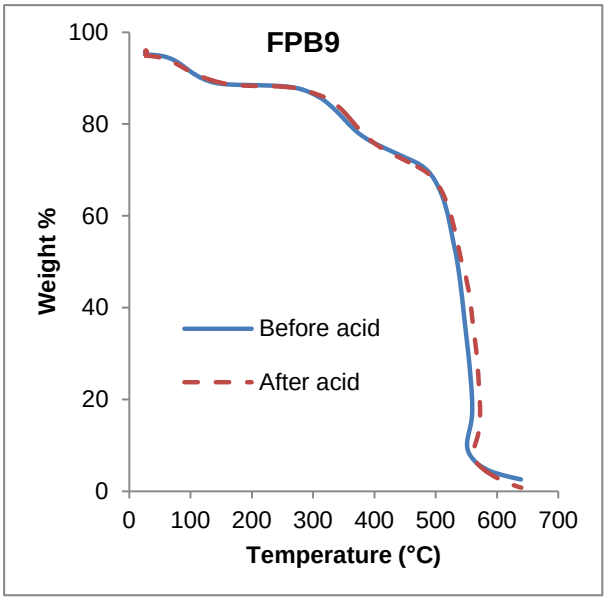
FPB9
Weight %
Temperature (°C)
Before acid
After acid
0
20
40
60
80
100
0
100
200
300
400
500
600
700

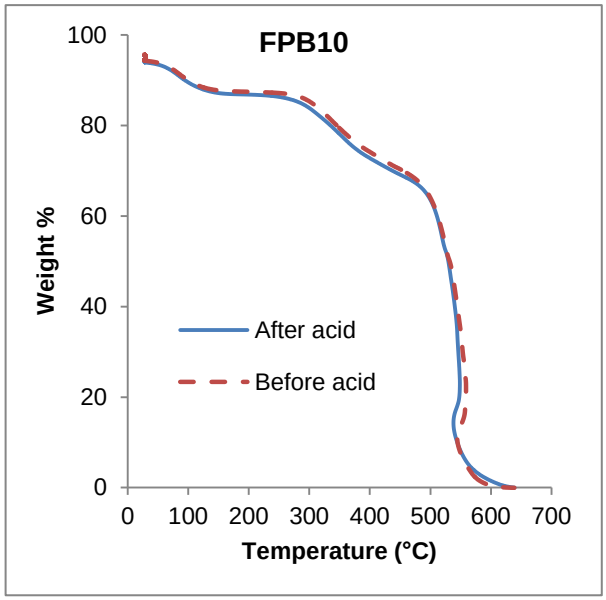
FPB10
Weight %
Temperature (°C)
After acid
Before acid
0
20
40
60
80
100
0
100
200
300
400
500
600
700

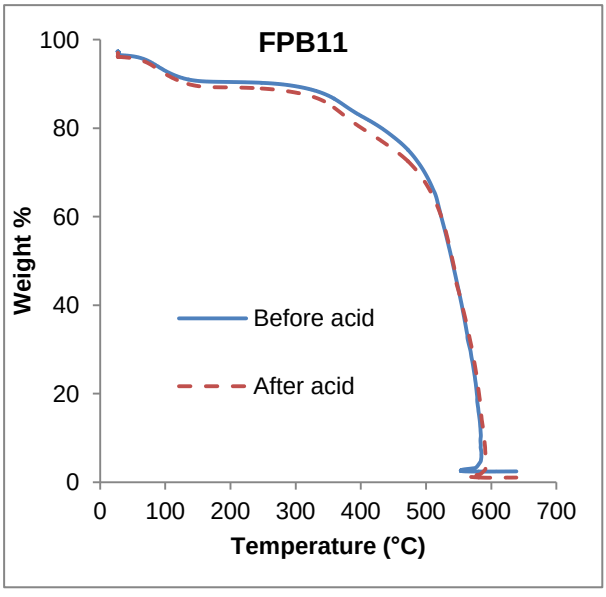
FPB11
Weight %
Temperature (°C)
Before acid
After acid
0
20
40
60
80
100
0
100
200
300
400
500
600
700